UNIVERSITY OF CALIFORNIA, SAN DIEGO

Acoustic communication in the Greater Sage-Grouse (*Centrocercus urophasianus*) an examination into vocal sacs, sound propagation, and signal directionality

A dissertation submitted in partial satisfaction of the requirements
for the Doctor of Philosophy degree

in

Biology

by

Marc Steven Dantzker

Committee in charge:

Professor Jack W. Bradbury, Chair
Professor Lin Chao
Professor Grant Deane
Professor James Moore
Professor Sandra Vehrencamp

2015

The Dissertation of Marc Steven Dantzker is approved, and it is acceptable in quality and form for publication on microfilm and electronically:

_____

_____

_____

_____
Chair

University of California, San Diego

2015

DEDICATION

For Heather, whose patience is nearly as unwavering as her love.

For my father, mother, and sister, whose support I have too often required.

For my kids, Charlie & Alice, who will henceforth address me as "Dr."

EPIGRAPH

Before you cross the street take my hand.
Life is what happens to you while you're busy making other plans.

-John Lennon

TABLE OF CONTENTS

LIST OF FIGURES

Chapter 1

Chapter 2

Chapter 3

LIST OF TABLES

PREFACE

I got my first break when, as an undergraduate in the Department of Zoology at the University of Texas at Austin, Dr. Michael J. Ryan asked me what I was doing for the summer.

"Probably working at REI and taking Physics," I said. "Why?"

"I was going to ask you if you wanted to go to Panama to work at the Smithsonian Tropical Research Institute."

"Did I say physics? I meant Panama. Yeah Panama!"

Sitting in a darkened lab being blasted with electronic *whines* and *chucks* well into the early morning hours would drive most people to pre-med. For me, it was profound and thrilling. We caught frogs, brought them inside and played sounds to them from a computer. With each hop, the frogs were answering fundamental questions about evolution.

I started my graduate training at Duke University where I learned a great deal about biomechanics and bioacoustics. In a lab devoted to the study of birdsong mechanisms, I began work to build a project on the evolution of vocal sacs in frogs. I had found a pair of species with a wide and well-studied hybrid zone where one species, the fire-bellied toad (*Bombina bombina*) had a vocal sac and its closest relative, the yellow-bellied toad (*Bombina variegata*) didn't. Hybrids were intermediate, which was possible only because the vocal sac in this group wasn't an independent structure, but more of a distension of the buccal cavity.

This would have been a great study to do except for two challenges. First, the hybrid zone was in the middle of Bosnia which was slipping into sectarian warfare.

Secondly, the Duke environment proved a poor fit for me personally. I left the program with a Master's degree and a handful of captive frogs.

I was supremely fortunate to find a new home in the Vehrenbury Lab where I could pursue my interest in signal evolution. I initially intended to stick with the *Bombina* system. One day Jack Bradbury pulled out the video tape of a displaying male sage grouse and said, "You think frog vocal sacs are cool, well check these out." I pretty much knew that my frog days were over right then and there.

We talked about the possible functions of the paired air sacs used by male sage grouse in their strut displays. I had no idea what to suggest based on the frog work. As I dug into the literature, I realized that, though much more spottily distributed than in frogs, many bird species also had vocal sacs and that some appeared to be used in vocal displays. Even more intriguing, no one had then tackled the functions of avian vocal sacs or even asked the relevant questions about mechanisms. I was captivated and hence filling this vacuum became the focus of my thesis.

The thesis is divided into three parts. The first is a general review of what is known about vocal sacs in birds. I discuss some of the possible functions, and what little is known about the mechanisms achieving those functions. My major attention in this chapter is given to the dual sacs in grouse, with a narrowing focus on sage grouse. This review, while not completed at the time, was the springboard for my subsequent research. In 2002, I was an invited speaker in a symposium on bird vocal communication as part of the 23 International Ornithological Congress in Beijing. All speakers provided a short summary of their presentations that were then published (Dantzker, M.S. and J.W. Bradbury. 2006. Vocal sacs and their role in avian acoustic

display. *Acta Zoologica Sinica* 52 (Supplement): 486-488). The current thesis chapter is a much expanded and updated version of that material. It has not yet been submitted for publication.

My review only reinforced my interest in Sage Grouse. They make the most dynamic use of a vocal sac of any animal. Jack and Sandy Vehrencamp had studied Sage Grouse in prior years with Robert Gibson, but both had recently switched organisms and study sites. While Dr. Gibson was continuing the research on the sage grouse mating system, Jack and I felt there was a more mechanistic set of questions to be asked about the role of the vocal sac that might help explain the evolution of this extraordinary display.

I set out to test various theories of the functions of the air sacs in Greater Sage-Grouse and I knew I would have to make extensive acoustic measurements on the leks where males display. My first field season using array recordings around strutting males proved to be a wakeup call. On analysis, the recordings seemed to point to interesting phenomena but were terribly inconsistent and seemed to have systematic errors. It was clear that I needed help. Jack pointed me down the hill to the Scripps Institute of Oceanography where acoustical physics was a major topic of study. I found a patient acoustical mentor in physicist Dr. Grant Deane. With Grant's help, I found that the problem I was having was principally due to my not factoring in the variability of sound propagation in the environment.

I knew from the bioacoustics literature that sound propagation near the ground presented additional challenges to both the birds and biologists. Clearly no measurements of male display acoustics could be interpreted without a suitable model

for sound propagation at the ground and under natural field conditions during the lek season. Grant and I developed a model of sound propagation in the environment that we then tested against extensive (and hard won) field data collected during lek seasons in California's Eastern Sierras. The results of this work constitute the content of Chapter 2 of this thesis. This chapter has not been submitted for publication but hopefully is now ready.

Finally, I turned to testing possible functions of the paired air sacs used in displays by male Greater Sage Grouse. Earlier studies by my advisor and his colleagues gave hints that strut sound amplitudes might be one of the criteria used by females in mate choice, but they had experienced considerable difficulty in obtaining consistent measurements from a given male. Part of this problem might have been variations in sound propagation processes at different temperatures or ground conditions. I hoped to account for this source of the variability with the results of Chapter 2. But there were still other possibilities suggested by my review in Chapter 1. If the main sources of emitted sound during a strut were the two sacs, there was a possibility that the waves emitted from the two nearby sources could interfere and generate a complex sound field around the bird. If so, the standardized procedure of recording a male only when he faced the microphone might give variable and even erroneous measures of amplitude. This is why I set out to record male strut displays in the field with a microphone array system. This would allow me to characterize the shape of the sound field around each male and use the peak lobes as the best measure of display amplitude but only if I could account for the transmission loss along each path.

There were no commercial systems or software available at the time, so I had to

devise my own. Luckily, my advisor and I had written and received two NSF grants to fund the relevant equipment, field costs, and computers (NSF IBN-9701201 and NSF IBN-940621). The system design was quite technically challenging and collecting sufficient data in the field required several very challenging lek seasons. Dr. Deane was a major collaborator in this project and provided key insights at every stage. The results constitute the third chapter of my thesis and this work has been published (Dantzker, M.S, Grant B. Deane, and J.W. Bradbury. 1999. Directional acoustic radiation in the strut display of male sage grouse, *Centrocercus urophasianus*. *Journal of Experimental Biology* 202: 2893-2909).

ACKNOWLEDGEMENTS

I'd like to thank the following people for their support.

The University of Texas TA, who got me into all of this – Steve Takata

My dearest friend and fellow Duke refugee – Michael Blum

Vehrenbury Lab members – Lisa Angelloni, Catherine deRivera, Laura Molles, Helen Neville.

UCSD Colleagues, Students and Faculty alike – Z Morgan Benowitz-Fredericks, David Holway, Randy Hampton, Daren & Jessica Irwin, Josh Kohn, Karen Marchetti, Karen Martien, Amy McGaraghan, Trevor Price, Kaustuv Roy, Andrew Suarez, & Neil Tsutsui.

From my life at the Cornell Lab of Ornithology – Erin Bohman, Kimberley Bostwick, John Bowman, Benjamin Clock, Charles Eldermire, John Fitzpatrick, Melissa Groo, Eric & Jillian Liner, Edwin Scholes, Tom Swartwout, & Gerrit Vyn.

For being pushy – Daniel Ardia & Martin Schlaepfer, you can let up now!

For being less pushy – Chris & Diji Behr, Jesse Ernst, Teddy Eisenman, & Ellie Rice.

For never ending positivity – Pat, J. Steele, and Steele M. Clark

My partner in many avian crimes – Gail Patricelli.

My committee members – Lin Chao, Jim Moore, & Sandy Vehrencamp

My collaborator and mentor – Grant Deane

And Jack Bradbury, whose role in my life defies any attempt at categorization.

Financial support for my years of graduate training came from the National Science Foundation through a Graduate Research Fellowship (MSD), a Doctoral Dissertation Research Grant IBN-9701201 (MSD with Jack W. Bradbury PI), and grant IBN-9406217 (Jack W. Bradbury, PI). Further support was provided by NIH training grant T32 GM–07240 (MSD).

Chapter 1, in part, is based upon a conference proceeding published in Vocal sacs and their role in avian acoustic display in Acta Zoologica Sinica 2006. Dantzker, Marc; Bradbury, Jack W. 2006. The dissertation author was the primary investigator and author of this paper.

Chapter 2, in full is currently being prepared for submission for publication of the material. Dantzker, Marc; Deane, Grant. The dissertation author was the primary investigator and author of this material.

Chapter 3, in full, is a reprint of the material as it appears in Directional acoustic radiation in the strut display of male sage grouse, *Centrocercus urophasianus* in Journal of Experimental Biology 1999. Dantzker, Marc; Deane, Grant; Bradbury, Jack W. 1999. The dissertation author was the primary investigator and author of this paper.

VITA

2015	University of California, San Diego Doctor of Philosophy in Biology
1995-2000	University Of California, San Diego Doctoral Candidate in Biology
1993-1995	Duke University Masters of Arts in Zoology
1988-1993	University Of Texas, Austin Bachelor of Science in Zoology

PEER REVIEWED PUBLICATIONS

Patricelli, G.L., **M.S. Dantzker** & J.W. Bradbury. 2008. Acoustic directionality of red-winged blackbird (*Agelaius phoeniceus*) song relates to amplitude and singing behaviours. *Animal Behavior*, **76**: 1389-1401.

Patricelli, G.L., **M.S. Dantzker** & J.W. Bradbury. 2007. Differences in acoustic directionality among vocalizations of male red-winged blackbird (*Agelaius pheoniceus*) are related to function in communication, *Behavioral Ecology and Sociobiology,* **61**(7):1099-1110.

Patricelli, G.L., **M.S. Dantzker** & J.W. Bradbury. 2006. Directionality in acoustic communication in Red-winged Blackbirds. *Journal of Ornithology,* **147**:225-226 Suppl. 1. (published abstract)

Dantzker, M.S. & J.W. Bradbury. 2006. Vocal sacs and their role in avian acoustic display. *Proceedings of the 23rd International Ornithological Congress, Acta Zoologica Sinica* **52**(Supplement):486-488.

Fitzpatrick, J.W., M. Lammertink, M.D. Luneau, Jr., T.W. Gallagher, B.R. Harrison, G.M. Sparling, K.V. Rosenberg, R.W. Rohrbaugh, E.C.H. Swarthout, P.H. Wrege. S. Barker, **M.S. Dantzker**, R.A. Charif, T.R. Barksdale, J.V. Remsen, Jr. S.D. Simon, & D. Zollner. 2006. Clarifications about current research on the status of Ivory-billed Woodpecker (*Campephilus principalis*) in Arkansas. *The Auk* **123**(2):1-7.

Fitzpatrick, J.W., M. Lammertink, M.D. Luneau, Jr., T.W. Gallagher, B.R. Harrison, G.M. Sparling, K.V. Rosenberg, R.W. Rohrbaugh, E.C.H. Swarthout, P.H. Wrege. S. Barker, **M.S. Dantzker**, R.A. Charif, T.R. Barksdale, J.V. Remsen, Jr. S.D. Simon, & D. Zollner. 2005. Ivory-billed Woodpecker (*Campephilus principalis*) persists in continental North America. *Science* **308**: 1460-1462.

Gaunt, S.L.L., D.A. Nelson, **M.S. Dantzker**, G.F. Budney and J.W. Bradbury. 2005. New Directions for Bioacoustics Collections. In: Commentary: Bird Collections: Development and Use of a Scientific Resource (K. Winkler ed). *The Auk*, **122**(3): 966-971.

Dantzker, M.S., G.B. Deane, & J.W. Bradbury. 1999. Directional acoustic radiation in

the strut display of male sage grouse *Centrocercus urophasianus*. *The Journal of Experimental Biology* **202**(21): 2893-2909.

Baer, C.F., **M.S. Dantzker**, & M.J. Ryan. 1995. A test for preference of association in a color polymorphic poeciliid fish: laboratory study. *Environmental Biology of Fishes* **43**: 207-212.

OTHER PUBLICATIONS

Dantzker, M.S., & D.O. Brown (Producers) 2009 Signals for Survival [DVD] Sinauer Associates 2009.

Dantzker, M.S. 2004. Preserving Visual Recordings at a Library of Animal Behavior, Part 1: From Submitted Media to Archival Masters. RLG DigiNews **8**(1).

ABSTRACT OF THE DISSERTATION

Acoustic communication in the Greater Sage-Grouse (*Centrocercus urophasianus*)
an examination into vocal sacs, sound propagation, and signal directionality

by

Marc Steven Dantzker

Doctor of Philosophy in Biology

University of California, San Diego, 2015

Professor Jack W. Bradbury, Chair

The thesis is an inquiry into the acoustic communication of a very unusual avian species, the Greater Sage-Grouse, *Centrocercus urophasianus.* One of the most outstanding features of this animal's dynamic mating display is its use of paired air sacs that emerge explosively from an esophageal pouch. My first line of inquiry into this system is a review of the form and function of similar vocal apparatuses, collectively called vocal sacs, in birds. Next, with a combination of mathematical models and field measurements, My collaborator and I investigate the acoustic environment where the Greater Sage-Grouse display. The complexities of this acoustic environment are

relevant both to the birds and to the subsequent examinations of the display's properties. Finally, my collaborators and I examine a cryptic component of the acoustic display — directionality — which we measured simultaneously from multiple locations around free moving grouse on their mating grounds.

CHAPTER 1:

Vocal sacs and their role in avian acoustic display

ABSTRACT

Much progress has been made in understanding the fundamental role of the avian syrinx in generating vocalizations. However, there is growing recognition that the rest of the avian vocal system may play an equally important part in sound production and emission. Here I examine the role that one such secondary structure, the avian vocal sac, may play in shaping the avian voice, addressing its function in chamber resonance, membrane resonance, acoustic coupling, directionality, and percussion. Special attention is given to the Greater Sage-Grouse, *Centrocercus urophasianus*, with its paired vocal sacs and unique strut display.

INTRODUCTION

The process of acoustic signaling can be understood as following three somewhat distinct stages — production, propagation, and reception. There are many degrees of freedom and constraints in each of these stages, the sum of which helps shape signal evolution (Bradbury & Vehrencamp, 2011). Here, I focus on the sound production stage.

Production is the process of creating and modifying vibrations, then transmitting them into the surrounding medium (here, air). This usually entails a primary vibration source, vibration modification in the internal environment, and finally emission into the air. I introduce each stage with a look at some of the more common variations in form found with special emphasis on birds. Thereafter I examine the role of a structure found in many terrestrial vertebrate taxa but not usually associated with birds, a vocal sac.

Vibration Sources

Most bird vocalizations begin in the syrinx – a uniquely avian voice-box built around specialized vibrating valves near the tracheal-bronchial split (King, 1989). Unlike the larynx and its vocal folds, the form of which is remarkably conserved across terrestrial vertebrates from frogs to mammals, the syrinx has proved evolutionarily labile. The syrinx is found in various forms in a variety of positions along the airway of different avian taxa (reviewed in King, 1989; and more recently in Bradbury & Vehrencamp, 2011). Physiologists have spent decades determining how the most common form of syrinx, the tracheobronchial syrinx, works (Goller & Larsen, 1997, 2002; Suthers et al., 1999; Larsen & Goller, 1999, 2002; Larsen et al., 2006; Jensen et al., 2007). Syringes whose vibratory membranes are elsewhere in the trachea or bronchi

have received less attention (but see Gaunt et al., 1976 on domestic chickens; Suthers & Hector, 1982 on Grey Swiftlets; Krakauer et al. 2009 on Greater Sage-Grouse). Surely there are still many puzzles to be solved.

Not all avian acoustic communication starts in a syrinx; birds have other ways of making sound. Feathers can be used to create sound either by percussion as in some manakins (Bostwick, 2000) and Ruffed Grouse, through stridulation as in sage grouse (Hjorth, 1970), and manakins (Bostwick, 2000), by aeroelastic flutter (Clark & Feo, 2008; Clark et al., 2013), or possibly by true vortex whistling (Fletcher 1992). All that said, most avian acoustic communication is vocal and produced internally with a syrinx.

Vibration Modification

When sounds are created internally, as they are with a larynx or syrinx, they are subject to modification by the structures and spaces in and around the airway[1]. These supplemental acoustic structures filter, amplify, radiate, and spatially configure the radiated vibrations. It has long been realized that the upper vocal tract of mammals acts as a resonance filter (reviewed by Fletcher, 1992). Acousticians have demonstrated the importance of the pharyngeal and other vocal tract anatomy on species such as lions, domestic cats, and non-human primates (Fitch & Hauser, 1995; Fitch, 1997, 2000; Weissengruber, 2002; Gamba et al., 2012). In great apes, anatomical changes to the vocal tract were an essential precondition for the evolution of human speech (Fitch, 2010).

[1] While it is helpful to consider modification as a separate step in sound production, there can be an interaction between the vibration source and the resonance of the vocal track that feeds back to alter the vibration pattern itself (Nowicki & Capranica, 1986; Mergell and Herzel, 1997; Riede et al., 2000,).

The syrinx is farther down the airway than the larynx so there is even more opportunity for the evolution of secondary acoustic structures. In fact, one adaptation that has evolved independently in multiple taxa is the extreme elongation of the trachea (Figure 1 and reviews by McLelland, 1989; Fitch, 1999) pushing the syrinx farther and farther away from the beak. This elongation appears to be an adaptation for size exaggeration, not by lowering frequency but by altering formant dispersion which is perceived as "richer" or "more resonant." This is an acoustic adaptation that works well for the broadband sounds of many non-songbirds, but the more musical song of passerines present a distinct challenge.

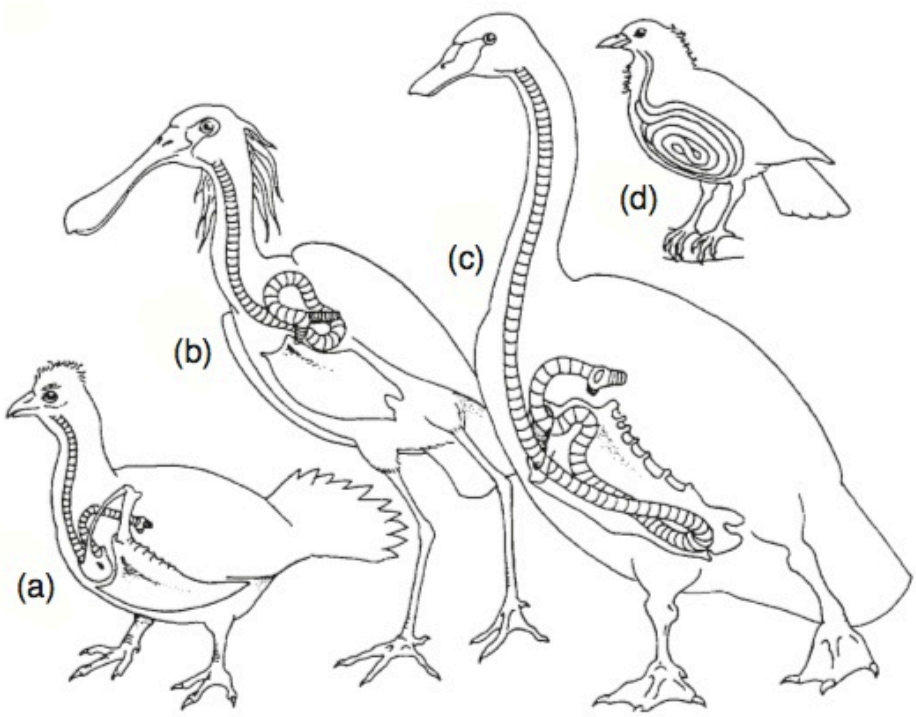

Figure 1. Four types of tracheal elongation. (a) intraclavicular coiling in the Crested Guinea-Fowl, *Guttera edouardii*; (b) intrathoracic coiling in the European Spoonbill, *Platalea leucorodia*; (c) intrasternal coiling in the trumpeter swan, *Cygnus buccinator*; and (d) subdermal coiling in the Trumpet Manucode, *Manucodia keraudrenii*. From Fitch, 1999.

Some bird songs are tonal, and these represent a particular acoustic challenge that many thought couldn't be explained by a source-filter model (e.g. Grenwalt, 1968). Tonal song has no overtones, and in many cases frequency modulation occurs rapidly without the appearance of any harmonics. In a source-filter model, to accomplish this, the vocal-tract filter must be narrow band and variable. Heliox experiments demonstrated that the vocal tract was responsible for the tonality of birdsong (Nowicki, 1987) but, at the time, the mechanism was unknown. Later, recordings made with implanted microphones directly demonstrated that filtering was responsible for tonal song (Beckers et al., 2003), at least in some doves.

Biologists did not know how songbirds could possibly reshape their vocal tract filter sufficiently to filter their highly variable sounds. The importance of aspects of the vocal tract beyond length became clearer with studies of beak posture (Westneat et al., 1993), which demonstrated an association between beak movements and vocalization. Others have found that the evolution of beak morphology for changes in feeding strategies can drive the diversification of vocal signals (Podos, 2001). But there are clear limits to the "rigid tube with variable opening" model that beak shape and movements can contribute to the capability of vocal tract filtering (Fletcher & Tarnopolsky, 1999) so acousticians have looked further. More advanced theoretical models later showed that adding the filtering components of other coupled vocal organs, in this case a distensible vocal cavity, would better explain the precise filtering required for songbird song (Fletcher et al., 2006). Researchers then used cineradiography to show that cardinals coordinate movements of the hyoid skeleton and the expansion of the cranial end of the esophagus during sound production (Riede et al., 2006). These

movements are consistent with the theoretical model and, taken together with that model, show how the precise nature of the vocal tract and associated structures can be critical to understanding the mechanism of sound production. Given the wide variety of sounds birds make, and the variety of associated structures they have available, there are clearly myriad other structures and mechanisms left to examine.

One such trait that has evolved multiple times in birds, yet has received almost no attention as a general phenomenon, is the vocal sac (Dantzker & Bradbury, 2006; Bradbury & Vehrencamp, 2011). All birds have air sacs as part of their respiratory system but these are not known to play a role in acoustics beyond their role in respiration. Many birds puff up their gular region to some extent when vocalizing, which may be a key component of tuning the vocal filter (Fletcher et al., 2006; Riede et al., 2006). However these minor expansions are not vocal sacs.

The vocal sac

Vocal sacs are a specialized structure, near the skin and unbounded by bone on at least one side, such that they can be inflated and deflated for vocalization. Vocal sacs protrude from the body but they may be covered by feathers or fur. Vocal sacs have flexible walls containing elastin, collagen and muscle fibers and thus they collapse when not under respiratory pressure through both passive and active components (Riede et al. 2008). Vocal sacs are generally associated with frogs (Figure 2). Except for a couple of basal clades, almost all frogs have vocal sacs. Frog vocal sacs are diverticula of the buccal cavity communicating with it through specific apertures (Tyler, 1971, 1972; Duellman & Trueb, 1994; Tyler & Duellman, 1995). There are more than four thousand species of frogs with vocal sacs, but frogs do not have a monopoly on the

acoustic apparatus.

Figure 2. Tungara frog, *Engystomops pustulosus*, with inflated vocal sac. Photo by author.

The mammalian vocal tract has provided ample fodder for the evolution of additional chambers (Kelemen, 1963; Negus, 1949) anterior to the vocal chords. Most of these are not vocal sacs because the structures are of a nearly fixed size regardless of vocal behavior or they are bounded on all sides by thick tissues or bone (Riede et al., 2008). The Mongolian Gazelle's (*Procapra gutturosa*) throat expansion is seasonal so, while it changes its posture during roaring, the chamber is fixed and not inflated (Frey & Gebler, 2003; Frey & Riede, 2003).

True vocal sacs do occur in mammals and some of the most intriguing are found in our closest relatives (Hewitt et al., 2002; Nishimura et al., 2006). All great apes except humans have a single fused ventricular sac extending from paired ventricles in the larynx (Raven, 1950; Starck & Schneider, 1960). The precise function of these air sacs is debated, but most hypotheses agree they are used in acoustic communication (Fitch and Hauser 2003; Hewitt et al. 2002). In adult male orangutans (*Pongo sp*.) the air sac is visible in the neck region when inflated (Figure 3a). In chimpanzees (Pan sp.) and gorillas (*Gorilla sp*.) the air sac extends into the pectoral and axillary regions which makes it less apparent (Starck & Schneider, 1960). It takes years for the sacks to fully develop (Nishimura et al., 2007) which I hypothesize may be the reason that only silverback gorilla's can do a full hoot-chest beat (Salmi et al. 2013).

Many other primates have laryngeal air sacs. Some of these qualify as vocal sacs and some do not. Siamangs (*Symphalangus syndactylus*) have perhaps the most conspicuous vocal sac of any primate, which both sexes use in their territorial display (Booth, 1957). The vocal sacs are inflated while vocalizing with mouths closed creating the "boom" sound, or held full of air while calling with mouth open (Figure 3b)

producing the “scream” (Riede et al. 2008). While the Siamang is a gibbon, the vocal sac has the same basic anatomy as the great apes (Starck & Schneider, 1960; Schneider, 1964.)

Figure 3. Laryngeal air sacs in primates. A) Orangutan, *Pongo spp*.[2]. B) Siamang, the largest of the gibbons, *Symphalangus syndactylus*.[3]

[2] photo by Sean Crane http://photo.net/photodb/photo?photo_id=9837008&size=lg

[3] "Symphalangus syndactylus, Chiba Zoo, Japan" by Suneko - http://www.flickr.com/photos/suneko/373310729/. Licensed under Creative Commons Attribution 2.0 via Wikimedia Commons - http://commons.wikimedia.org/wiki/File:Symphalangus_syndactylus,_Chiba_Zoo,_Japan.jpg#mediaviewer/File:Symphalangus_syndactylus,_Chiba_Zoo,_Japan.jpg

As with the air sacs of apes and siamangs, most mammalian vocal sacs are connected to the airway through apertures in the larynx. One example is the Diana monkey (*Cercopithecus diana*) (Riede & ZuRiede et al., 2005). Other mammalian vocal sacs include the "hubmaseakkha" of reindeer (*Rangifer tarandus*) (Frey et al., 2007), and the pharyngeal pouches of male epomophorine bats (Kingdon, 1984).

That said, there are many laryngeally connected chambers that fill with air but should not be considered vocal sacs. Howler monkeys (*Alouatta spp*.) have superficially similar air cavities, called Bulla hyoidea, below their chins but these are not inflatable (Riede et al., 2008, Frey & Gebler, 2010). In bears (*Ursidae*), there is a laryngeal air sac but it is deep between tissues and its inflation and deflation cannot be seen externally (Ganzberger et al. 1995; Weissengruber et al., 2001). Musk Oxen (*Ovibos moschatus*) also have a very small inflatable chamber adjacent the larynx, but it is deep inside their thick necks (Frey et al., 2006). None of these are vocal sacs. The only mammalian vocal sac that is not laryngeal is the super nose-balloon of hooded seals (Berland, 1966).

BIRDS WITH VOCAL SACS

The throats of most birds expand during vocalization and recent work by Riede, Fletcher and colleagues explains the significance of this (Fletcher et al., 2006; Riede, T. et al., 2006). But, no matter how big a bird's mouth gets, the buccal cavity isn't a vocal sac. This is more like the pharyngeal adaptations for mammalian roaring and human speech. True vocal sacs have evolved in at least eleven distinct avian lineages. There are three basic anatomical types of vocal sacs – esophageal, tracheal, and gular – and we shall review the diversity of species and forms in each type, plus a few more

mysteries.

Esophageal vocal sacs

The most familiar avian vocal sac, at least if you've spent any time in an urban park, is that of the common Rock Pigeon, *Columba livia*. In fact the same basic structure is found in many of the approximately 310 pigeon and dove species in the order Columbiformes (Baptista et al., 1997) . Because their sacs are covered in feathers, cooing is often described as fluffing up of feathers, but it is actually an inflated esophagus. One can see the air sac more clearly in some breeds of domesticated fancy pigeon including the Norwich Cropper, which have been artificially selected to increase sac volume and inflation behavior. The vocal sac of the dove is also the best studied avian vocal sac so we will return to a discussion of this structure below in the section on vocal sac functions (Beckers et al., 2003).

Figure 4. Esophageal vocal sac of the Rock Pigeon is inflated in the cooing courtship display. A) a wild Rock Pigeon male displays to a female[4]. B) A fancy pigeon breed, the Norwich Cropper.[5].

[4] "Rock pigeons (*Columba livia*) courting, taken in Santa Barbara, California " by Dori. Licensed under CC BY-SA 3.0 US -http://commons.wikimedia.org/wiki/File:Pigeons_courting_4867.jpg

[5] Norwich Cropper 102 by Mike Krochter is licensed under CC BY-NC 4.0
Based on a work at http://www.vancouverfancypigeon.ca/wintershowreport2012.htm.

A review of anatomy and observational behavior inevitably takes one into the deep literature of early naturalists and their observations during collecting expeditions. That is where we find mention of a number of other feathered esophageal vocal sacs that have largely not been studied since. One example is found in the American Bittern (*Botaurus lentiginosus*), whose vocal sac anatomy was described in 1922 (Figure 5; Chapin, 1922). Chapin argued that they were a critical vocal apparatus for the production of the dramatic pump-er-lunk display.

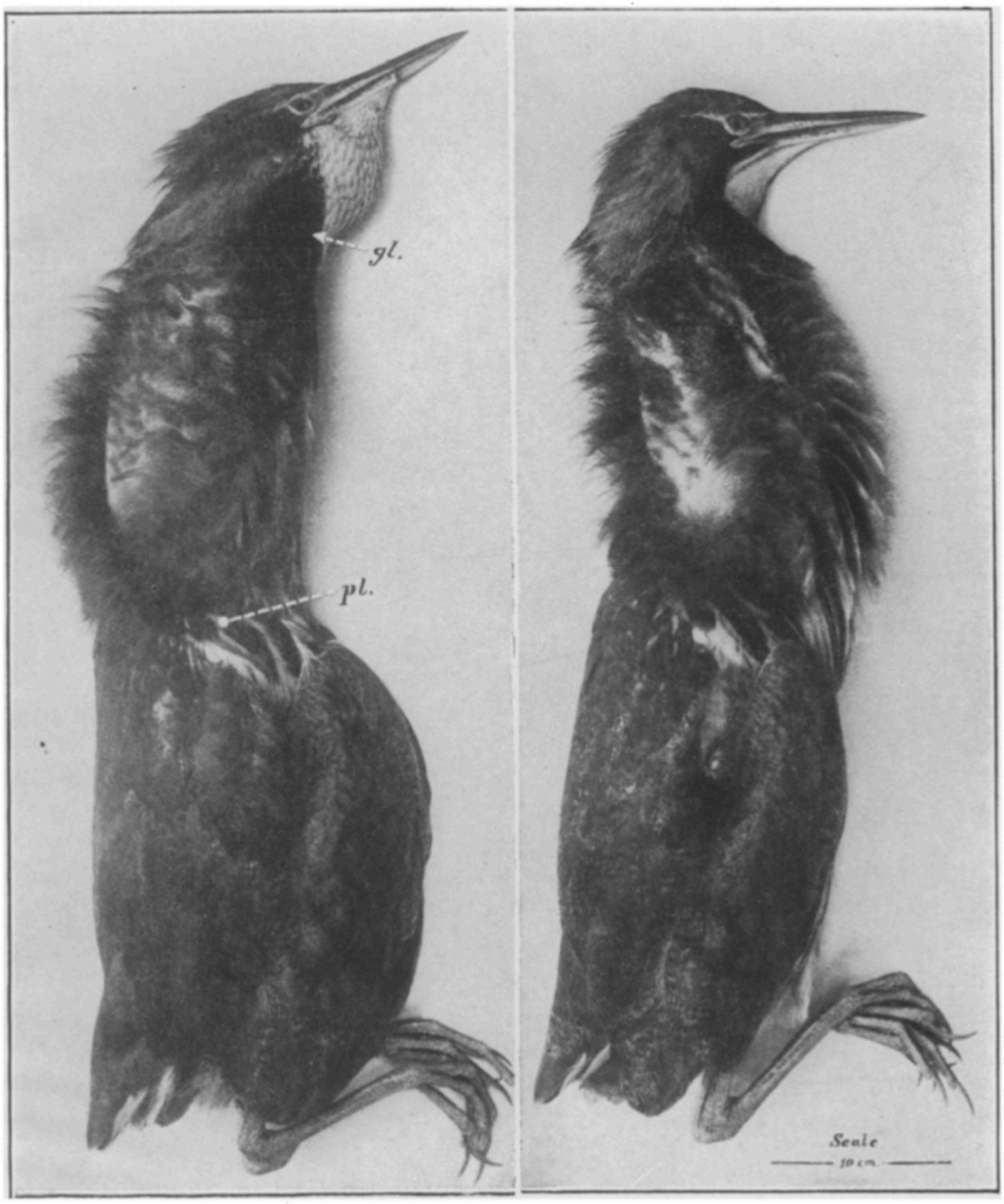

Figure 5. Photographs of a dead American Bittern inflated and deflated (Chapin, 1922).[6]

[6] Photographs from Chapin, 1922. Available at www.jstor.org/stable/4073951

Many medium to large bustards (*Otididae*) have esophageal vocal sacs that are often covered in elaborate feathering; and some but not all inflating bustard species vocalize while inflated. The Kori Bustard (*Ardeotis kori*) combines its inflation, called a "balloon display" with booming (Hellmich J, 1988, Lichtenberg & Hallager, 2007). While they hold their balloon stance for as long as an hour and don't vocalize the entire time, the boom is only made with the vocal sac inflated. Many other bustard species including the Great Bustard (*Otis tarda*), Denham's Bustard (*Neotis denhami*), Australian Bustard (*Ardeotis australis*) and Great-Indian Bustard (*Ardeotis nigriceps*) combine inflation and booming (Collar, 1996).

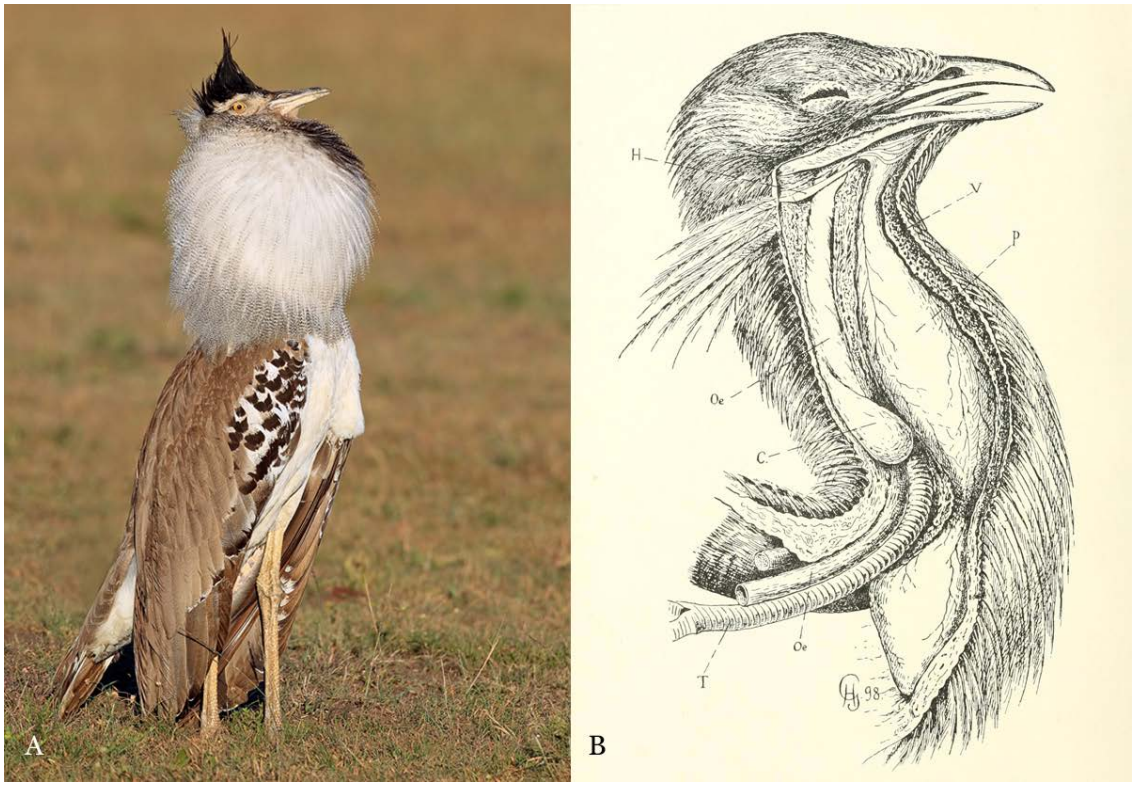

Figure 6. Bustard vocal sacs A) Kori Bustard (*Ardeotis kori)* balloon display.[7]. B) Great Bustard (*Otis tarda*) vocal sac. P= Pouch Œ=Esophagus T=Trachea H=Hyoid V=Vascular tissue. ([8].)

[7] Photo by Jalil El Harrar, www.naturfotografie-costa-rica.de
[8] Illustration from Pycraft, 1910 Biodiversity Heritage Library: www.biodiversitylibrary.org/item/31751

Buttonquails (family: *Turnicidae*), which inflate as well, are unique insofar as they are the only sexually-dimorphic group in which females, not males, have the vocal sac. The display of the Painted Buttonquail (*Turnix varia*) "recalls that of the male of the Common Pigeon, the crop being inflated with air, the while the proud suitor bows and "coos" to the chosen mate (Pycraft, 1910)." While we can't be certain without specific anatomical study, Pycraft's account implies that the air sac is esophageal. It isn't clear if all 16 species of Buttonquail have vocal sacs but it seems likely.

All three Umbrellabirds (*Cephalopterus spp*.) have pendulous esophageal vocal sacs (Sick, 1954). The sac is bare in the aptly named Bare-necked Umbrellabird (*Cephalopterus glabricollis*, Figure 7A) and covered with feathers in the other two (Figure 7B). The Bare-necked Umbrellabird's vocal sac is unique in having a wattle hanging off of it.

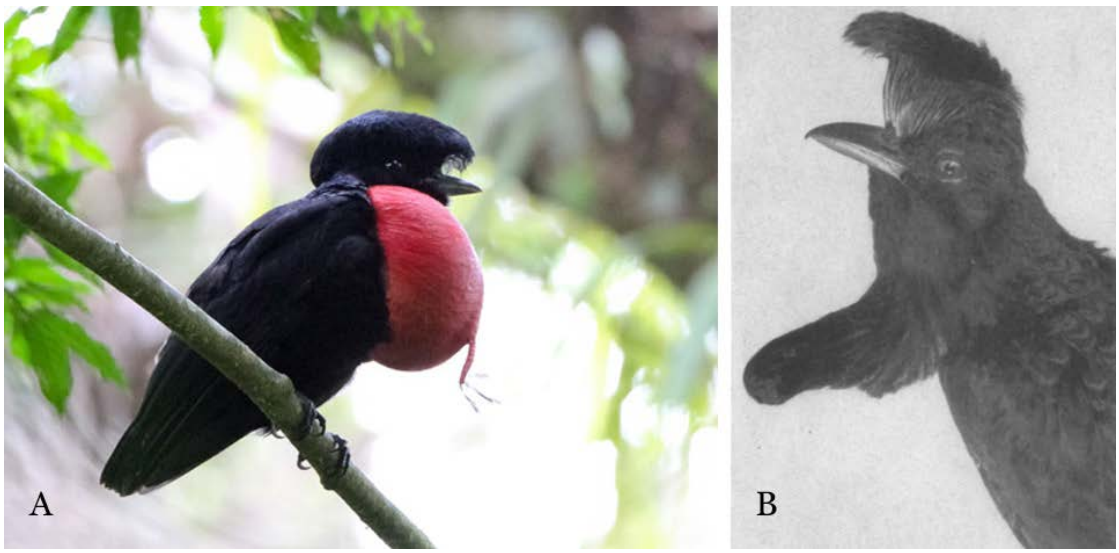

Figure 7. Vocal sacs of Umbrella birds. A) Displaying wild Bare-necked Umbrellabird (*Cephalopterus glabricollis*)[9]. B) Dead Amazonian umbrellabird, *Cephalopterus ornatus*, from (Sick, 1954).

[9] Photo by Frank Hummel www.birdquest-tours.com/

A stunning group of chicken-like birds in the family Tetraonidae have esophageal air sacs that have the distinction of being the only paired vocal sacs in birds. A few frog species, such the Neotropical veined tree frog (*Trachycephalus venulosus*) and the North American wood frog (*Lithobates sylvaticus*) have paired sacs but grouse are the only bird examples. The sacs are paired on the surface, but internally, they are parts of the same expansion of the esophagus. Black grouse (*Tetrao tetrix*) show what is likely the ancestral condition. They have a single broadly inflatable neck, much like doves. In North America the three species in the Genus *Tympanuchus* have paired apteral regions of bare skin (Figure 8A). The vocal sacs are brightly colored in all three species, and it is entirely possible that the acoustic mechanism is identical to the single vocal sac of black grouse, with an added paired visual component superimposed.

Figure 8. Grouse vocal sacs. A) Greater Prairie Chicken (*Tympanuchus cupido*) booming[10]. B) Gunnison Sage-Grouse (*Centrocercus minimus*) strut display[11].

[10] , photo by Gerrit Vyn
[11] , photo by the author

The same is less likely for the two species of Sage Grouse (Centrocercus spp., Figure 7B), which have a sac that, when put under pressure as part of the display, clearly becomes a paired structure, even if there is still communication between the two parts internally. The air sac changes shape so rapidly in the strut display that it is entirely possible that the vocal sac plays different roles at different moments of the 3 second strut. On the outside of the vocal sac there are stiff feathers that the bird stridulates like a güiro. During these wing swishes, the thin membranes may act like the open end of the musical instrument. Then the air sacs are expelled rapidly and pushed through the skin by bringing the head down onto them.

Tracheal vocal sacs

Not all avian vocal sacs are esophageal. Some species have an air sac that is communicated to the vocal tract through an aperture in the trachea. One such vocal sac is found in the Emu (Dromaius novaehollandiae). Adult emus have large ovoid vocal sacs on their lower neck that extend up to 35 cm long down to the sternum and are 8-10 cm in diameter (Murie, 1867). Little is known beyond a few dissections over the last 150 years (McLelland, 1989), but it is believed that the sac is larger in females than males (Murie, 1867). The sac is inflated during low-frequency booming. It appears that all of the large members of the order Struthioniformes probably have this same structure. Ostriches (Struthio sp.), and Rheas (Rhea sp.) have both been repeatedly documented as booming with an inflated air sac (Folch, 1992). More recently Cassowaries (Casuarius sp.) were observed booming with the neck nearly doubling in size during inflation (Mack & Jones, 2003). A more recent video by James Reardon vimeo.com/80171843 clearly demonstrates this inflation in a Dwarf Cassowary

(Casuarius bennetti). While there are no anatomical studies of the air sacs of these other Struthioniformes, it is reasonable to presume that they share the same basic anatomy with a tracheal origin.

Male Ruddy Ducks (*Oxyura jamaicensis*) and their sister species the Andean Duck (*Oxyura ferruginea*) have an air sac that originates from an aperture in the trachea as well, but in their case just below the larynx (Wetmore, 1917, 1918). They use this in an unusual display where they pound their bills against the air sac repeatedly (Figure 9, Johnsgard, 1971; Johnsgard & Carbonell, 1996). Based on similar anatomy in the skins of other ducks, Wetmore hypothesizes that a number of other duck species likely have vocal sacs in the same location. Based on current phylogeny, the trait likely occurs in two other genera, Thalassornis (White-backed Duck), and Nomonyx (Masked duck) (Wetmore, 1917). If present in all of these species, then tracheal air sacs would have a disjointed dispersion on the Anatid family tree. Oxyura and Nomonyx are in the same subfamily with many species that lack air sacs, and Thalassornis is thought to be distantly related but convergent on other fronts. If so, it would be interesting to know if the they have the same tracheal origin, or if the anatomical similarity is only skin (sac) deep.

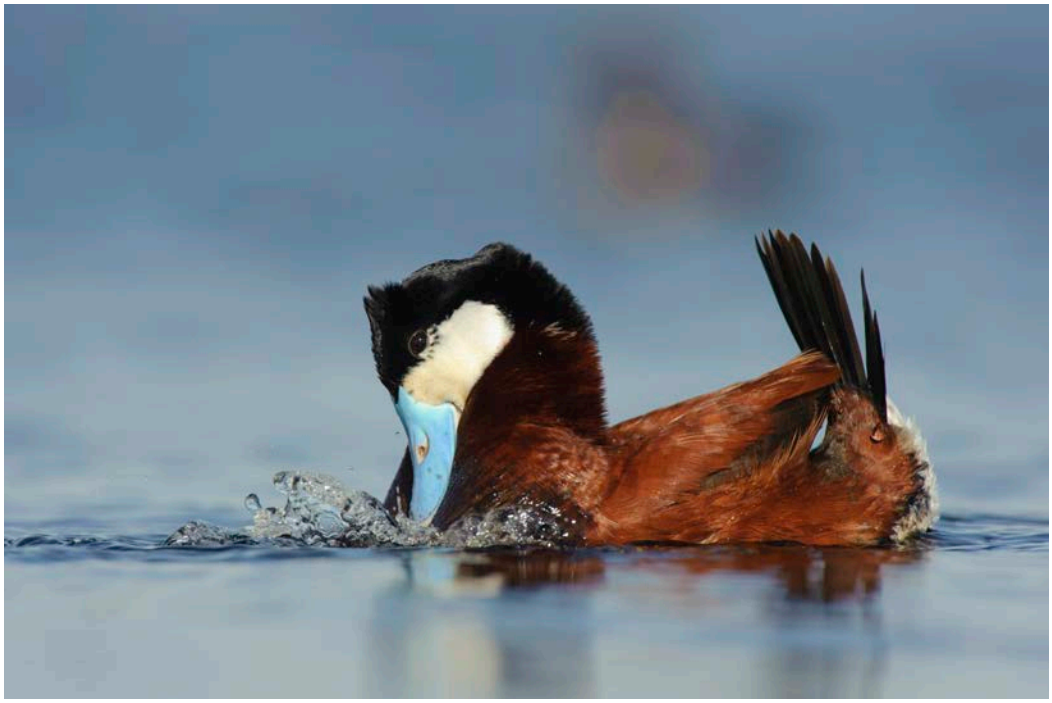

Figure 9. Ruddy Duck (*Oxyura jamaicensis*) thumping its air sac. [12]

[12] Photo by Gerrit Vyn.

Two storks, the Jabiru Stork (*Jabiru mycteria*) and the somewhat closely related Marabou Stork (*Leptoptilos crumeniferus*) both inflate a region in their necks as part of their displays. The external anatomy is consistent with a tracheal air sac but I can find no anatomical studies in the literature. These air sacs are often held fully inflated for lengthy periods in a strictly visual display. However, they are inflated during both voiced phonation and bill clattering, in which they likely play an acoustic role. The Marabou has the broadest repertoire of all the storks making moos, whines, whistles and hiccups during courtship.

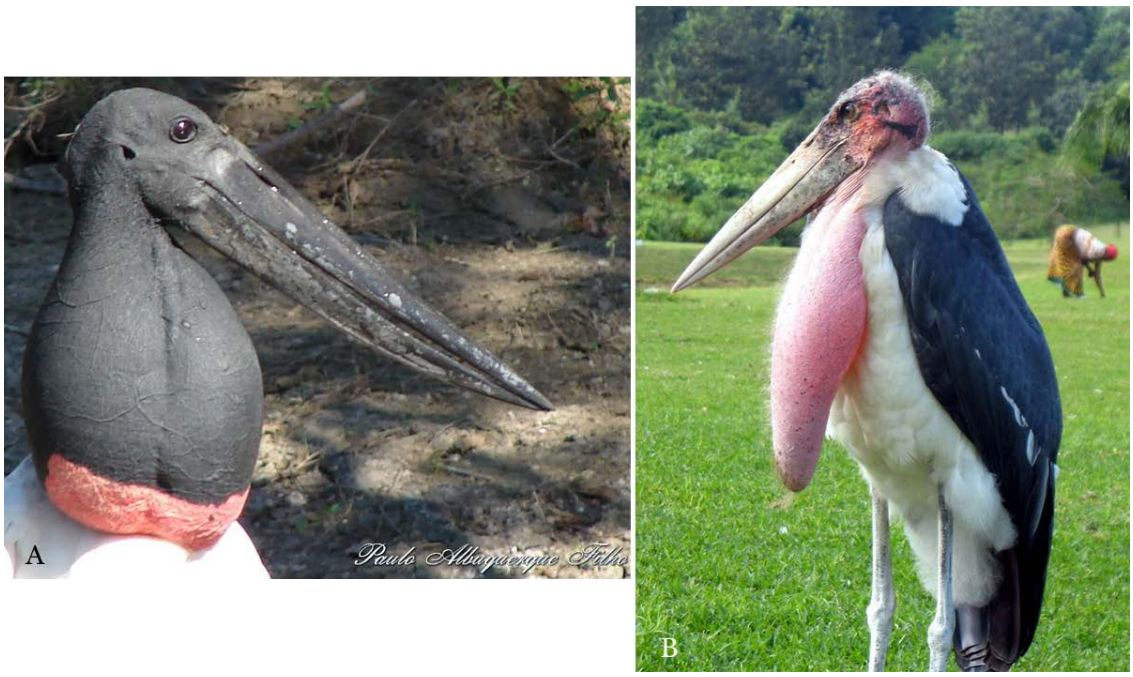

Figure 10. The air sacs of storks: A) Jabiru Stork (*Jabiru mycteria*)[13], B) Marabou Stork (*Leptoptilos crumeniferus*)[14].

[13] photo by Paulo Albuquerque Filho
[14] creepyanimals.com/2013/04/marabou-stork/

Gular vocal sacs

While an enlarged buccal cavity isn't a vocal sac, a gular pouch adapted for inflation might be. That may be what has happened in the Pelicaniformes, possibly twice. The five species of Frigatebird (Fregatidae) have bright red medial air sacs (Figure 10). The flame red is a strong indicator that the sac is used for visual communication as well, and at least the Frigatebird often inflates its sack when not vocalizing at all, as in flight (Figure 10b). In a recent review of the family, Orta (1992) has said this is a gular sac, but it is not clear if this is based on anatomical study. A hundred years earlier Pycraft (1910) identified this as a cervical air sac, which is almost certainly not true. Given that the bird can maintain inflation with its mouth open (Figure 10a), it must have a constriction which, unless it has a tracheal origin, actually makes this an esophageal air sac that inflates under the skin of the gular region.

Figure 11. The vocal sac of the Magnificent Frigatebird (*Fregata magnificens*). A) with mouth agape B) in flight.[15]

[15] Photos by Gerrit Vyn.

The African pink-backed pelican (*Pelecanus rufescens*, Figure 12) has been reported to use its gular pouch to produce sounds. “The inflated pouch may be flapped from side to side, this movement being likewise accompanied by a blowing sound and the mandibles may be widely spread, revealing the red interior of the pouch. (Serle, 1943).” It isn’t clear if these are vocal sounds or if these are blowing created at the gular pouch itself. Without more information this candidate vocal sac gets only an honorable mention.

Figure 12. Gular pouch of the Pink-backed Pelican (*Pelecanus rufescens*) [16].

[16] "Pink backed Pelican (Pelecanus rufenscens)" photo by Anette Mossbacher http://anettemossbacher.com, licensed under CC BY-NC-ND 3.0

Unknown anatomy and suspect sacs

Air sacs can be quite hard to discern beneath neck and breast plumage so many other taxa may still be hiding them from biologists. At minimum there have been suggestions that both the Pectoral Sandpiper (*Calidris melanotos*) and the African Rail (*Rallus caerulescens*) may have sacs (Chapin, 1922) and both have acoustic displays that are consistent with this early observation.

One of the most exaggerated examples of feather-covered inflation is seen in Kakapo (*Strigops habroptilus*), a critically endangered flightless parrot from New Zealand. Already the largest parrot in the world, during their booming display (Figure 13) they seem to double their body size as part of their rarely-witnessed display (Merton, 1999, Cockrem 2002). The anatomy of this vocal sac is unknown, or at least unpublished.

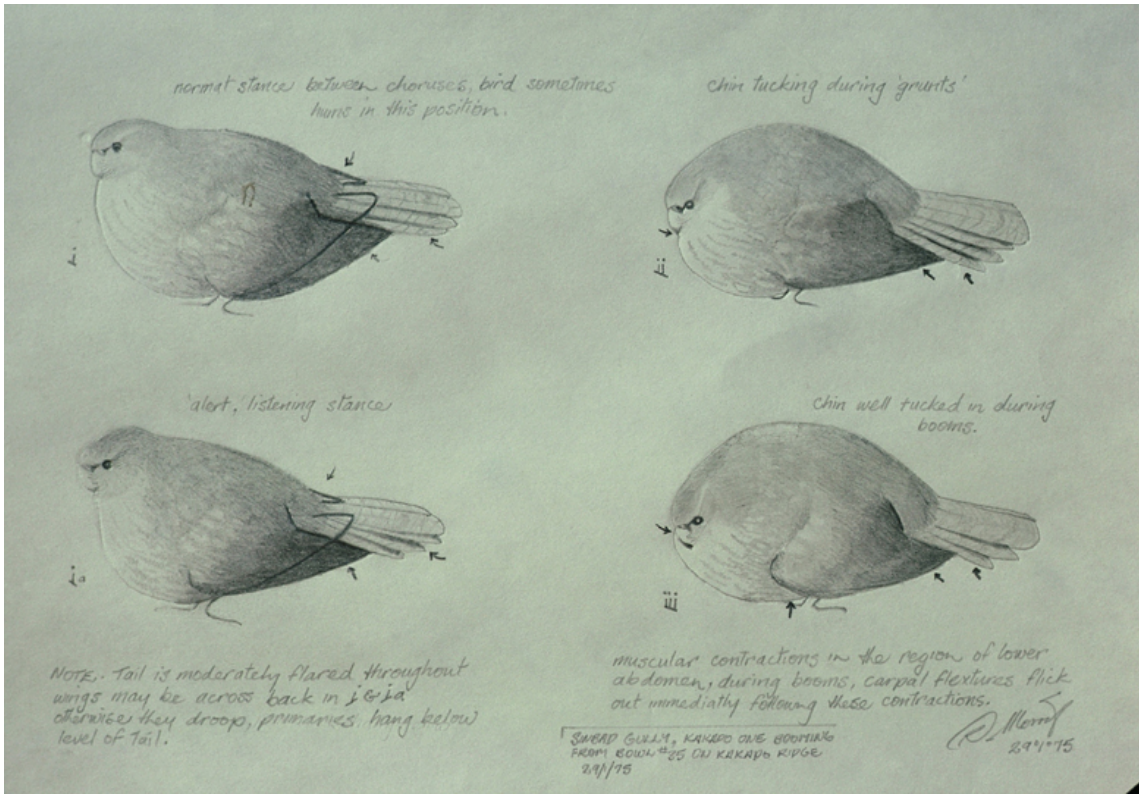

Figure 13. Illustration of the booming display of the Kakapo (*Strigops habroptilus*).[17]

[17] by Don Merton. Used by permission from Department of Conservation, New Zealand kakaporecovery.org.nz/breeding

VOCAL SAC FUNCTIONS

The air sacs profiled in this review are all proposed to be used in sound production, which is why I have lumped them in the functional category of vocal sac. However, the actual role that each inflated structure plays in the production of acoustic signals remains mostly unstudied for almost all of these examples.

In this section, I will lay out the roles that air sacs could play in an acoustic system. For each function I will note where research has attributed this function to the vocal sacs of individual species. I will also propose hypotheses where logical links can be drawn. While we will continue to focus on birds, we will add mammals and frogs back into our discussion since lessons from these other taxa can inform our understanding of birds.

Breathing for Sound Production

In frogs, the vocal sac plays a critical non-acoustic role in the production of the acoustic signal. Frogs lack a diaphragm so they inhale slowly by gulping air and pumping it into their lungs using the musculature of their mouths (De Jongh & Gans, 1969). Without a vocal sac to retain the air and strain energy in an elastic structure between exhalations, frogs would have a much slower maximum call rate at a much higher energetic cost (Ryan, 1985; Dudley & Rand, 1991; Jaramillo et al., 1997). Without vocal sacs, frogs would be as soft-spoken as salamanders.

Birds have a far more capable respiratory system. There is no evidence that any avian vocal sac serves this air-storage return-reserve function as it does for frogs.

Chamber resonance

Sets of natural resonant frequencies result from the size, shape, and constrictions of the vocal tract. Introduced vibrations that match the resonant peaks of the vocal tract will experience a relative gain while others will be selectively filtered out. The addition of any air filled space can alter the resonant spectrum of the vocal tract and change the character of the voice. This is the explanation of the effects of opening and closing the beak (Westneat et al., 1993). Experimental manipulations of beak gape led to a mismatch between this filter and syringeal output, and the result was less tonal sound (Hoese et al., 2000). Later studies have questioned whether the beak actually changes resonance, or if it just attenuates higher frequencies (Nelson et al., 2005). Attention has recently turned to spaces in the upper vocal tract such as the oropharyngeal-esophageal cavity (Riede et al. 2006), and restrictions at the larynx (Riede et al., 2004) that seem to actually change tracheal resonance frequencies (Fletcher et al. 2005).

For larger birds with lower frequency calls, the vocal tract resonance can be changed with chambers such as the bullae in ducks (King, 1989) or tracheal lengthening of cranes as discussed earlier. For the lower frequency vocalizations of larger birds, modifications to resonance by secondary structures like this affect formant dispersal and shape the richness of the voice. This is still chamber resonance, but the effect of the resonance on the signal probably arises for distinct reasons (Fitch, 1999).

Can the addition of a “balloon” change the resonant properties of the vocal tract? Certainly the size and shape of the airway are changed with inflation of such a sac, and this in turn should result in a change in the resonant peaks. However, there is some doubt whether a flexibly walled sac can act as an efficient chamber resonator

because so much sound energy is transferred across the membrane that there is insufficient overlap of successive vibrations, which is required to amplify or attenuate particular frequencies (Watkins et al., 1970; Bradbury & Vehrencamp, 2011). When a frog, for example, is made to vocalize in a helium atmosphere as an assay for this kind of resonance, there is no evidence that the vocal sac plays a significant role (Capranica and Moffat, 1983; Rand and Dudley, 1993). In doves, the resonance of the vocal sac doesn't change as the volume of the chamber increases as it should if the resonance of the chamber is serving as an amplifier or filter (Reide et al., 2004).

That the vocal sac of frogs and doves does function for selective chamber resonance does not necessarily mean that air sacs in other taxa are incapable of such sound modification. If chamber resonance is a factor, it is likely to be at higher frequencies or with thicker air sac walls. Perhaps this is the case for Bitterns. It is also possible that chamber resonance is more important for species that hold their vocal sacs at a constant volume while they vocalize such as storks, ostriches, and emus.

Selective radiation and coupling

In most birds, internally produced sound is transmitted to the surrounding medium through the nose or mouth. This seemingly simple process is complicated by the impedance mismatch between the airway aperture and the open air environment. Depending on the shape of the aperture, much of the sound may actually be reflected back into the vocal tract. One way that animals can avoid such transference problems is to pass the sound through a membrane which has an intermediate impedance value (Bradbury and Vehrencamp, 2011). An inflated air sac can have a more favorable impedance match with surrounding air, and therefore be able to transfer sound energy to

the environment more efficiently.

This type of trans-membrane sound transfer has another effect, since the membranes themselves will act as Helmholtz resonators with their own resonant frequencies. The precise nature of the frequency dependence is determined by the size, shape, and micro-anatomical makeup of the membrane tissue. In so much as these air sac walls can be tuned, it is likely that selection will bring the natural resonant frequencies of membranes in line with important components of species-specific vocalizations. That is exactly what seems to have occurred in the frogs and doves.

Purgue (1997) showed that various anurans have membrane transfer functions with peaks that are aligned with key components of species-specific vocalizations. The anuran vocal sac is an important selective resonator; but it is the transfer function of the membrane that matters, not that of the chamber. This helps to explain how such small animals can make such low frequency sounds so loudly. The same measurements that ruled out chamber resonance for the dove vocal sac showed just how important this membrane resonance could be. The dove's vocal sac actually amplified the fundamental frequency by transferring the energy from the higher frequencies into the fundamental (Riede et al., 2004).

While no formal studies have been made on the Siamang vocal sac, it appears to illustrate this phenomenon perfectly since, unlike frogs, these apes vocalize both with their mouths shut and open. The boom call, made with the mouth shut is nearly tonal near the resonant frequency of the vocal sac membrane (Riede et al., 2008). In contrast, when the mouth is opened, even with the vocal sac inflated, vocalizations are rich in harmonic content (personal obs.). The same differences between open mouthed and

vocal sac inflating vocalizations holds for both the Lesser and Greater Prairie-Chickens (*Tympanuchus pallidicinctus* and *T. cupido*) (personal obs.).

Selective radiation and coupling might be an important feature of air sacs in many birds, specifically those that inflate their vocal sac while vocalizing such as the Kakapo and some elements of the Greater Sage-Grouse strut display. It is not clear if this could be a factor in species that limit inflation to calling, but rather exhibit inflated balloons for long quiet periods as do the Frigatebirds and Storks.

Rapid modulation of resonance

Rapid changes in sac volume or shape might also cause fluctuations in resonance effects and thus create qualitatively novel sounds. Such an effect is likely to be found in animals that use their sacs in a dynamic fashion such as both species of Sage Grouse (*Centrocercus spp*.) or the Bare-Necked Umbrellabird (*Cephalopterus glabricollis*). Through rapid body movements and muscle contractions, these birds modify the shape of their vocal sacs wildly during display, creating rapid changes in the shape of the sac, which might alter chamber resonant profiles. At least in Sage Grouse, this also modulates the size and thickness of tympanic portion of the membrane, which could affect its resonance profile. The bare-necked umbrellabird has a fleshy projection attached to the middle-bottom of its air sac (Crandall, 1945) that might serve as a weight to help modulate the resonance.

Directionality

Air sacs that are used to couple sound to the environment have the potential to modify more than just the frequency composition of those sounds. This mode of radiation also alters the shape of the sound field significantly. An animal that relies on expired air to carry the pressure waves from its mouth or beak into the environment will have an acoustic field generally biased forwards. The intensity of the waves will be much greater in line with the opening, and have frequency-dependent lobes of lower intensity to the sides and rear (Patricelli et al. 2007). In contrast, a single air sac emitting sound will likely act as an acoustic monopole where pressure waves are of nearly equal intensity in all directions. This is generally what has been found in anurans with a single vocal sac (Gerhardt, 1975).

It is less clear what pattern would be radiated from paired sacs since two nearby radiators could generate interference. This type of interference has been demonstrated for horseshoe and leaf-nosed bats that emit sounds for both nares (Thomas et al. 2002). It is possible that paired vocal sacs, such as those in grouse, may create interference patterns that, depending on the distance between the sacs, frequencies, and phase differential between the sacs. This could lead to directional sound fields that may be advantageous for communication. Bradbury (personal communication) has suggested that components of the vocalization of the Greater Sage-Grouse are less apparent head-on. If this is confirmed, it might be due to this type of interference.

Acoustic directionality may be a hidden factor in many species. Patricelli and colleagues (including myself) have found adaptive differences in directionality between vocalization types in songbirds (Partrcelli et al. 2007; Yorzinski & Patricelli 2010).

Moreover, Frey (2007) suggested that the vocal system of the reindeer allows for sideways projection for 'broadside acoustic display.' Neither of these examples include vocal sacs, but as argued above, species with multiple sacs may indeed prove to have unusual sound fields as a result.

Percussion

In some cases, air sacs may serve not only in the modification of syringeally produced sounds, but also in the production of novel vibrations. Vocal sacs are clearly used as drums to be struck with the bill in male ruddy ducks and the hands in gorillas. The bare-necked umbrellabird shakes its body from side to side, and the fleshy projection on its vocal sac slaps rhythmically back and forth against the inflated sac to produce a drumming sound (Crandall, 1945). In the sage grouse there are no projections to bang against the inflated air sacs. Instead, the paired air sacs are slapped against each other, possibly producing the loud "pop" components of the display. These may be examples of percussion but it is important to bear in mind that the sound produced by percussion may not be the primary reason for the behavior. Rather, the behavior might serve more to start rapid movement of the air sac membrane to lead to the dynamic modulation of resonant and/or consequent radiation patterns.

In other species percussion is adjacent to a constantly inflated air sac, such as beak clattering in Storks and Frigatebirds. In these cases the air sac might ring in response to the percussion.

Conclusions

Evolutionary biologists see convergence as a signpost for adaptation. The vocal sac appears to be an excellent example of such convergent evolution given that it has evolved independently at least eight times in birds. However, the complexity and diversity of the ways that vocal sacs are used, and the different physical processes that seem to be invoked in different species, suggest that considerably more research on different vocal sac systems will be needed to determine whether this, and other secondary acoustic structures in birds, follow common rules.

Acknowledgements

Chapter 1, in part, is based upon a conference proceeding published in Vocal sacs and their role in avian acoustic display in Acta Zoologica Sinica 2006. Dantzker, Marc; Bradbury, Jack W. 2006. The dissertation author was the primary investigator and author of this paper.

REFERENCES CITED

Baptista, L.F. 1997. Order Columbiformes. Pages 60-243 *in Handbook of the birds of the world. Volume 4. Sandgrouse to Cuckoos*. (J. del Hoyo, A. D. Elliott, and J. Sargatal, Editors). Lynx Edicions, Barcelona, Spain.

Beckers, G. J. L., R. A. Suthers, and C. ten Cate. 2003. Pure-tone birdsong by resonance filtering of harmonic overtones. *Proceedings of the National Academy of Sciences of the United States of America* **100**, 7372–7376.

Berland, B. 1966. The hood and its extrusible balloon in the hooded seal - *Cystophora cristata* Erxl. *Norsk Polarinstitutt Arbok* **1965**, 95–102.

Bostwick, K. S. 2000. Display behaviors, mechanical sounds, and evolutionary relationships of the Club-winged Manakin (*Machaeropterus deliciosus*). *Auk* **117**, 465–478.

Bostwick, K. S. & Prum, R.O. 2005. Courting bird sings with stridulating wing feathers. *Science* **309** (5735) 736-736.

Bradbury, J. W. & Vehrencamp, S. L. 2011. *Principles of animal communication, 2nd edition*. Sunderland, MA: Sinauer Associates.

Capranica, R. R., Moffat, A. J. M. 1983. Neurobehavioral correlates of sound communication in anurans. In: Ewert J. P., Capranica R. R., Ingle D. J. ed. *Advances in Vertebrate Neuroethology*. New York: Plenum Press, 701–730.

Chapin, J. P. 1922. The function of the oesophagus in the bittern's booming. *Auk* **39**, 196-202

Clark, C. J. & Fe, T. J. 2008. The Anna's Hummingbird Chirps with Its Tail: A New Mechanism of Sonation in Birds**.** *Proceedings: Biological Sciences*. **275** (1637) 955-962.

Clark, C.J., Elias, D.O., Prum, R.O. 2013. Hummingbird feather sounds are produced by aeroelastic flutter, not vortex-induced vibration. *Journal of Experimental Biology,* **216** (18) 3395-3403.

Cockrem, J. F. 2002 Reproductive biology and conservation of the endangered kakapo (*Strigops habroptilus*) in New Zealand. *Avian And Poultry Biology Review. **13**(3) 139-144.*

Collar, N. J. 1996. Family Otididae (Bustards). Pages 240–273 *in Handbook of the birds of the world. Volume 3. Hoatzin to auks*. (J. del Hoyo, A. D. Elliott, and J. Sargatal, Editors). Lynx Edicions, Barcelona, Spain.

Crandall, L. S. 1945. The umbrella bird is not a dull fellow any more. *Animal Kingdom* **48**, 109–112.

Dantzker, M. S., Deane, G. B., Bradbury, J. W. 1999. Directional acoustic radiation in the strut display of male sage grouse, Centrocercus urophasianus. *Journal of Experimental Biology* **202**, 893–909.

Dantzker, M. S. and J. W. Bradbury. 2006. Vocal sacs and their role in avian acoustic display. *Acta Zoologica Sinica* **52**(Suppl): 486–488.

De Jongh, H.J. & Gans, C. 1969. On the mechanism of respiration in the bullfrog, *Rana catesbeiana:* A reassessment. *Journal of Morphology*. **127***,* 259–290.

Duellman, W. E. & Trueb L. 1994 *Biology of Amphibians*. *Chapter 4: Vocalization*. Baltimore: The Johns Hopkins University Press.

Fitch, W. T. and M. D. Hauser. 1995. Vocal production in nonhuman primates - acoustics, physiology, and functional constraints on honest advertisement. *American Journal of Primatology***,** 191–219.

Fitch, W. T. 1997. Vocal tract length and formant frequency dispersion correlate with body size in rhesus macaques. *Journal of the Acoustical Society of America* **102**, 1213–1222.

Fitch, W. T. 1999. Acoustic exaggeration of size in birds via tracheal elongation: comparative and theoretical analyses. *Journal of Zoology* **248**, 31–48.

Fitch, W. T. 2000. The phonetic potential of nonhuman vocal tracts: Comparative cineradiographic observations of vocalizing animals. *Phonetica* **57**: 205–218.

Fitch, T. & Hauser, M. D. 2003. Unpacking "honesty": vertebrate vocal production and the evolution of acoustic signals. In *Acoustic Communication* (A. Simmons, R. R. Fay, and A. N. Popper, eds.), pp. 65–137. New York: Springer.

Fitch, W. T. 2010. *The evolution of language.* Cambridge: Cambridge University Press.

Fletcher, N. H., 1992. *Acoustic systems in biology*. New York: Oxford University Press.

Fletcher, N. H. & Tarnopolsky, A. 1999. Acoustics of the avian vocal tract, *Journal of the Acoustical Society of America,* **105**, 35-49.

Fletcher, N. H., T. Riede, and R. A. Suthers. 2006. Model for vocalization by a bird with distensible vocal cavity and open beak. *Journal of the Acoustical Society of America* **119**, 1005–1011.

Folch, A. 1992. Order Struthioniformes. Pages 75-110 *in Handbook of the birds of the world. Volume 1. Ostrich to Ducks*. (J. del Hoyo, A. D. Elliott, and J. Sargatal, Editors). Lynx Edicions, Barcelona, Spain.

Frey, R., Gebler, A. & Fritsch, G. 2006. Arctic roars - laryngeal anatomy and vocalization of the muskox (*Ovibos moschatus* Zimmermann, 1780, Bovidae). *Journal of Zoology* **268**, 433–448.

Frey, R., Gebler, A. 2010 Mechanisms and evolution of roaring-like vocalization in mammals. In. Brudzynski, S. M. ed. *A Handbook Of Mammalian Vocalization: An Integrative Neuroscience Approach*, Series, *Handbook of Behavioral Neuroscience* **19**, 439-450.

Gamba, M., Friard, O. & Giacoma, C. 2012. Vocal Tract Morphology Determines Species-Specific Features in Vocal Signals of Lemurs (Eulemur), *International Journal of Primatololgy,* **33**, 1453–1466.

Gautier, J. P. 1971. Etude morphologique et fonctionnelle des annexes extra- laryngées des cercopithecineae; liaison avec les cris d'espacement. *Biologica Gabonica* **7**, 230–267.

Gaunt, A. S., Gaunt, S. L. L., & Hector, D. H. 1976. Mechanics of the syrinx in Gallus gallus. I. A comparison of pressure events in chickens to those in oscines. Condor **78**, 208–223.

Gerhardt, H.C. 1975. Sound pressure levels and radiation patterns of the vocalizations of some North American frogs and toads. J. Comp. Physiol. **102**, 1–12.

Goller, F. & Larsen, O. N. 1997. A new mechanism of sound generation in songbirds. Proceedings of the National Academy of Sciences of the United States of America **94**, 14787–14791.

Goller, F. & Larsen O. N. 2002. New perspectives on mechanisms of sound generation in songbirds. Journal of Comparative Physiology A-Neuroethology Sensory Neural and Behavioral Physiology **188**, 841–850.

Greenwalt, C. H. 1968. *Bird Song: Acoustics and Physiology*. Washington, D.C.: Smithsonian Institution.

Hellmich J. 1988. Zum Balz-verhalten der Riesentrappe (*Ardeotis kori*). *Zool Garten NF*. **58**, 345–352.

Hewitt, G., MacLarnon, A., & Jones, K. E. 2002. The functions of laryngeal air sac in primates: A new hypothesis. *Folia Primatologica*, **73**, 70–94.

Hill, W. C. O. & Booth, A. H. 1957**.** Voice and Larynx in African and Asian Colobidae. Journal of the Bombay Natural History Society **54**, 309–321.

Hjorth, I. 1970. Reproductive behavior in Tetraonidae with special reference to males. *Viltrevy* **7**, 381–587.

Hoese W. J., Podos J., Boetticher N. C., Nowicki S., 2000. Vocal tract function in birdsong production: experimental manipulation of beak movements. Journal of Experimental Biology **203**, 845–855.

Jaramillo, C., Rand, A. S., Ibanez, R., & Dudley, R. 1997. Elastic structures in the vocalization apparatus of the Tungara frog *Physalaemus pustulosus* (Leptodactylidae). *Journal of Morphology* **233**, 287–295.

Jensen, K. K., Cooper B. G., Larsen, O. N. & Goller, F. 2007. Songbirds use pulse tone register in two voices to generate low-frequency sound. Proceedings of the Royal Society B-Biological Sciences **274**, 2703–2710.

Johnsgard, P. A. 1965. *Handbook of Waterfowl Behavior*. Ithaca, NY: Comstock Publishing Associates.

Johnsgard, P. A. & Carbonell, M. 1996. *Ruddy Ducks and Other Stifftails*. Norman, OK: University of Oklahoma Press.

Kelemen, G. 1963. Comparative anatomy and performance of the vocal organ in vertebrates. In *Acoustic Behaviour of Animals* (R.-G. Busnel, ed.), pp. 489–521. Amsterdam: Elsevier Publishing Company.

King, A. S. 1989. Functional anatomy of the syrinx. In *Form and Function in Birds, Vol. 4* (A. S. King and J. McLelland, eds.), pp. 105–192. New York: Academic Press.

Krakauer, A. H., M. Tyrrell, K. Lehmann, N. Losin, F. Goller, and G. L. Patricelli. 2009. Vocal and anatomical evidence for two-voiced sound production in the greater sage-grouse Centrocercus urophasianus. Journal of Experimental Biology **212**, 3719–3727.

Larsen, O. N. and F. Goller. 1999. Role of syringeal vibrations in bird vocalizations. Proceedings of the Royal Society of London Series B-Biological Sciences **266**, 1609–1615.

Larsen, O. N. and F. Goller. 2002. Direct observation of syringeal muscle function in songbirds and a parrot. Journal of Experimental Biology **205**, 25–35.

Larsen, O. N., F. Goller, and J. L. van Leeuwen. 2006. Aspects of syringeal mechanics in avian phonation. Acta Zoologica Sinica **52**(Suppl) 478–481.

Lichtenberg, E. & Hallager, S. 2007. A description of commonly observed behaviors for the Kori Bustard (*Ardeotis kori*). *Journal of Ethology*. **26**(1) 17-34.

Mack A.L. & Jones J. 2003. Low-Frequency Vocalizations By Cassowaries (*Casuarius* Spp.). *Auk* 120: 1062.

McLelland, J. 1989. Larynx and trachea. In *Form and Function in Birds, Vol. 4* (A. S. King and J. McLelland, eds.), pp. 69–103. New York: Academic Press.

Mergell P, Herzel H, 1997. Modeling biphonation — the role of the vocal tract. Speech Commun. **22**, 141–154.

Merton, D.V. 1999 Kakapo in: HIGGINS, P.J. (Ed.) Handbook of Australian, New Zealand and Antarctic birds, pp. 633-646 (Melbourne, Oxford University Press).

Murie, J. 1867. On the tracheal pouch of the Emu (*Dromaeus novaehollandiae*). Proceedings of the Zoological Society of London **35**, 405–415.[18]

Negus, V. E. 1949. *The Comparative Anatomy and Physiology of the Larynx*. New York: Hafner Publishing Company.

Nelson, B. S., Beckers, G. J. L. & Suthers,R. A. 2005. Vocal tract filtering and sound radiation in a songbird. *Journal of Experimental Biology*. **208**, 297-308.

Nishimura, T., Mikami, A., Suzuki, J. & Matsuzawa, T. 2007 Development of the Laryngeal Air Sac in Chimpanzees, *International Journal of Primatology*, **28**, 483-492.

Nowicki, S. & Capranica, R. 1986. Bilateral syringeal interaction in vocal production of an oscine bird sound. *Science* **231**, 1297–1299.

Nowicki S, 1987. Vocal tract resonances in oscine bird sound production: evidence from birdsongs in a helium atmosphere. *Nature*. **325**, 53–55.

Orta, J. 1992. Family Fregatidae (Frigatebirds). Pages 362-374 *in Handbook of the birds of the world. Volume 1. Ostrich to Ducks*. (J. del Hoyo, A. D. Elliott, and J. Sargatal, Editors). Lynx Edicions, Barcelona, Spain.

Patricelli, G. L., Dantzker, M. S. & Bradbury, J. W. 2007. Differences in acoustic directionality among vocalizations of the male red-winged blackbird (*Agelaius pheoniceus)* are related to function in communication. *Behavioral Ecology and Sociobiology*. **61**, 1099–1110.

Podos J., 2001. Correlated evolution of morphology and vocal signal structure in Darwin's finches. *Nature*. **409**, 185–188.

[18] Rare text online at
http://archive.org/stream/proceedingsofzoo1867zool/proceedingsofzoo1867zool_djvu.txt

Purgue A. P., 1997. Tympanic sound radiation in the bullfrog *Rana catesbeiana*. *Journal of Comparative Physiology A* **181**, 438–445.

Rand A. S., Dudley R., 1993. Frogs in helium: the anuran vocal sac is not a cavity resonator. *Physiological Zoology* **66**, 793–806.

Raven, H. C. 1950. *The Anatomy of the Gorilla*. Columbia University Press, New York.

Riede T., Herzel H., Mehwald D., Seidner W., Trumler E., Böhme G., Tembrock G., 2000. Nonlinear phenomena in the natural howling of a dog-wolf mix. Journal of the Acoustical Society of America. **108**, 435–442.

Riede, T. & Zuberbühler, K. 2003. Pulse register phonation in Diana monkey alarm calls. *Journal of the Acoustical Society of America*. **113**, 2919-2926.

Riede, T., Bronson, E., Hatzikirou, H. & Zuberbühler, K. 2004. Vocal production mechanisms in a non-human primate: morphological data and model. *Journal of Human Evolution*, **48**, 85-96.

Riede, T., Suthers, R. A., Fletcher, N. H. & Blevins W. E. 2006. Songbirds tune their vocal tract to the fundamental frequency of their song. *Proceedings of the National Academy of Sciences of the United States of America* **103**, 5543–5548.

Riede, T., Tokuda, I. T., Munger, J. B. & Thomsom, S. L. 2008. Mammalian laryngseal air sacs add variability to the vocal tract impedance: Physical and computational modeling. *Journal of the Acoustical Society of America*. **124** (1) 634-647.

Ryan, M.J. 1985. *The Túngara Frog: A Study of Sexual Selection and Communication*. Chicago: University of Chicago Press.

Ryan M. J., 1988. Energy, calling and selection. *American Zoologist,* **28**, 885–898.

Salmi, R., Hammerschmidt, K. & Doran-Sheehy, D. M. 2013. Western Gorilla Vocal Repertoire and Contextual Use of Vocalizations, *Ethology* **119**, 831–847.

Schneider, R. 1964. Der Larynx der Säugetiere (The larynx of mammals), Handbuch der Zoologie **5**, 1–128.

Serle W., 1943. Further field observations on northern Nigerian birds. *Ibis* **85**: 264–300.

Sick, H. (1954) Zur Biologie des amazonischen Schirmvogels, *Cephalopterus ornatus. Journal ffir Ornithologie* **95**, 233-244

Starck, D. & Schneider, R. 1960 Respirationsorgane A. Larynx. *Primatologia* **3**, 423–587.

Suthers, R. A., Goller, F., & Pytte, C. 1999. The neuromuscular control of birdsong. *Philosophical Transactions of the Royal Society of London Series B- Biological Sciences* **354**, 927–939.

Suthers, R. A. and D. H. Hector. 1982. Mechanism for the production of echolocating clicks by the grey swiftlet, Collocalia spodiopygia. Journal of Comparative Physiology A-Neuroethology Sensory Neural and Behavioral Physiology **148**, 457–470.

Thomas, J. A., Moss, C. F., & Vater, M. (eds). 2002. *Echolocation in Bats and Dolphins*. Chicago IL: The University of Chicago Press.Tyler,

M. J. 1971. The phylogenetic significance of vocal sac struc- ture in hylid frogs. *University of Kansas publications, Museum of Natural History* **19**, 319 – 360.

Tyler, M. J. 1972. Superficial mandibular musculature, vocal sacs and the phylogeny of Australo-Papuan leptodactylid frogs. *Records of the South Australian Museum* **16**, 1–20.

Tyler, M. J. & Duellman, W. E. 1995, Superficial mandibular musculature and vocal sac structure in hemiphractine hylid frogs. *Journal of Morphology* **224**, 65–71.

Watkins W. A., Baylor E. R., Bowen A. T., 1970. *The call of Eleutherodactylus johnstonei, the whistling frog of Bermuda*. Copeia 3: 558–561.

Westneat M. W., Long J. H. J., Hoese W., Nowicki N., 1993. Kinematics of birdsong: functional correlation of cranial movements and acoustic features in sparrows. J. Exper. Biol. 182: 147–171.

Wetmore, A. 1917. On certain secondary sexual characteristics in the male Ruddy Duck, *Proceedings of the United States National Museum*. **52,** 479-482.

Wetmore, A. 1918. A Note on the Tracheal Air-Sac in the Ruddy Duck. *The Condor*, **20**, 19-20.

Weissengruber, G. E., Forstenpointner, G., Peters, G., Kubber-Heiss, A., & Fitch, W. T. 2002. Hyoid apparatus and pharynx in the lion (*Panthera leo*), jaguar (*Panthera onca*), tiger (*Panthera tigris*), cheetah (*Acinonyx jubatus*) and domestic cat (*Felis silvestris f. catus*). *Journal of Anatomy* **201**, 195–209

Yorzinski, J. L. & Patricelli, G. L. 2010. Birds adjust acoustic directionality to beam their antipredator calls to predators and conspecifics. *Proceedings of the Royal Society B-Biological Sciences* **277**, 923–932.

CHAPTER 2:

Environmental Acoustics of Near Ground Communication: Acoustic adaptation and the Greater Sage-Grouse, *Centrocercus urophasianus*

ABSTRACT

Environmental effects on propagating sound can drive signal evolution but our restricted understanding of the physics of acoustic degradation hampers our efforts to understand the nature and degree of this acoustic adaptation. Here we present a model of transmission loss in near-ground non-reverberative environments. This model allows us to understand and predict the effects of changing habitat or of source-receiver geometry on frequency-dependent transmission loss; however, one major question is whether there is sufficient physical theory to predict propagation in a specific context, or whether direct measurement is the only option. Here we extend the classical models of sound propagation near the ground, estimate the relative parameters, and compare model predictions of sound propagation across a Greater Sage-Grouse lek to direct measurements. We find that our three-component model adequately predicts propagation on the lek but within a limited frequency range and temperature regime. While this model may have limited applicability, invoking it suggested solutions to several puzzling behaviors of the grouse on the leks. We thus see the combined use of appropriate models and direct measurements as the best research strategy.

INTRODUCTION

It's not what's said, but what's heard that is communicated. Sound is degraded by the environment through which it propagates, often making what is heard significantly different from what is said. When the fidelity or range of the message is important, the environment can exert selection on senders to account for degradation patterns in their signaling behavior. Patterns of acoustic degradation can vary with habitat, time of day, and the relative positions of the sender and receiver (Embleton, 1996). Signaling behavior can be shaped by these environmental effects whenever a population experiences predictable, or predictably variable, patterns of acoustic degradation. All aspects of acoustic signaling behavior can be affected, including the temporal and frequency properties of the vocalizations, as well as where and when those sounds are broadcast.

The degree to which acoustic communication is shaped by the propagation environment has been of broad interest since Morton proposed that differences between the frequencies used in songs of birds that live in different habits are due to habitat-specific degradation (attenuation) (Morton, 1975). This seminal work was followed by studies of Marten and Marler suggesting that singing perch height plays an even more significant role on acoustic degradation than does overall habitat structure (Marten & Marler, 1977; Marten et al., 1977). The methodologies of these early studies, as well as the generality of their conclusions, have been justifiably criticized (Wiley & Richards, 1978; Roberts et al., 1979; Roberts et al., 1981; Wiley & Richards, 1982). However, the basic findings of this collective work, that both habitat type and microhabitat

selection can shape acoustic communication, are now supported by the results of many studies (Bradbury and Vehrencamp, 2011).

This hypothesis, sometimes referred to as the Acoustic Adaptation Hypothesis (Morton, 1975; Hansen, 1979; Rothstein & Fleischer, 1987; Wiley, 1991)**,** has been investigated with varied results across a broad suite of taxa and habitats (Boncoraglio & Saino 2007, Bradbury and Vehrencamp, 2011). While the results of some of these studies have generally agreed with this hypothesis (Hansen, 1979; Hunter & Krebs, 1979; Gish & Morton, 1981; Lemon et al., 1981; Shy 1983; Cosens & Falls, 1984; Anderson & Conner, 1985; Ryan & Brenowitz, 1985; Sorjonen, 1986; Handford, & Lougheed, 1991; Wiley, 1991; Dabelsteen et al., 1993; Tubaro & Segura, 1994; Mathevon et al., 1996; Badyaev & Leaf, 1997; Crawford et al.,1997; Mitani & Stuht, 1998; Doutrelant &Lambrechts, 2001; Nemeth et al., 2001; Balsby et al., 2003; Lugli et al., 2003; Nelson, 2003; Christie et al., 2004; Couldridge & van Staaden, 2004; Kopuchian et al., 2004; Patton et al., 2004; Mathevon et al., 2004; Nicholls & Goldizen, 2006; Sugiura et al., 2006; Tubaro & Lijtmaer, 2006), others have failed to find convincing evidence that species specific sounds have been shaped by environmental effects (Lougheed & Handford, 1992; Williams & Slater, 1993; Daniel & Blumstein, 1998; Penna & Solis, 1998; Kime et al., 2000; Brown & Handford, 2000; Sueur & Aubin, 2003; Blumstein & Turner, 2005; Saunders & Slotow, 2004; Boncoraglio & Saino, 2007; Jain & Balakrishnan, 2o12). Some of the variation in these results is due, not to differences in the response of signaling behavior to environmental selection, but to differences in either the scale or methodology of the investigations. Progress has been hampered by a dearth of understanding of sound propagation physics and the lack

of suitably complex yet usable models of sound propagation in the environment. In this study, we examine the acoustic environment of a Greater Sage-Grouse lek using a combination of *in situ* measurements and acoustical modeling.

During the mating season, the male Greater Sage-Grouse (*Centrocercus urophasianus*) of Mono county California gather mostly on alkali flats to strut for females. The alkali flats are indeed quite flat and, owing to their inhospitable soil, are free of standing vegetation. The relative homogeneity of this habitat makes it reasonable to develop an acoustic propagation model. Both the dancing males and the searching females are standing on the ground so the dominant feature of the acoustic environment is the ground itself. While this model is explicitly for flat, open habitats, it can be generalized to approximate conditions faced by many other organisms, especially other lekking grouse. In addition, the acoustics of this system are of broad relevance insofar as the ground plays a dominant role in shaping degradation patterns in even more complex and heterogeneous habitats whenever communication occurs near this reflective boundary.

MATERIALS AND METHODS

Field Recordings

All acoustic measurements were made at Lek 8 in Long Valley, Mono County, California, USA (37°40'N, 118°50'W) from April 4 to 21 of 1997, during the period of high display activity. Lek 8, like most of the leks in this region, is located on a mostly flat alkali meadow surrounded by rolling hills of sagebrush. The vegetation on the meadow (*Carex sp.* and saltgrass) was sparse and low.

Our method for the measurement of transmission loss is described in detail in previous work (see Appendices A and B of Dantzker et al., 1999). Therefore, only a brief summary is included here.

The acoustic system had the following components. For a sound source, a Kudelski powered speaker was driven by a Stanford Research DS340 function generator or a recording of the function generator. The receiver channels were Audiotechnica MB1000L microphones coupled to a custom-built amplifier through impedance-matching transformers. We arranged a linear array of microphones along a relatively flat stretch of the lek at 4,6, 8, 12, 16, 24, & 32 meters. The signals were recorded on a TASCAM DA88 digital recorder. The acoustic system was calibrated for its free field response as described in detail previously (Appendix A, Dantzker et al., 1999). Measurements were analyzed as in appendix B of the same publication (Dantzker et al., 1999).

The Model

Figure 1 shows the assumed geometry for the problem of sound propagation when the source and receiver are positioned near flat ground—as are Greater Sage-

Grouse while communicating on an alkali flat. In this simple scenario, the source and receiver are placed in homogeneous air above a uniform half space representing the ground. The calculation of the acoustic field in this situation has been a topic of empirical and mathematical investigation in the acoustics literature since the 1940's (Rudnick, 1947) and a source of confusion in the bioacoustics literature since the 1970's (Roberts et al., 1979; Roberts et al., 1981; Martin, 1981). The mathematical roots of the solution are drawn from investigations of radio wave propagation that date back to the turn of the twentieth century (Sommerfeld, 1909; 1926; Van Der Pol, 1935). The formulation that we present here (and in more detail in the Appendix), is known as the Van Der Pol equation, since it is essentially unchanged from his early formulation. The Van Der Pol equation requires, but does not contain, an acoustical model of the ground. Experimental and theoretical acoustics continue to wrestle with characterizations of the ground. Here we employ a single parameter ground model that has been shown to adequately describe transmission loss over many different types of soils (Embleton et al., 1983).

To develop the complete model of transmission loss on the grouse lek, we first present a didactic explanation of the field components that make up the Van Der Pol equation. We then explain the single parameter model of the ground and its place in the formulation of transmission loss estimation. Finally we present the complete formulation of the Van Der Pol equation and review its utility. These explanations do not constitute a derivation of the Van Der Pol equation and we do not provide one. However a technical discussion of its derivation and theoretical backing are found in the Appendix.

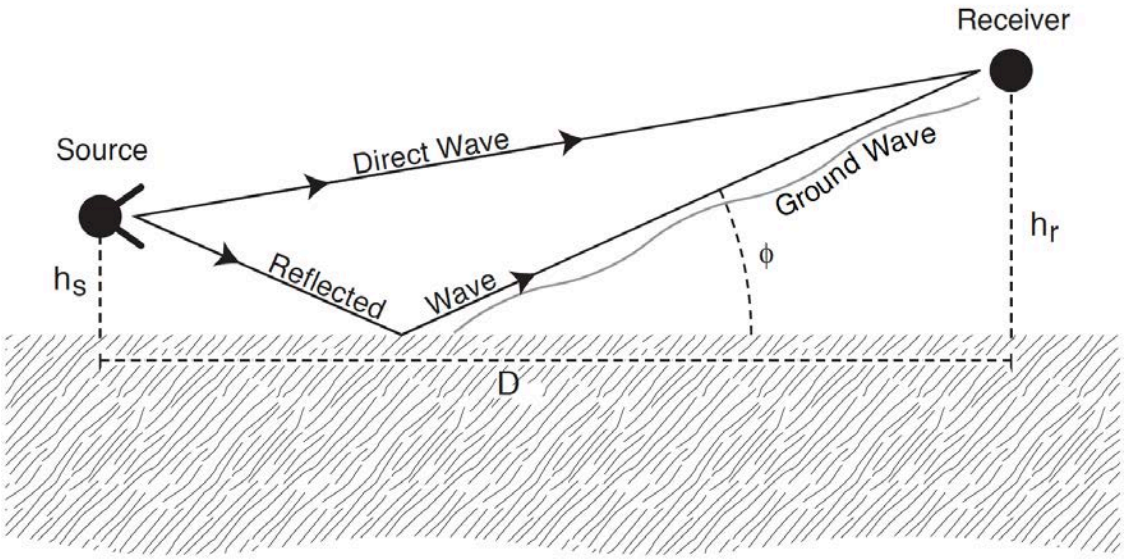

Figure 1. Source-receiver geometry for an acoustic sender and receiver near the ground. Sound source height is h_s. Receiver height is h_s. The distance between the two is given by D which is referred to elsewhere as range.

Components of the Acoustic Field

For the source-receiver geometry of Figure 1, the total acoustic field at the receiver, p_r, can be expressed as the sum of the wavefronts propagated along three paths,

$$p_r = p_d + p_m + p_g \ , \tag{1}$$

where p_d is the direct path pressure, p_m is the specularly reflected pressure, and p_g is the pressure due to ground waves. The last two terms, p_m and p_g, are direct effects of the proximity of the ground and are therefore collectively known as the ground effect[19]. Without other objects to reflect, scatter, or absorb sound, and without impedance profiles in the air or ground, the acoustic degradation, or transmission loss, TL, between the source and receiver can be described as,

$$\mathrm{TL} = \frac{p_r}{p_0} \ , \tag{2}$$

where p_0 is the acoustic pressure generated by the source. If one wishes to calculate a relative measure of transmission loss, as we do later, one can simplify this equation by assuming unity source pressure.

The pressure of the direct wave, p_d, is calculated simply as a spherically spreading wave, inversely proportional to the path length,

$$p_d = \frac{p_o e^{ik_1 r_d}}{r_d} \ , \tag{3}$$

[19] An alternative visualization of this problem, common in the physics and acoustic literature, shows sound propagation along the ground as if every source had a mirrored source image equidistant below the surface of the ground. The source image is then considered the origin of the ground effect. The difference between these representations is strictly pedagogic.

where r_d is the length of the direct path, and k_1 is the wave number in air. The wave number $k_1 = 2\pi f / c_1$ where f is frequency and c_1 is the speed of sound in the air. The length of the direct path, r_d, can be calculated from the more easily measured descriptors of source-receiver geometry, using the Pythagorean theorem. Thus $r_d = \sqrt{(h_r - h_s)^2 + D^2}$, where h_s and h_r are the heights of the source and receiver, and D is the distance between the two along the ground.

The equation for the pressure from the specularly reflected wave, p_m, is very similar to that of the direct wave except that path length is longer and there is an additional term to account for the changes in amplitude and phase that occur on reflection. The reflected wave is

$$p_m = \frac{p_0 e^{ik_1 r_r} R_p}{r_r}, \tag{4}$$

where the length of the reflected path is $r_r = \sqrt{(h_r + h_s)^2 + D^2}$, and R_p is the plane-wave reflection coefficient defined by

$$R_p = \frac{\sin\phi - \frac{Z_1}{Z_2}\sqrt{1 - \left(\frac{k_1}{k_2}\right)^2 \cos^2\phi}}{\sin\phi + \frac{Z_1}{Z_2}\sqrt{1 - \left(\frac{k_1}{k_2}\right)^2 \cos^2\phi}}. \tag{5}$$

Here Z_1 and Z_2 are the specific acoustic impedances of the air and ground respectively, k_2 is the wave number in the ground, ϕ is the angle of incidence,

$$\phi = \tan^{-1}\left(\frac{h_r + h_s}{D}\right),$$

and $Z_1 = \rho_1 c_1$ where ρ_1 is the density of the air. Further explanation of the ground properties, Z_2 and k_2, is best left to our presentation of our ground model below. The plane-wave reflection coefficient is heavily dependent on the angle of incidence and the acoustic properties of the ground. These factors therefore determine the effect of reflection on the amplitude and phase of the reflected wave. The amplitude and phase of this reflected wave combine with the loss due to spherical spreading over the length of its propagation path to determine the contribution of the reflected wave to the resulting sound field.

There is a third component of the sound field, the ground wave, which is often neglected in the bioacoustics literature. Specifically, the sole formal model of sound propagation over the ground previously available in the bioacoustics literature (Roberts et al., 1979) includes only the direct and specularly reflected components, not the ground wave. This omission was the subject of a spirited exchange (Roberts et al., 1981; Martin, 1981). As we will show below, the ground wave can contribute significantly to the field, providing an alternative channel for communication that many animals like the grouse rely on.

The equation for the specularly reflected wave, equation 4 above, is for plane waves. The ground wave can't be dealt with in the same way. Since most natural sound sources, and all animals, produce waves that are mostly spherical not planar, we must account for the non-planar component of the ground reflection. The planar component is identified in equation 4 by the plane wave reflection coefficient, R_p. It follows, then, that the complementary component of the reflected wave, $1 - R_p$, accounts for the non-

planar component. Whereas the planar portion of the reflected wave bounces precisely off of one spot on the ground, the non-planar ground wave comes from a smeared point of reflection. This smearing causes predictable shifts in this field component, which can be accounted for by a complex "ground wave" function (Norton, 1936). Hence, the ground wave can be modeled as

$$p_g = \frac{p_0\left(1 - R_p\right)F(w)e^{ik_1 r_r}}{r_r}, \tag{6}$$

where *F(w)* is the complex ground wave function [Norton (1936) derived in his Appendix as the variable A_1]. An exact equation for the complex ground wave function is found in the Appendix, but it is easy enough to approximate using the infinite series expansion derived by Norton (1941, equation 47),

$$F(w) = 1 + i\sqrt{w\pi}e^{-w} - 2w + \frac{2w}{1 \bullet 3} - \frac{2w}{1 \bullet 3 \bullet 5} + \ldots, \tag{7}$$

where *w* is the "numerical distance" as formulated by Rudnick (1947)[20]

$$w = i\frac{2k_1 r_r}{\left(1 - R_p\right)^2}\left(\frac{Z_1}{Z_2}\right)^2\left[1 - \left(\frac{k_1}{k_2}\right)^2 \cos^2\phi\right]. \tag{8}$$

Norton (Norton, 1941) used a different formulation of the numerical distance that he termed "*p*," but we shall use Rudnick's *w* instead.

While the series expansion provided by Equation (7) is correct for all values of w, it converges very slowly for large w. Norton therefore provided an asymptotic expansion (1941, equation 48), to be used when w is large,

[20] Our formulation of numerical distance follows directly from Rudnick (1947). In one influential paper, Embleton (1983), attempted to use this same formulation but made an important numerical error that affected the remainder of his calculations.

$$F(w) = -\frac{1}{2w} - \frac{1 \bullet 3}{2w^2} - \frac{1 \bullet 3 \bullet 5}{2w^3} - \frac{1 \bullet 3 \bullet 5 \bullet 7}{2w^4} - \cdots \quad . \tag{9}$$

The ground wave is sometimes referred to by its various physical manifestations, specifically the "ground" or "boundary" wave, or the "surface" wave (Embleton, 1996; Bradbury & Vehrencamp, 2011). This formulation of the complex ground wave function is robust in that it accounts for all of these manifestations. Other forms of the complex "ground wave" function are less general and may exclude surface waves.

Model of the ground

Given the three descriptors of source-receiver geometry, h_s,h_r and D from Figure 1, the speed of sound in air, c_1, and the equations given above for the transmission loss between a source and receiver placed near a homogeneous flat boundary, the only data lacking are the parameters that describe the acoustic interactions with the soil, Z_2 and k_2. Both properties are frequency dependent and both can be measured directly for a given soil sample. Many measurement techniques have been developed but none work for all kinds of soils and all are difficult to implement in the field (see review in Section IV.D. of Embleton, 1996).

The difficulty of measuring the acoustical properties of soil directly in the field has motivated acousticians to develop models of Z_2 and k_2 from non-acoustic properties of the soil. The most complete of such models to date is Attenborough's (1983) model that uses five parameters, each clearly related to a relevant property of the ground; these are porosity, flow resistivity, tortuosity, steady-flow shape factor, and dynamic shape factor. While highly precise, the use of a five-parameter model for the ground is so complex that it is difficult to implement. A more practical option uses a

single parameter, effective flow resistivity, σ_e, to describe the ground. This single term combines the two most significant parameters of Attenborough's model (1983), porosity and flow resistivity, suitably describing much of the variation in ground types (Embleton, 1996). Where empirical measurements of transmission loss are available or can be made (see methods and materials below), this single parameter can be varied to give a best-fit estimate of the effective flow resistivity of the soil. This best-fit technique has been used by Embelton and colleagues to assess the effective flow resistivity of a broad diversity of ground types (Table 1). Their measurements can be used as a reasonable estimate for many natural ground types or as a starting point for a best-fit approximation.

To be useful in our effort to generate a general model for the sound field above a homogeneous boundary, a ground model must be translated into useful measures of Z_2 and k_2. Empirical measurements by Delany and Bazley (1971) with the important correction of a change of sign by Embleton (Embleton et al., 1983) established the relationship between the impedance and wave number in air and their corresponding value in the ground as a function of effective flow resistivity of the ground and frequency. The ratio of the impedances is

$$\frac{Z_1}{Z_2} = \left[1 + 9.08\left(\frac{f}{\sigma_e}\right)^{-0.75} + 11.9i\left(\frac{f}{\sigma_e}\right)^{-0.73}\right]^{-1}, \tag{10}$$

and the ratio of the wave numbers is

$$\frac{k_1}{k_2} = \left[1 + 10.8\left(\frac{f}{\sigma_e}\right)^{-0.70} + 10.3i\left(\frac{f}{\sigma_e}\right)^{-0.59}\right]^{-1}. \tag{11}$$

While these relationships were determined by measurement of propagation over synthetic substrates, Embleton's work (Embleton et al., 1983) shows that they function well for more natural ground types with effective flow resistivities that vary from snow to asphalt.

The Van Der Pol Equation

The transmission loss is the ratio of the measured pressure, p_r, to the initial source strength, p_0. Substituting equations 3, 4, and 6 into equation 1, and solving for transmission loss, TL, from equation 2, we get the Van Der Pol equation

$$\mathrm{TL} = \frac{p_r}{p_0} = \left(\frac{e^{ik_1 r_d}}{r_d}\right) + R_p\left(\frac{e^{ik_1 r_r}}{r_r}\right) + \frac{\left(1 - R_p\right)F(w)e^{ik_1 r_r}}{r_r} \quad . \tag{12}$$

Since we are now concerned only with the amplitude information, plots of transmission loss only show the magnitude of this solution. Excess attenuation (*EA*) is a measure of transmission loss relative to what would be expected due to spherical spreading of the direct wave alone. Therefore, excess attenuation is related to transmission loss by,

$$EA = r_d \bullet \left|TL\right| . \tag{13}$$

RESULTS

Model Assessment

The complete model for propagation across the lek derived above consists of Equation 12 for the transmission loss. The plane wave reflection coefficient, R_P, was calculated using equation 5 and equations 10 and 11, which comprises the acoustic model for the ground. The complex ground wave function was calculated using whichever of equations 7 or 9 is appropriate depending of the value of the numerical distance, *w*. This has been implemented numerically and is in complete agreement with Embelton's (Embleton et al., 1983, Embleton, 1996) published results (not shown here).

The model as implemented assumes that the ground can be considered a homogeneous half-space. Embelton and colleagues (1983) conducted a number of experiments using naturally occurring granular materials and soils to construct such homogenous half-spaces, and their propagation measurements made over these surfaces show good agreement with the model predictions. To first order, it is reasonable to expect that the lek can be modeled as a homogeneous half-space. Although there are small mounds present, it is largely flat, and because of the presence of alkali salts, relatively free of vegetation. The soil consists of a mixture of fine particulate matter and water (mud), which freezes each night during the breeding season. We will explore the half-space assumption further later. Given these assumptions and equations we now compare the model's computed predictions to the actual field measurements.

Contrasts between Model Predictions and Field Measurements

Figure 2 shows a comparison of the model predictions with the actual transmission loss measured on Lek 8 as a function of frequency at four source-receiver

separations (ranges). The experimental transmission loss curves (black curves) were obtained using the measurement protocol described earlier. The grey curves show the model predictions for the equivalent source receiver geometry. The effective flow resistivity of the ground, σ_e, was set to 400. This was the value found to give the best qualitative agreement between the modeled and observed transmission loss curves and is consistent with the value expected for roadside dirt (see Table 1), although any value in the range of 300-500 yields similar results. The model is able to reproduce the general features of the field results quite well. The level of increasing transmission loss with increasing range and the broad null in the curves between 1 and 2.5 kHz predicted by the model are reproduced in the observed results. In addition, the observed tendency of the null to deepen and decrease in frequency with increasing range is also predicted by the model. However, the model over-predicts the transmission loss at ranges greater than about 20 meters and frequencies above about 2 kHz. This can be seen in the 32 meter curves in Figure 2.

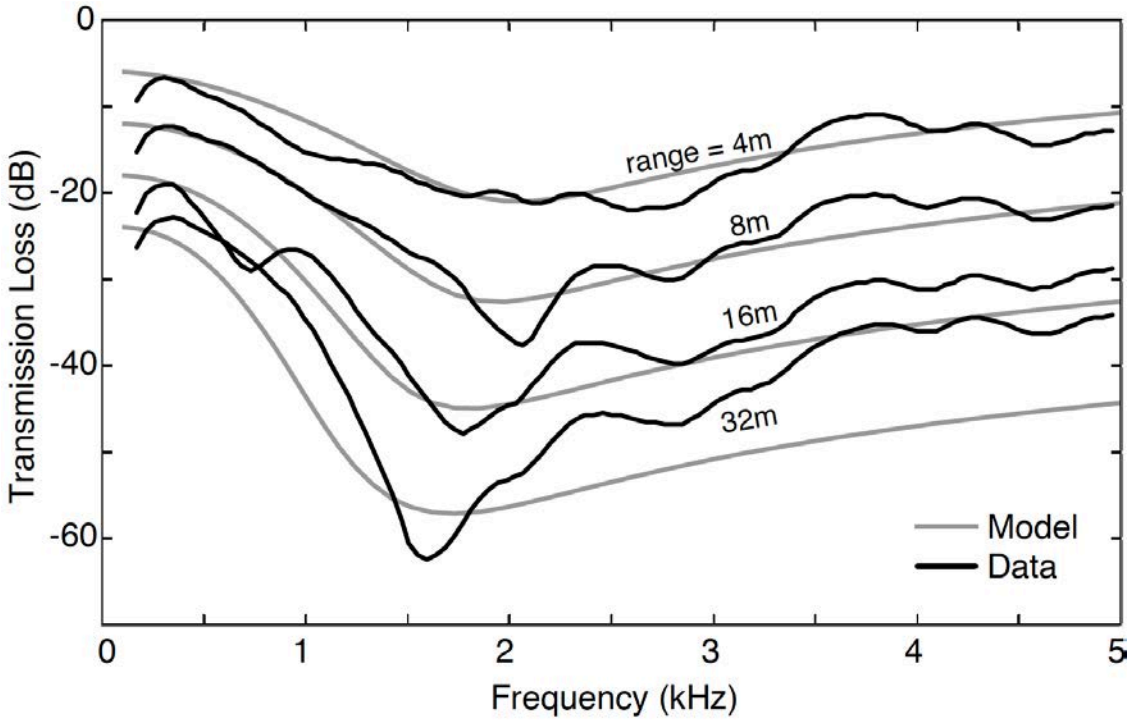

Figure 2. Comparisons of model predictions with measured transmission loss over four source-receiver distances. The experimental (measured) transmission loss is shown in black. The model predictions for the equivalent source receiver geometry are in grey. For the model, the flow resistivity of the ground, σ_e, was set to 400.

Table 1. Ranges of effective flow resistivity, σ_e, for various types of ground surface according to Embleton et al., 1983.

Surface Description	**Flow resistivity**
Dry snow, new fallen 0.1 m over about 0.4 m older snow	10-30
Sugar snow	25-50
In forest, pine or hemlock	20-80
Grass: rough pasture, airport, lawns	150-300
Roadside dirt, ill-defined small rocks up to 0.1 m mesh	300-800
Sandy silt, hard packed by vehicles	800-2500
“Clean” limestone chips, thick layer	1500-4000
Old dirt roadway, fine stones (0.05m mesh) interstices filled.	2000-4000

The data shown in figure 2 were measured in the early morning hours when the ground was frozen. Since it was known that the ground alternates between frozen and thawed over a diurnal cycle, transmission loss curves were obtained over a 24 hour period to study the impact of temperature on propagation. The results are shown in Figure 3B as a grey-scale contour of transmission loss versus frequency and time. Although there is considerable variability in the transmission loss data, there is a general trend for the transmission loss null to broaden and increase in frequency during the daylight hours. Figure 3a shows the air temperature measured during the 24 hour experiment period. These significant changes in the transmission loss behavior coincide with the warming of the lek during the day.

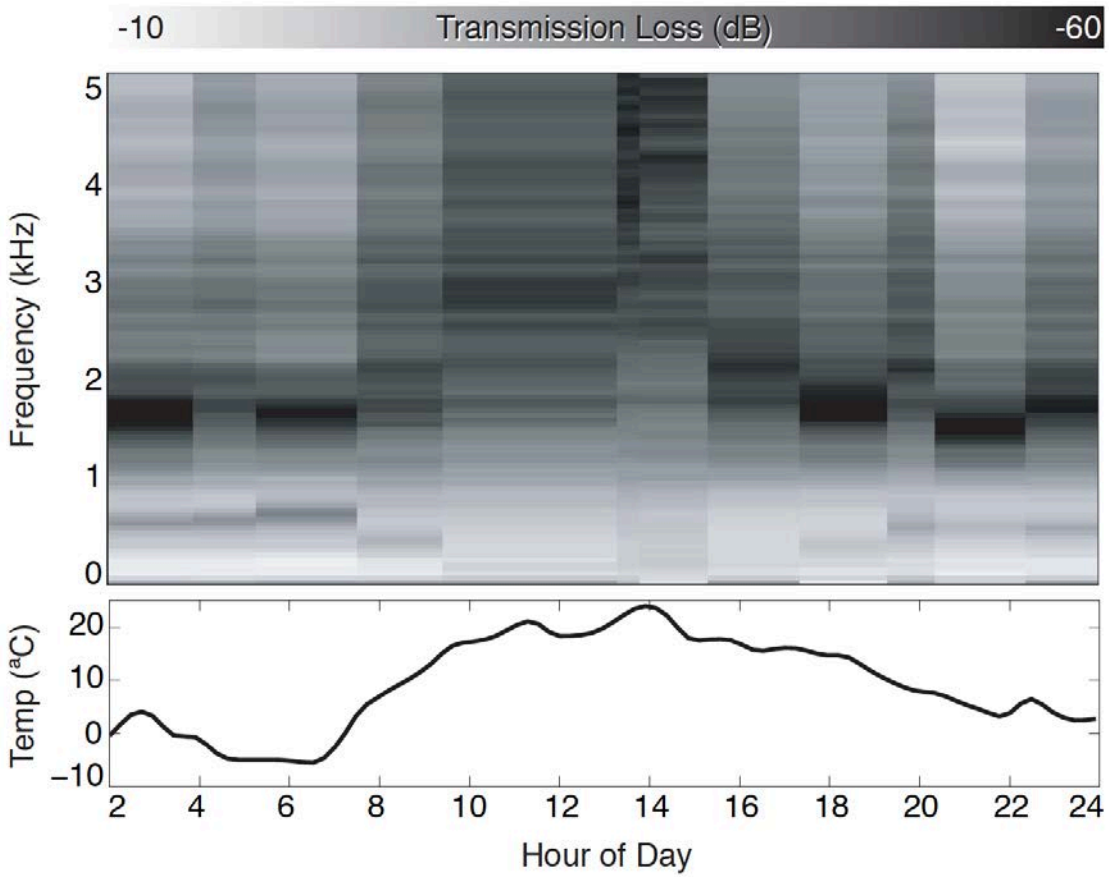

Figure 3. Transmission Loss as a function of time and temperature. Figure 3a is a grey-scale contour of transmission loss versus frequency and time. Figure 3b shows air temperature measured during the same 24 hour period. There is a general trend for the transmission loss null to broaden and increase in frequency during the daylight hours. The changes in transmission loss coincide with the warming of the lek during the day.

Figure 4 shows the results of an attempt to model the variations in transmission loss throughout the day by varying the effective flow resistivity of the ground. The three black curves show transmission loss measured during predawn, early morning, and mid day (corresponding to air temperatures respectively of -2, 12, and 20 ºC). Although the transmission loss curves show a similar behavior below about 1.5 kHz, propagation effects above this frequency varied by as much as 20 dB depending on temperature. The homogeneous half-space model is unable to reproduce this temperature dependence at higher frequencies, suggesting that a more complicated representation of the lek is required to fully characterize the transmission properties. In retrospect, it would have been helpful to measure the temperature profile in the top 20 cm or so of the soil, but this was not done. However, we can do some simple calculations to estimate the impact of layering near the lek surface. Calculations of the acoustic wavelength in the soil (assuming an effective flow resistivity of 400) show that the wavelength varies from approximately 5 cm at 100 Hz to less than a cm at 5 kHz. The thermal skin depth associated with diurnal radiation forcing cannot be calculated accurately without more information about the soil properties than is currently available, but we expect it to be on the order of a few cm. The close correspondence of this scale with the range of acoustic wavelengths over the frequencies of interest lead us to expect a strong interaction between sound reflected from the ground and any layers associated with thermal effects. We suspect that such an interaction may be the source of the deep null seen at 1.5 kHz during the night and the wide variations in transmission loss observed at higher frequencies with changes in temperature.

Notwithstanding the thermal effects discussed above, the propagation measurements shown in Figure 2 demonstrate that the half-space model can adequately reproduce transmission loss across the lek between 100 Hz and 5 kHz at ranges from 4 to approximately 20 meters during the early morning hours when the lek is frozen and the birds are displaying.

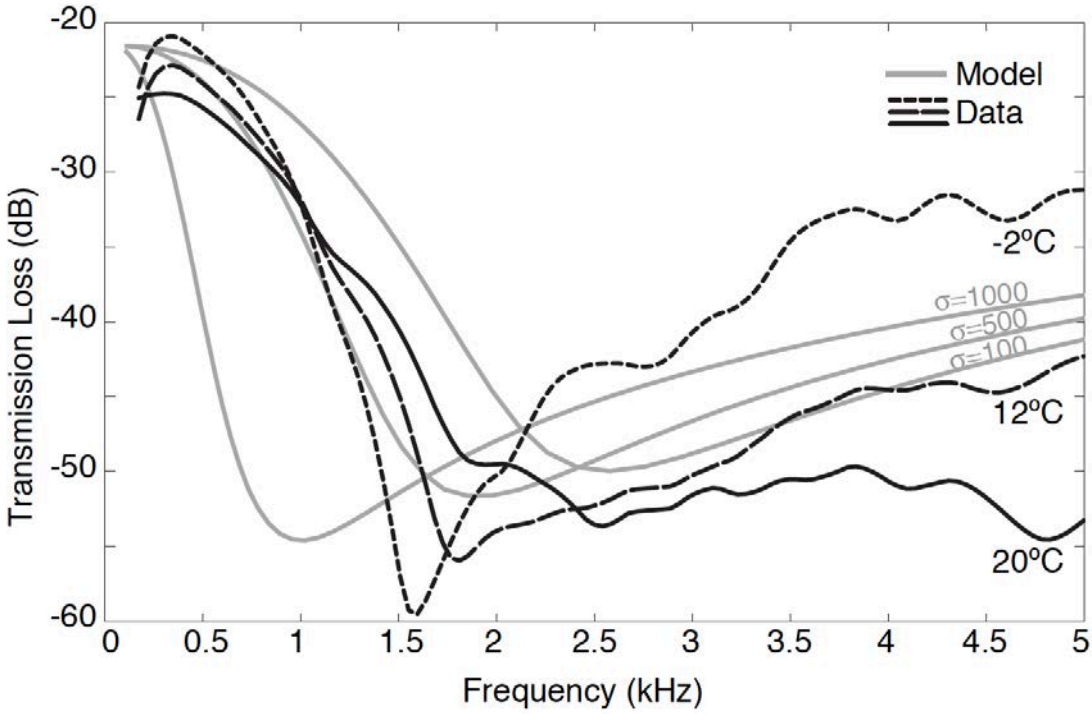

Figure 4. Varying the effective flow resistivity of the ground in an attempt to model the variations in transmission loss observed throughout the day. The three black curves show measured transmission loss measured during predawn (-2 ºC, dotted line), early morning (12 ºC, dashed line), and mid day (20 ºC, solid line). The transmission loss curves show a similar behavior below about 1.5 kHz. Above this frequency, transmission loss varies as much as 20 dB between curves.

DISCUSSION

Modeling propagation

The main focus of this paper has been the application of a terrestrial propagation model to explain the complicated interaction between acoustic transmissions and the ground for sound propagating over an alkali-flat Greater Sage-Grouse lek. The field observations presented show that sound propagation is sensitive to the details of the source-receiver geometry, as suggested previously by Gerhardt (1983), and the temperature of the ground over a broad band of frequencies. The sensitivity of acoustic transmissions to the details of the local environment is not limited to alkali flats such as Lek 8, and is more the rule than the exception in both terrestrial and marine acoustics. It is not safe to assume that low frequencies are always attenuated near the ground (e.g. Nemeth et al., 2001), nor is it safe to either assume a particular phase relationship between direct and reflected waves or to ignore the ground wave (e.g. Nelson, 2003). Generalizations and rules-of-thumb are instructive and illustrative (Bradbury & Vehrencamp, 2011) but should not be taken as formal mathematical treatments on which to base hypotheses, models, or analyses (e.g. Parris, 2002).

We have examined a very specific acoustic signaling environment using both experimental measurement and an existing model for transmission loss. We have confirmed that the model characterizes the experimentally measured frequency dependence of acoustic propagation in this environment at least at some temperatures and ranges. Thus, we have experimentally determined that this model has a range of applicability in this environment. It characterizes well propagation between 4 and 20 meters, and between about 0.1 and 5 kHz when the surface of the lek is frozen. While

this is a limited range of applicability on the lek, the half-space model pioneered by Embleton and others (Delany & Bazley, 1971; Embleton et al., 1976; Embleton et al., 1983; Embleton, 1996) is likely to be useful in understanding near-ground communication in other species and contexts. This model has been cited often in the bioacoustics literature but not implemented and not well understood. Perhaps because of its complexity, recent modeling efforts have avoided applying the model even where it was clearly relevant (Brown & Handford, 1996, 2000; Parris, 2002; Nelson, 2003), choosing instead to use their own less rigorous approximations or generalizing measurements from other studies into "rules".

The limits of applicability of this model are due to the limited suitability of the single parameter model of the ground to this, and likely any, complex environment. While Delany & Bazley (1971) found that the single parameter model worked well over synthetic surfaces, and Embelton (Embleton et al., 1983) found that it characterized propagation well over more natural (yet constructed) surface types, our results show that a single parameter model works for the lek environment only over a limited range of frequencies, distances, and temperatures.

The model might be improved by incorporating range dependent scattering effects (Bullen & Fricke, 1982), temperature dependent vertical stratification in the soil, heterogeneity of the soil in the horizontal plane of the lek, wind and thermal effects in the air (Daigle et al., 1983, 1986), and shadowing and refraction by small scale topography (Rasmussen, 1985; Heimann & Gross, 1999). The model also might be improved by using a more complicated description of the ground than as a homogeneous half-space. However, there is a limit to the utility of developing an

increasingly accurate model. The main utility of the model for behavioral studies is being able to predict propagation. If the data needed to make those predictions are sufficiently complicated, it may be better simply to measure propagation directly. This point is discussed in greater detail in the concluding remarks.

Behavioral ramifications of diurnal cycles

The data show that transmission loss changes with temperature (Figure 3). In the early morning, when the ground is frozen, the ground effects generate a characteristic transmission loss. As solar radiation heats the surface of the lek, it melts and the transmission loss changes dramatically. In the 2-5 kHz range, it can vary by as much as 40 dB. Grouse acoustic signals therefore experience increasing attenuation in the middle frequencies once the day warms up.

There is some evidence that suggests that Greater Sage-Grouse are affected by this diurnal cycle of transmission loss changes. Grouse follow a diurnal and seasonal display cycle. Early in the breeding season, males display until late in the morning, whereas late in the season, males finish displaying earlier in the morning (Gibson et al., 1991). This is consistent with our measurements, which predict that the increase in mid-frequency attenuation should occur earlier and earlier in the season as temperatures rise. The decision to cease display when the ground is soft may be driven by male grouse choosing to limit display, or by female grouse who might avoid choosing mates when attenuation is greater.

It may seem absurd to suggest that Greater Sage-Grouse are directly measuring attenuation. There is, of course, no direct way that a grouse can assess the transmission loss for his own vocalizations. However, they might detect the changes in the

frequency characteristics of the vocalizations of other displaying males. A 40 dB drop in the mid frequencies might be directly perceived as changes in the timbre of the orchestra. Of course, there is another way grouse might avoid vocalizing during heightened attenuation: they can probably feel it with their feet. When the ground softens and warms, they may simply take that as a cue to stop. These are predictions that can be directly tested with future work.

Ramifications of common Greater Sage-Grouse behaviors on signaling

Within the identified accuracy of the model it is possible to study the acoustical implications of three common Greater Sage-Grouse mating behaviors: females approaching males for active comparison, females raising and lowering their heads, and males standing on small knolls.

Approach

While they are choosing a mate, Greater Sage-Grouse females walk back and forth across the lek, visiting territories of multiple males (Dantzker et al., 1999). We can use the homogeneous half-space model to examine the consequences of this movement on the frequency dependent transmission loss that is filtering the surrounding males' vocalizations. Figure 5, shows model predictions of how transmission would change as a female approaches a male under idealized frozen (Figure 5a) and thawed conditions (Figure 5b). In both conditions, as she approaches the propagation null disappears and she improves her ability to assess frequency and amplitude variables in a male's acoustic display.

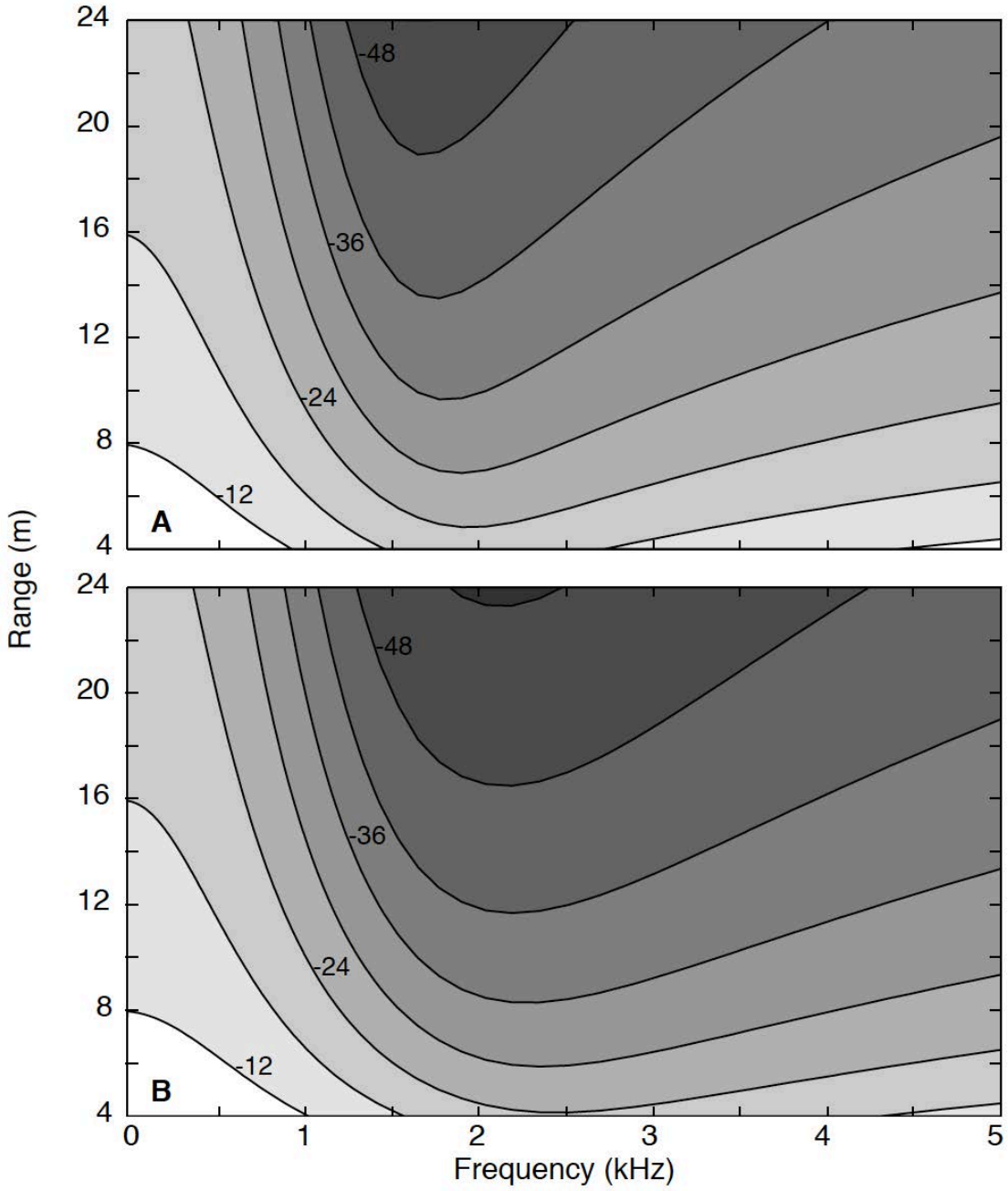

Figure 5. Model predictions of how acoustic transmission changes as a female approaches a male under idealized frozen (Figure 5a) and thawed conditions (Figure 5b).

Gibson (1996) showed that female Greater Sage-Grouse exhibit two distinct stages of pre-mating behavior, distant attraction and nearby active comparison. Our results suggest that the relative amplitude of each male's acoustic display may play a role in distant attraction just because louder males have a larger active space and thus greater range of detectability. However, in this environment it is difficult, if not impossible, for a female to judge the absolute amplitude of a male's vocalization when at a distance. However, as the female approaches, the transmission loss effects decrease and, within 1-2 meters, she should be able to reliably assess amplitude in her comparisons of potential mates.

Female head height

Female Greater Sage-Grouse raise and lower their heads as they walk around the lek. They usually hold their heads high as they walk, and duck them when they sit, bringing them very close to the ground at times. While these behaviors may have primary functions ranging from avoiding predation to soliciting copulation, it is interesting to examine the effects that this small movement will have on transmission loss. Figure 6A, shows that once a female is close to a male even a 20 cm movement in head height can have a greater than 10 dB effect on the transmission loss of some frequencies. As she ducks her head to the ground, she improves her reception of energy below 2 kHz and decreases her reception of higher frequency energy. It is interesting to speculate that females use this in some way during assessments.

Standing on knolls

On Lek 8 we observed that male Greater Sage-Grouse seek out and often display from small knolls. These knolls are not apparent from the surrounding hillsides, and are

small enough to avoid notice to even careful, qualitative observers on the lek. Some knolls can be 40-60 cm higher than the surrounding plane and tens of meters across. Other males' territories contain only a small mound, a meter or so wide and 10-20 cm tall, and still other males may have no appreciable knoll at all. However, when males do have a knoll on their territory, they were often observed displaying from the edge of them. As we've shown, the frequency dependent transmission loss is very sensitive to source-receiver geometry. Standing just inside the edge of a knoll has the effect of changing the source height, whereas moving to the center of the knoll just puts him closer to the ground somewhere else. Figure 6B shows the results of the model where effective flow resistivity, range, and receiver (female) height are held constant, and the source (male's) height is varied from 0.2 meters (the approximate height of the male's chest in display posture on flat ground) to 0.8 meters (the approximate height of the male's chest when standing on a 60 cm knoll). The grey curves from the model are plotted against the data from the propagation experiment (black, source height o.2 m) for comparison. We see that males achieve a systematic propagation advantage in the range of 1.5-5 kHz from standing on progressively higher knolls. Above 2 kHz, a male standing on a 60 cm knoll has a greater than 10 dB advantage over a male standing on flat ground. This is a tremendous advantage across a broad range of relevant frequencies. This advantage might help males attract females to their territory from farther away, or even be heard by females at a greater distance against the din of other males' persistent strutting.

Gibson (1996) showed that an acoustic parameter of the Greater Sage-Grouse strut display (inter-pop interval) is correlated with long-range attraction. Any advantage

to broadcast that signal should therefore lead to greater mating success. We can make three predictions from this model: 1) successful males will preferentially display from positions in their territory that have a favorable geometry with females, at least when those females are at a distance, 2) we expect that males who are able to defend territories with features like knolls will be more likely to attract females into their territories than males who do not, and 3) while it may not be true every year, the territory of the most successful males should include some propagation advantage. Not all grouse leks are on alkali flats however; even when they are in other micro-habitats, we predict there will be similar knolls or other environmental heterogeneities that lead certain specific places to be beneficial for acoustic transmission.

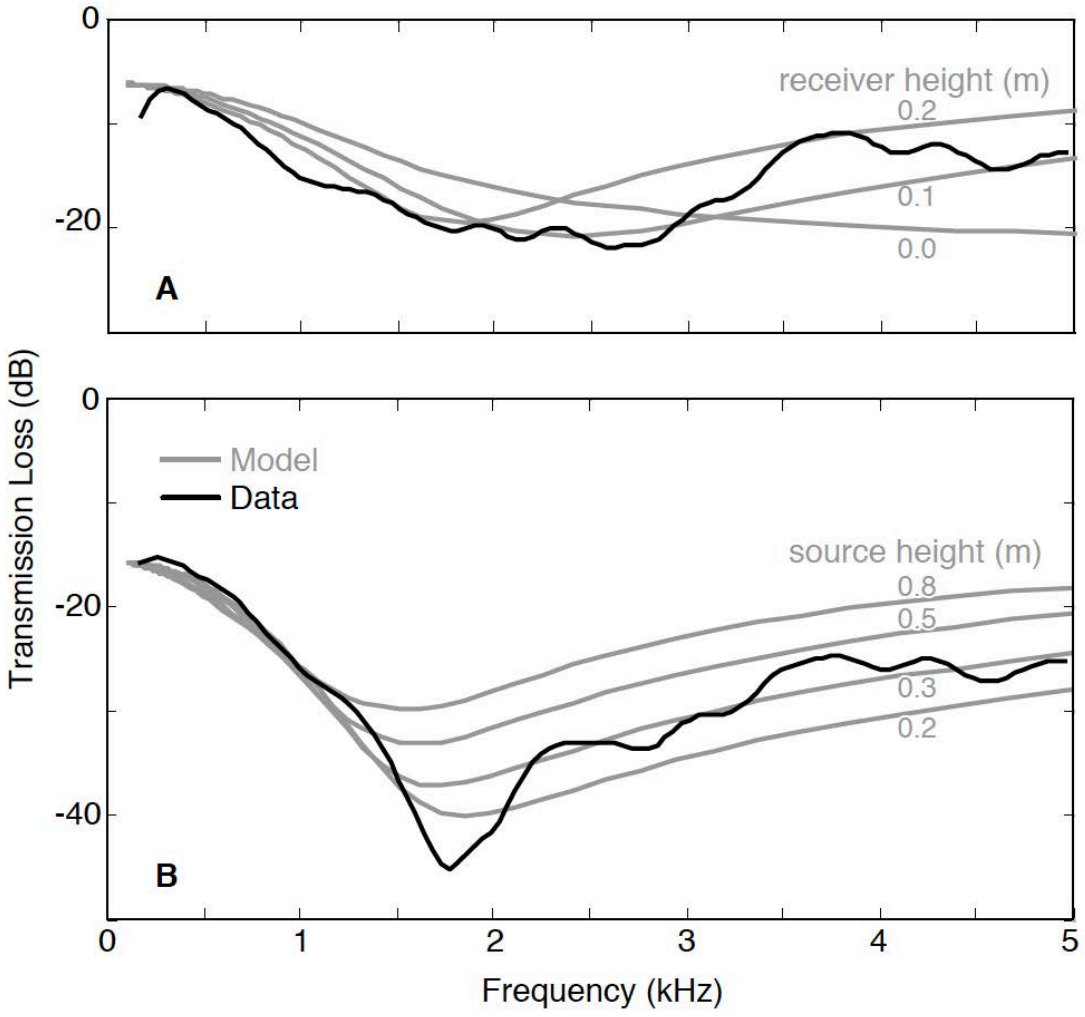

Figure 6. Model predictions of how acoustic transmission changes with different common female and male behaviors. (Figure 6a) As a female at close proximity sits and lowers her head toward the ground, she becomes better able to assess the lower frequencies of a male's display. (Figure 6b) Males who find small rises to stand on effectively raise their acoustic source, which the model shows us decreases transmission loss significantly.

If true, this may provide a link between the concept of a fixed "mating center" and active female choice. Many observers of Greater Sage-Grouse mating behavior have noted that successful males tend to occupy the same territories year after year (Scott, 1942; Patterson, 1952; Wiley, 1973b). Gibson and others showed that differences in male behavior mostly determine mating success (Gibson & Bradbury, 1985; Gibson et al., 1991). Both explanations can be right in a system where conspicuous environmental factors bolster the efficacy of display. Males who seek the advantageous topography on their lek will tend to have higher mating success. Over time, males will be selected to compete over those display territories and soon the more fit individuals will tend to be found on the better display territories. Such a process has already been proposed to explain territoriality around light gaps in some tropical lekking birds that use visual signals to attract mates (Endler & Théry, 1996). Wiley found no differences in the microhabitat at the location of the mating center and concluded that the position of the mating center was arbitrary (Wiley, 1973a, 1973b). However, he did not make the type of acoustic measurements necessary to evaluate territories for their propagation tendencies, and the variations in small-scale topography are difficult to detect without measurement (for a description of how to measure small-scale topography see Dantzker et al., 1999), so his conclusions are not necessarily incompatible with our results. We now know that specific differences between the acoustic signals of individual males attract females from a distance (Gibson & Bradbury, 1985; Gibson et al., 1991; Gibson, 1996). From this we can predict that while mating centers might move around from year to year, on average they ought to occur on a knoll.

More general issues

From the perspective of two animals using sound to communicate, interactions between the traveling pressure waves and the environment result in sound being distorted and degraded during its propagation between the two parties (Bradbury & Veherencamp, 2011). Bioacousticians tend to categorize environmental interactions into attenuation considered in the frequency domain and distortion or degradation (corresponding to the effects of scattering and reverberation) considered in the time domain (Catchpole & Slater, 1995; Bradbury & Veherencamp, 2011). Contemporary studies of environmental interactions in the bioacoustics literature have tended to focus on time domain effects, probably because of the difficulties in identifying consistent trends and patterns through analysis in the frequency domain. Those that examine amplitude have used coarse measures, such as SPL, that ignore the frequency dependence that might be crucial for signaling (e.g. Balsby et al., 2003, Jain & Balakrishnan 2o12). Some of the early absorption studies did identify two patterns of absorption associated with ground interactions: a propagation notch between 300 and 800 Hz within which sound does not propagation well for sources and receivers close to the ground, and the strong attenuation of high frequency sounds for sources and receivers on the ground. A propagation notch can be seen in our lek measurements, although its center frequency, depth, and width are all highly dependent on the ground properties and the source-receiver geometry. The propagation studies of Embleton and our model predictions show that there are, in fact, multiple interference nulls and that the depth and location of these nulls is a sensitive function of geometry and ground type.

These observations lead to two important questions: 1) Is it, in fact, possible to derive general and useful rules of thumb for transmission loss over ground, and 2) what level of environmental detail is required to predict transmission loss to a specified level of accuracy? Our results suggest that the answer to the first question is no. There is simply too much sensitivity to geometry and ground effective flow resistivity for useful generalizations to be made even in the simplified case of a homogeneous half-space model. With the exception of boundaries of a known type (for example, homogeneous layers of snow or concrete) the minimum level of effort required is a transmission loss experiment or some other methodology to identify the acoustical properties of the substrate. Once identified, these properties permit the general features and trends of absorption to be described but, as can be seen from the lek data, there will be range and frequency limitations. This is, in part, an answer to question 2: a single parameter description for the substrate used by displaying grouse is sufficient to enable calculation of the transmission loss curves to within 3-6 dB over ranges between 4 and 20 meters, and between about 0.1 and 5 kHz when the surface of the lek is frozen. This level of detail is sufficient to study general trends in transmission loss, for example, with source and receiver height. However, it is insufficient to study effects which require a more precise knowledge of the propagation characteristics. For example, Dantzker et al. (1999) were able to infer the directional radiation patterns of Greater Sage-Grouse vocalizations on the same study lek, but only by a direct calibration of the transmission loss over each transmission path. In general this is probably going to be true for other environments as well. The level of environmental characterization required to model the transmission loss to better than several dB is impractical or impossible to obtain,

and the most expedient way to calibrate the acoustic environment is by direct measurement.

More specifically, we conclude that to make detailed measurements of the sounds emitted in this environment you must have a measured transmission loss curve for the path over which the measurement is made. Measurements of any acoustic parameter that would be affected by frequency dependent transmission loss will vary in both systematic and non-systematic ways depending on propagation path and source receiver geometry. This calls into question many of the measured acoustic traits that have been investigated in their relationship to mating success (Hartzler, 1972; Wiley, 1973a; Gibson & Bradbury, 1985; Gibson et al., 1991; Spurrier et al., 1994; Gibson, 1996; Young, 1994; Young et al., 1994). For example, the measurement protocols of Gibson and colleagues were not sufficient to measure at least 4 of 9 traits they examined in 1985 (Gibson & Bradbury, 1985) and 11 of the 16 acoustic traits they examined in 1991 (Gibson et al., 1991). These traits include peak amplitudes of individual call notes and peak frequencies. Gibson and colleagues (Gibson & Bradbury, 1985; Gibson et al., 1991; Gibson, 1996) acknowledged that propagation effects may have affected their measurements but they accounted for them only insomuch as they examine their data for spurious correlations that might have resulted from frequency dependent transmission loss. This statistical method allowed them to exclude the possibility that frequency dependent transmission loss was biasing their results, but it did not correct for the influence of the environment which, our results show, would cause significant measurement errors. Our results strongly suggest that a reexamination of the Greater Sage-Grouse acoustic display, using either explicit calibration for

propagation effects or recordings made very close to the male (perhaps 1-2 meters) may yet discover acoustic correlates with mating success. The use of robotic females outfitted with calibrated recording systems, as being used by Patricelli & Krakauer (2010), is promising in this regard.

Greater Sage-Grouse have evolved a highly ritualized and spectacular acoustic display which is obviously important to the birds' mate selection. It has been a longstanding puzzle for bioacousticians that no robust acoustic metric has been found as a correlate of mating success despite years of searching. This work may provide an answer to this puzzle: the acoustic environment of the lek, heretofore uncharacterized, plays a central role in the communications dynamic of the birds.

Acknowledgements

Chapter 2, in full is currently being prepared for submission for publication of the material. Dantzker, Marc; Deane, Grant. The dissertation author was the primary investigator and author of this material.

APPENDIX

General Theory

The goal of this appendix is to elucidate the underpinnings of the Van Der Pol equation, which forms the basis of our propagation model. The general acoustic theory describing the effect of the nearby ground on a source-receiver pair is well established. Its origins trace back to studies of radio wave propagation by Sommerfeld, Van Der Pol, and Norton, which were subsequently applied to the problem of acoustic propagation along a boundary by Rudnick (Sommerfeld, 1909, 1926; Van Der Pol, 1935; Norton, 1936, 1937, 1941; Rudnick, 1947).

Figure 1 shows the assumed geometry for the problem. A source-receiver pair are placed in air with uniform sound speed c_1 and density ρ_1 above a stratified half space representing the ground. The ground, with sound speed c_2 and density ρ_2 is assumed to be uniform in the horizontal, but in its most general form can have layers or be continuously variable in the vertical. For this geometry, the total acoustic field at the receiver can be expressed as the sum of two terms, one of which represents the direct path energy and the other the energy reflected by the ground. For a harmonic source of unity strength and frequency, *f*, the field can be expressed as

$$p_r = \frac{e^{ik_1 r_d}}{r_d} + i\int_0^\infty R_p J_0(\xi_1 D) e^{i\gamma_1(h_s+h_r)} \frac{\xi_1}{\gamma_1} d\xi_1 \qquad \text{(A1)}$$

where $k_1 = 2\pi f / c_1$ is the total wave number of the acoustic field in the air, R_p is the plane wave reflection coefficient (discussed below), $\gamma_1 = \sqrt{k_1^2 - \xi_1^2}$ is the vertical wave number and the variable of integration ξ_1 is the horizontal wave number, J_0 is the zero-

order Bessel function of the first kind, and the distances D,h_s,h_r and $\mathrm{r_d}$ are defined in Fig. 1. Equation (A1) has a simple physical interpretation. The leading term on the right hand side, equivalent to Equation 3 for unity source strength, accounts for the spherically spreading wave fronts radiated by the source that do not interact with the ground. The integral accounts for the wave fronts reflected from the ground. The form of this integral results from expressing the spherically spreading wave field incident on the ground as a superposition of plane waves. In a cylindrical coordinate system, this amounts to Bessel transform, integral representation for the field. Reflection by the ground modifies the amplitude and phase of each plane wave component by the factor R_p which appears inside the integral. Equation A1 is equivalent to Rudnick's Equation 12 (Rudnick, 1947; also see Brekhovskikh & Lysanov, 1991, p. 79, Eq. 4.3.2). Equation A1 is exact provided that the ground is horizontally stratified and obeys the boundary conditions that pressure and the first derivative of pressure are continuous across the air-ground interface.

Although Equation A1 is exact, it is not in a convenient form for numerical evaluation because the presence of γ_1 in the denominator of the integral introduces a pole close to the path of integration and the integral kernel is highly oscillatory. This integral has received a great deal of attention in the underwater acoustics community and asymptotic forms for it have been developed (e.g., see chapter 4 of Brekhovskikh & Lysanov, 1991). The standard approach in the literature on outdoor propagation over ground (e.g. Albert, 2003) is to use the Weyl-Van Der Pole equation, which is derived from Equation A1 by assuming that the ground is sufficiently absorbing [see the

discussion by Rudnick (1947) and the original treatment by Norton (1936, 1937, 1941)]. The approximate form for the pressure field is,

$$p_r = \frac{\exp\left(ik_1 r_d\right)}{r_d} + \left[R_p + \left(1 - R_p\right)F(w)\right]\frac{\exp\left(ik_1 r_r\right)}{r_r} \qquad \text{(A2)}$$

where F(w) is the complex "ground wave" function (Norton, 1936, derived this function as *A* in equation (45) of his appendix)

$$F(w) = 1 + i\sqrt{w\pi}e^{-w}\operatorname{erfc}\left(-i\sqrt{w}\right) \qquad \text{(A3)}$$

where w is the "numerical distance" defined in Equation (8) , and the complex error function is

$$\operatorname{erfc}(x) = \frac{2}{\sqrt{\pi}}\int_x^\infty e^{-u^2}\,du. \qquad \text{(A4)}$$

If one chooses to calculate the complex ground wave function directly from these equations, care must be taken to insure that the solution to the error function allows for complex values. An alternate and equivalent tack is to employ the series expansions for F(w) that are presented in Equations 7 and 9.

LIST OF SYMBOLS

c_1	speed of sound in the air (m/s)
c_2	speed of sound in the ground (m/s)
D	distance along flat ground between the source and receiver (m)
EA	Excess attenuation (dB)
erfc(x)	complex error function of variable x
f	frequency of vibration (Hz)
$F(w)$	complex ground wave function of variable w
h_r	receiver height (m)
h_s	source height (m)
k_1	wavenumber in air (rad/m)
k_2	wavenumber in the ground (rad/m)
J_0	the zero-order Bessel function of the first kind
p_d	direct path pressure measured at the receiver (Pa)
p_g	pressure due to the ground wave measured at the receiver (Pa)
p_o	acoustic pressure generated by the source (Pa)
p_m	specularly reflected pressure measured at the receiver (Pa)
p_r	total acoustic field measured at the receiver (Pa)

r_d	length of the shortest path between the source and receiver (m)
r_r	length of the reflected path between the source and receiver (m)
R_p	plane wave reflection coefficient
TL	transmission loss (dB)
u	dummy variable of integration
w	numerical distance
Z_1	specific acoustic impedance of the air
Z_2	specific acoustic impedance of the ground
γ_1	vertical wavenumber in air
ξ_1	horizontal wavenumber in air
ρ_1	density of air (kg/m^3)
ρ_2	density of the ground (kg/m^3)
σ_e	effective flow resistivity
ϕ	angle of incidence (degrees)

REFERENCES CITED

Anderson, M. E. & Conner, R. N. 1985. Northern cardinal song in 3 forest habitats in eastern Texas. *Wilson Bulletin* **97**, 436–449.

Albert, D.G. 2003. Observations of acoustic surface waves in outdoor sound propagation, *Journal of the Acoustical Society of America*. **113** 2495-2500.

Attenborough, K. 1983. Acoustical characteristics of rigid fibrous absorbents and granular materials. *Journal of the Acoustical Society of America*, **73,** 785-799.

Badyaev, A. V. & Leaf, E. S. 1997. Habitat associations of song characteristics in Phylloscopus and Hippolais warblers. *Auk*, **14**(1) 40-46.

Balsby, T. J. S., Dabelsteen, T. & Pedersen, S. B. 2003. Degradation of whitethroat vocalisations: Implications for song flight and communication network activities. *Behaviour*, **140**(6) 695-719.

Blumstein, D. T. & Turner A. C. 2005. Can the acoustic adaptation hypothesis predict the structure of Australian birdsong? Acta Ethologica, **8**(1) 35–44.

Boncoraglio, G. & Saino N. 2007. Habitat structure and the evolution of bird song: a meta-analysis of the evidence for the acoustic adaptation hypothesis. Functional Ecology **21**(1) 134–142.

Bradbury, J. W. & Vehrencamp, S. L. 2011. *Principles of animal communication, 2nd edition*. Sunderland, MA: Sinauer Associates.

Brekhovskikh, L. M. & Lysanov, Y. P. 1991. *Fundamentals of Ocean Acoustics*. New York: Springer-Verlag.

Brown, T.-J. & Handford, P. 1996. Acoustic signal amplitude patterns: A computer simulation investigation of the acoustic adaptation hypothesis. *The Condor*, **98**(3) 608-623.

Brown, T.-J. & Handford, P. 2000. Sound design for vocalizations: Quality in the woods, consistency in the fields. *The Condor*. **102**(1) 81-92.

Bullen, R. & Fricke, F. 1982. Sound Propagation through Vegetation. *Journal of Sound and Vibration*. **80**(1) 11-23.

Catchpole, C. K. & Slater, P. J. B. 1995. Bird song: Biological themes and variations. In: *Bird song: Biological themes and variations. 1995; viii+248p* (Ed. by Catchpole, C. K. & Slater, P. J. B.): Cambridge University Press, The Pitt Building, Trumpington Street, Cambridge CB2 1RP, England; Cambridge University Press, 40 W. 20th Street, New York, New York 10011-4211, USA.

Christie, P. J., Mennill, D. J. & Ratcliffe L. M. 2004. Chickadee song structure is individually distinctive over long broadcast distances. *Behaviour* **141**(1) 101–124.

Couldridge, V. C. K. & van Staaden M. J. 2004. Habitat-dependent transmission of male advertisement calls in bladder grasshoppers (Orthoptera; Pneumoridae). *Journal of Experimental Biology* **207**, 2777–2786.

Cosens, S. E. & Falls, J. B. 1984. A Comparison of Sound Propagation and Song Frequency in Temperate Marsh and Grassland Habitats. *Behavioral Ecology and Sociobiology*. **15**(3) 161-170.

Crawford, J. D., Jacob P., & Benech V. 1997. Sound production and reproductive ecology of strongly acoustic fish in Africa: *Pollimyrus isidori*, Mormyridae. *Behaviour* **134**(9/10) 677–725.

Dabelsteen, T., Larsen, O. N. & Pedersen, S. B. 1993. Habitat-induced degradation of sound signals: Quantifying the effects of communication sounds and bird location on blur ratio, excess attenuation, and signal-to-noise ratio in blackbird song. *Journal of the Acoustical Society of America* **93**(4) 2206-2220.

Daigle, G. A., Embleton, T. F. W. & Piercy, J. E. 1986. Propagation of Sound in the Presence of Gradients and Turbulence near the Ground. *Journal of the Acoustical Society of America*, **79**(3) 613-627.

Daigle, G. A., Piercy, J. E. & Embleton, T. F. W. 1983. Line-of-Sight Propagation through Atmospheric-Turbulence near the Ground. *Journal of the Acoustical Society of America*, **74**(5) 1505-1513.

Daniel, J. C. & Blumstein, D. T. 1998. A test of the acoustic adaptation hypothesis in four species of marmots. *Animal Behaviour*, **56**(6) 1517–1528.

Dantzker, M. S., Deane, G. B. & Bradbury, J. W. 1999. Directional acoustic radiation in the strut display of male sage grouse Centrocercus urophasianus. *The Journal of Experimental Biology*, **202,** 2893-2909.

Delany, M. E. & Bazley, E. N. 1971. A note on the effect of ground absorption in the measurement of aircraft noise. *Journal of Sound and Vibration*, **16,** 315-322.

Doutrelant, C. & Lambrechts, M. M. 2001. Macrogeographic variation in song a test of competition and habitat effects in blue tits. *Ethology* **107**(6) 533–544.

Embleton, T. F. W. 1996. Tutorial On Sound Propagation Outdoors. *Journal of the Acoustical Society of America*, **100,** 31-48.

Embleton, T. F. W., Piercy, J. E. & Daigle, G. A. 1983. Effective flow resistivity of ground surfaces determined by acoustical measurements. *Journal of the Acoustical Society of America*, **74,** 1239-1244.

Embleton, T. F. W., Piercy, J. E. & Olson, N. 1976. Outdoor sound propagation over ground of finite impedance. *Journal of the Acoustical Society of America*, **59,** 267-277.

Endler, J. A. & Théry, M. 1996. Interacting effects of lek placement, display behavior, ambient light, and color patterns in three neotropical forest-dwelling birds. *American Naturalist*, **148**(3) 421-452.

Gerhardt, H. C. 1983. Communication and the environment. In: *Communication* (Ed. by Halliday, T. R. & Slater, P. J. B.), pp. 82-113. New York: W. H. Freeman and Company.

Gibson, R. M. 1996. Female choice in sage grouse: the roles of attraction and active comparison. *Behavioral Ecology and Sociobiology*, **39**(1) 55-59.

Gibson, R. M. & Bradbury, J. W. 1985. Sexual Selection in Lekking Sage Grouse *Centrocercus-urophasianus* Phenotypic Correlates of Male Mating Success. *Behavioral Ecology and Sociobiology*, **18**(2) 117-124.

Gibson, R. M., Bradbury, J. W. & Vehrencamp, S. L. 1991. Mate choice in lekking sage grouse revisited: the roles of vocal display, female site fidelity, and copying. *Behavioral Ecology*, **2**(2) 165-180.

Gish, S. L. & Morton, E. S. 1981. Structural Adaptations to Local Habitat Acoustics in Carolina Wren Thryothorus-Ludovicianus Songs. *Zeitschrift fuer Tierpsychologie*, **56**, 74-84.

Handford, P. & Lougheed, S. C. 1991. Variation in Duration and Frequency Characters in the Song of the Rufous-Collared Sparrow Zonotrichia-Capensis with Respect to Habitat Trill Dialects and Body Size. *The Condor*, **93**, 644-658.

Hansen, P. 1979. Vocal learning: its role in adapting sound structures to long- distance propagation, and a hypothesis on its evolution. *Animal Behaviour* **27**, 1270–1271.

Hartzler, J. E. 1972. *An analysis of sage grouse lek behavior*. University of Montana, Missoula.

Heimann, D. & Gross, G. 1999. Coupled simulation of meteorological parameters and sound level in a narrow valley. *Applied Acoustics*, **56**, 73-100.

Hunter, M. L. & Krebs, J. R. 1979. Geographical variation in the song of the great tit *Parus major* in relation to ecological factors. *Journal of Animal Ecology* **48**, 759–785.

Jain, M. & Balakrishnan, R. 2o12. Does acoustic adaptation drive vertical stratification? A test in a tropical cricket assemblage, Behavioral Ecology **23**, 343–354.

Kime, N. M., Turner, W. R. & Ryan, M. J. 2000. The transmission of advertisement calls in Central American frogs. *Behavioral Ecology* **11**, 71-83.

Kopuchian, C., Lijtmaer, D. A., Tubaro, P. L., & Handford, P. L. 2004. Temporal stability and change in a microgeographical pattern of song variation in the rufous- collared sparrow. *Animal Behaviour* **68**, 551–559.

Lemon, R. E., Struger, J., Lechowicz, M. J. & Norman, R. F. 1981. Song features and singing heights of American warblers: maximization or optimization of distance. *Journal of the Acoustical Society of America*, **69,** 1169-1176.

Lougheed, S. C. & Handford, P. 1992. Vocal dialects and the structure of geographic variation in morphological and allozymic characters in the rufous- collared sparrow, Zonotrichia capensis. Evolution **46**, 1443–1456.

Lugli, M., Yan, H. Y. & Fine M. L. 2003. Acoustic communication in two freshwater gobies: the relationship between ambient noise, hearing thresholds and sound spectrum. *Journal of Comparative Physiology A-Neuroethology Sensory Neural and Behavioral Physiology* **189**, 309–320.

Marten, K. & Marler, P. 1977. Sound transmission and its significance for animal vocalization. I. Temperate habitats. *Behavioral Ecology and Sociobiology*, **2,** 291-302.

Marten, K., Quine, D. & Marler, P. 1977. Sound transmission and its significance for animal vocalization. II. Tropical forest habitats. *Behavioral Ecology and Sociobiology*, **2,** 291-302.

Martin, G. R. 1981. Avian vocalizations and the sound interference model of Roberts et al. *Animal Behaviour*, **29,** 632-633.

Mathevon, N., Aubin, T. & Dabelsteen, T. 1996. Song degradation during propagation: Importance of song post for the wren Troglodytes troglodytes. *Ethology*, **102,** 397-412.

Mathevon, N., Aubin, T., Dabelsteen, T. & Vielliard, J. M. E. 2004. Are communication activities shaped by environmental constraints in reverberating and absorbing forest habitats? *Anais Da Academia Brasileira De Ciencias* **76**, 259–263.

Mitani, J. C. & Stuht, J. 1998. The evolution of nonhuman primate loud calls: Acoustic adaptation for long-distance transmission. *Primates*, **39,** 171-182.

Morton, E. S. 1975. Ecological sources of selection on avian sounds. *American Naturalist*, **109,** 17-34.

Nelson, B. S. 2003. Reliability of sound attenuation in Florida scrub habitat and behavioral implications. *Journal of the Acoustical Society of America*, **113**(5) 2901-2911.

Nemeth, E., Winkler, H. & Dabelsteen, T. 2001. Differential degradation of antbird songs in a neotropical rainforest: Adaptation to perch height? *Journal of the Acoustical Society of America* **110**, 3263-3274

Nicholls, J. A. & Goldizen, A. W. 2006. Habitat type and density influence vocal signal design in satin bowerbirds. *Journal of Animal Ecology* **75**, 549–558.

Norton, K. A. 1936. The propagation of radio waves over the surface of the earth and in the upper atmosphere: Part I. *Proceedings of the the Institute of Radio Engineers*, **24,** 1367-1387.

Norton, K. A. 1937. The propagation of radio waves over the surface of the earth and in the upper atmosphere: Part II. *Proceedings of the the Institute of Radio Engineers*, **25,** 1203-1236.

Norton, K. A. 1941. The calculation of ground-wave field intensity over a finitely conducting spherical Earth. *Proceedings of the Institute of Radio Engineers***, December 1942**, 623-639.

Parris, K. M. 2002. More bang for your buck: The effect of caller position, habitat and chorus noise on the efficiency of calling in the spring peeper. *Ecological Modelling,* **156**(2) 213-224.

Patricelli, G. L. & Krakauer A. H. 2010. Tactical allocation of effort among multiple signals in sage grouse: an experiment with a robotic female. *Behavioral Ecology,* **21**, 97–106

Patten, M. A., Rotenberry, J. T., Zuk, M. 2004. Habitat selection, acoustic adaptation, and the evolution of reproductive isolation. *Evolution* **58**(10)2144-2155.

Patterson, R. L. 1952. *The sage grouse in Wyoming*. Denver: Sage books.

Penna, M. & Solis, R. 1998. Frog call intensities and sound propagation in the South American temperate forest region. *Behavioral Ecology and Sociobiology* **42**, 371–381.

Rasmussen, K. B. 1985. The Effect of Terrain Profile on Sound Propagation Outdoors. *Journal of Sound and Vibration* **98**(1) 35-44.

Roberts, J., Hunter, M. L. & Kacelnik, A. 1981. The ground effect and acoustic communication. *Animal Behaviour*, **29,** 633-634.

Roberts, J., Kacelnik, A. & Hunter, M. L. 1979. A model of sound interference in relation to acoustic communication. *Animal Behaviour*, **27,** 1271-1273.

Rothstein, S. I. & Fleischer, R. C. 1987. Vocal dialects and their possible relation to honest status signalling in the brown-headed cowbird. *The Condor*, **89,** 1-23.

Rudnick, I. 1947. Propagation of an acoustic wave along a boundary. *Journal of the Acoustical Society of America*, **19,** 348-356.

Ryan, M. J. & Brenowitz, E. A. 1985. The role of body size, phylogeny, and ambient noise in the evolution of bird song. *The American Naturalist*, **126,** 87-100.

Saunders, J. & Slotow, R. 2004. The evolution of song structure in southern African birds: an assessment of the acoustic adaptation hypothesis. *Ostrich* **75**, 147–155.

Scott, J. W. 1942. Mating behavior of the sage grouse. *Auk*, **59,** 477-498.

Shy, E. 1983. The relation of geographical variation in song to habitat characteristics and body size in North American tanagers (Thraupinae, Piranga). *Behavioral Ecology and Sociobiology* **12**, 71–76.

Sommerfeld, A. 1909. *Annalen der Physik*, **28,** 665.

Sommerfeld, A. 1926. Uber die Ausbreitung der Wellen in der drahtlosen Telegraphie. *Annalen der Physik*, **81,** 1135-1153.

Sorjonen, J. 1986. Factors affecting the structure of song and singing behavior of some northern European passerine birds. *Behaviour*, **98,** 286-304.

Spurrier, M. F., Boyce, M. S. & Manly, B. F. J. 1994. Lek behaviour in captive sage grouse *Centrocercus urophasianus*. *Animal Behavior*, **47,** 303-310.

Sueur, J. & Aubin, T. 2003. Is microhabitat segregation between two cicada species (Tibicina haematodes and Cicada orni) due to calling song propagation constraints? *Naturwissenschaften* **90**, 322–326.

Sugiura, H., Tanaka, T. & Masataka, N.. 2006. Sound transmission in the habitats of Japanese macaques and its possible effect on population differences in coo calls. *Behaviour* **143**, 993–1012.

Tubaro, P. L. & Segura, E. T. 1994. Dialect differences in the song of *Zonotrichia capensis* in the southern Pampas: A test of the acoustic adaptation hypothesis. *The Condor* **96**(4) 1084-1088.

Tubaro, P. L. & Lijtmaer, D. A. 2006. Environmental correlates of song structure in forest grosbeaks and saltators. *The Condor* **108**, 120–129.

Van Der Pol, B. 1935. *Physica*, **2,** 843.

Wiley, R. H. 1973a. The strut diplay of male sage grouse: a 'fixed' action pattern. *Behaviour*, **47,** 129-152.

Wiley, R. H. 1973b. Territoriality and non-random mating in sage grouse, *Centrocercus urophasianus*. *Animal Behaviour Monographs*, **6,** 85-169.

Wiley, R. H. 1991. Associations of song properties with habitats for territorial oscine birds of eastern North America. *American Naturalist*, **138,** 973-993.

Wiley, R. H. & Richards, D. G. 1978. Physical constraints on acoustic communication in the atmosphere: Implications for the evolution of animal vocalizations. *Behavioral Ecology and Sociobiology*, **3,** 69-94.

Wiley, R. H. & Richards, D. G. 1982. Adaptations for acoustic communication in birds: sound transmission and signal detection. In: *Acoustic Communication in Birds* (Ed. by Kroodsma, D. E. & Miller, E. H.), pp. 131-181. New York: Academic Press.

Williams, J. M. & Slater, P. J. B. 1993. Does Chaffinch (*Fringilla coelebs*) song vary with the habitat in which it is sung? *Ibis,* **134**, 1115-1121.

Young, J. R., Hupp, J. W., Bradbury, J. W. & Braun, C. E. 1994. Phenotypic divergence of secondary sexual traits among sage grouse, Centrocercus urophasianus, populations. *Animal Behaviour* **47**(6) 1353-1362.

Young, J. R. 1994. The influence of sexual selection on phenotypic and genetic divergence among sage grouse populations. Purdue University.

CHAPTER 3:

Directional Acoustic Radiation in the Strut Display of Male Sage Grouse *Centrocercus Urophasianus*

The Journal of Experimental Biology 202, 2893–2909 (1999)
Printed in Great Britain © The Company of Biologists Limited 1999
JEB2242

DIRECTIONAL ACOUSTIC RADIATION IN THE STRUT DISPLAY OF MALE SAGE GROUSE *CENTROCERCUS UROPHASIANUS*

MARC S. DANTZKER[1,*], GRANT B. DEANE[2] AND JACK W. BRADBURY[1]

[1]*University of California, San Diego, Department of Biology, 9500 Gilman Drive, La Jolla, CA 92093-0116, USA* and [2]*Marine Physical Laboratory, Scripps Institute of Oceanography, La Jolla, CA 92093-0238, USA*

*e-mail: mdantzker@ucsd.edu

Accepted 11 August; published on WWW 13 October 1999

Summary

We present evidence that the acoustic component of the strut display of male sage grouse *Centrocercus urophasianus* is highly directional and that the nature of this directionality is unique among measured vertebrates. Where vertebrate acoustic signals have been found to be directional, they are most intense anteriorly and are bilaterally symmetrical. Our results show that sage grouse acoustic radiation (beam) patterns are often asymmetric about the birds' anterior–posterior axis. The beam pattern of the 'whistle' note is actually strikingly bilobate with a deep null directly in front of the displaying bird. While the sage grouse display serves to attract potential mates, male sage grouse rarely face females head on when they call. The results of this study suggest that males may reach females with a high-intensity signal despite their preference for an oblique display posture relative to those females. We characterized these patterns using a novel technique that allowed us to map acoustic radiation patterns of unrestrained animals calling in the wild. Using an eight-microphone array, our technique integrates acoustic localization with synchronous pressure-field measurements while controlling for small-scale environmental variation in sound propagation.

Key words: sage grouse, *Centrocercus urophasianus*, strut display, acoustic communication, mate attraction, directionality, beam pattern, lek, airsac, acoustic radiation pattern, environmental acoustics, sound propagation, sound production, directivity index.

Introduction

Studies of acoustic mate-attraction displays have concentrated on the role of spectral and temporal characteristics in signal evolution. Despite the likely importance of signal directionality (Bradbury and Vehrencamp, 1998; Witkin, 1977), the fitness consequences of directional patterns of acoustic display have been largely overlooked because these patterns have been considered too difficult to map in the field. In this paper, we present measures of the acoustic radiation (beam) patterns of the male sage grouse strut display. The spectral and temporal aspects of this display have been extensively examined (Gibson, 1996; Gibson and Bradbury, 1985; Gibson et al., 1991; Hartzler, 1972; Spurrier et al., 1994; Wiley, 1973a; Young, 1994). However, despite anecdotal observations of strong directionality (Wiley, 1973a; J. W. Bradbury and M. S. Dantzker, personal observation), these directional patterns have not been quantified and their consequences have not been explored.

The strut display of the male sage grouse is highly stereotyped and elaborate (Hjorth, 1970; Honess and Allred, 1942; Wiley, 1973a; Young et al., 1994). Prior to display, a male sage grouse inflates a region of his esophagus that sits in a muscular bag at the base of his neck. The strut display is a series of three heaves of this esophageal expansion through outreached wings held stiffly at either side (Fig. 1). Sage grouse keep their beak closed for most of the display; sound production coincides instead with tandem anterior expansions of the esophageal air sac through ventral apteria (featherless regions) on the neck (Hjorth, 1970; Young et al., 1994). These dark, inflated skin patches bulge repeatedly through a dense region of white feathers to create a dramatic and unusual acoustic (Fig. 2) and visual (Fig. 1) display. While many other groups of vertebrates use external air sacs in sound production and radiation, this explosive use of dual anterior air sacs is unique to the *Centrocercus* grouse strut display. This mate-attraction display has evolved under the intense sexual selection of a lek mating system (Höglund and Alatalo, 1995). However, male sage grouse do not appear to direct their display efforts towards females by facing them during display (Simon, 1940; Wiley, 1973a). In this study, we examine the directionality of the acoustic signal produced by this unusual display mechanism of sage grouse.

Directional patterns of acoustic radiation, beam patterns, have usually been measured under laboratory conditions where the animal's position and orientation are held constant and repeated measurements are made on induced or coaxed phonation. Similar methods can be used in the field when the animals of interest remain stationary during display and will tolerate movements around them (Gerhardt, 1998). Sage

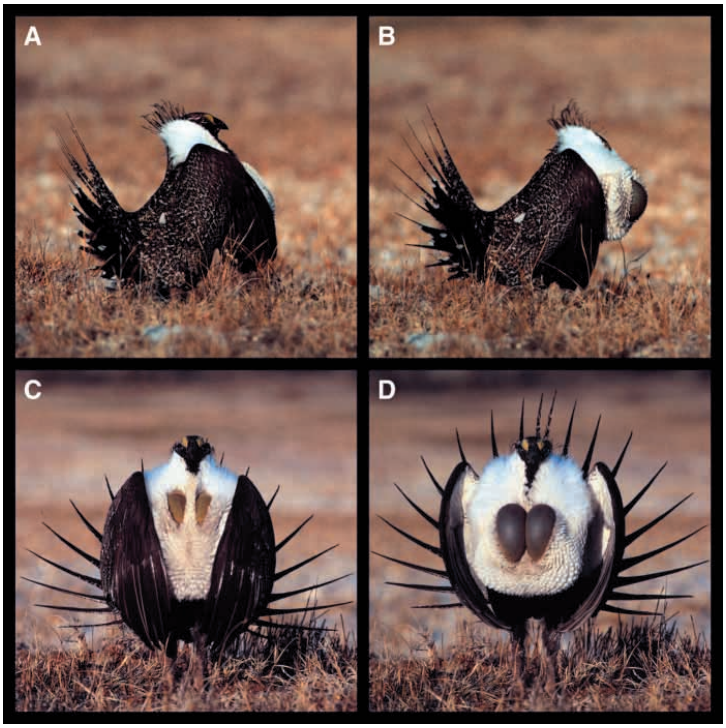

Fig. 1. Strut display of male sage grouse. (A) Profile with white esophageal sac held behind the two outstretched wings. (B) Profile with sac fully expanded and visible through the anterior apterium on the sac. Note that the head is no longer visible. (C) Pre-expansion thrust of the air sac from the front. The apteria are visible but not distended. (D) Full expansion of the apteria, accompanied by an opening of the wings. Note that the expanded apteria touch along the midline. The exposed air sacs and the beak face forwards for the duration of the strut. The vegetation at the male's feet is typical of the lek. All exposures are either 1/4000 s or 1/8000 s.

grouse afford neither such opportunity as they are rarely available for captive study and wild birds travel rapidly around their territories between consecutive displays. We developed a novel method for the measurement and calculation of these beam patterns which allows for the use of unrestrained and actively mobile wild individuals while correcting for heterogeneity in the acoustic environment.

Here, we present evidence that acoustic radiation patterns of the sage grouse strut display are unlike any previously measured in a vertebrate. Where vertebrate acoustic signals have been found to be directional, they are most intense anteriorly and are bilaterally symmetrical (see Discussion). Our results show that sage grouse beam patterns are variably asymmetric about the animal's anterior–posterior axis. The beam pattern of one of the call elements, the 'whistle', has a deep minimum (null) directly in front of the displaying bird and is instead most intense to the sides and behind.

Materials and methods

Sage grouse *Centrocercus urophasianus* (Bonaparte) travel across the mostly flat display arena (lek) on foot; therefore, we focused our efforts on characterizing acoustic directionality in the horizontal plane. The sound field surrounding an acoustic source, in this case a strutting sage grouse, is considered to be directional when the amplitudes of the induced pressure waves

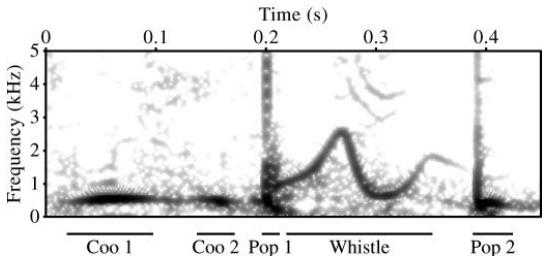

Fig. 2. Spectrogram of the acoustic component of a male sage grouse strut display showing the time limits of each note as well as the notes' names as used by Gibson and Bradbury (1985) and Wiley (1973a). Spectrogram parameters: frame size, 512 point; sampling rate, 22.5 kHz; windowing function, Hanning; frame overlap, 94 %.

vary as a function of angle. This angular variation is described by a normalized function called the beam pattern (Kinsler et al., 1982, p.175). Here, we describe a method for measuring beam patterns of unrestrained animals in complicated acoustic environments.

Measurement summary

We recorded male sage grouse using an eight-microphone array that we deployed around their display territories

(described in greater detail below). The essential problem we faced in determining the beam pattern from these recordings was to separate the superimposed effects of source directionality, which were inherent to the calling bird, and directionality introduced by the environment. In our case, this environmental effect arose primarily from interfering acoustic reflections from the lek surface. To discriminate between the directional effects of the source and those that were environmentally induced, we measured the directionality of the signal received from a known, calibrated source positioned inside our array. This calibration procedure allowed us to identify and quantify the effects of the environment across the range of frequencies used by the sage grouse. We could then calculate beam patterns generated only by the directional properties of the source. The mathematical basis underlying our calibration procedure, as well as the concept of beam pattern relevant to this study, are developed in some detail below.

Beam pattern and the directional factor

In the far field, the pressure field in a horizontal plane, $p_s(r,\theta)$, can be expressed as a function of distance, r, and horizontal angle, θ, from the sound source such that:

$$p_s(r,\theta) = p_{s,axis}(r)H(\theta)\,. \quad (1)$$

$H(\theta)$ is the directional factor that has been normalized so that the maximum value is unity (Kinsler et al., 1982). The value of θ for which $H(\theta)=1$ defines the acoustic axis of the radiation pattern. The term $p_{s,axis}(r)$ is the far-field pressure on the acoustic axis. Therefore, $p_{s,axis}(r)$ is dependent on both range and source level, while $H(\theta)$ is dependent only on angle. The directional factor is usually represented as its decibel (dB) equivalent, the beam pattern, $b(\theta)$ (Kinsler et al., 1982) using:

$$b(\theta) = 10\log H^2(\theta)\,, \quad (2)$$

where the maximum value of the beam pattern, $MAX[b(\theta)]$, is 0 dB.

In general, both source strength and directionality vary with frequency of vibration, f. Accordingly, the directional factor, $H(f,\theta)$, is most generally expressed as function of both angle and frequency, a convention we will adopt. Additionally, since the directional factor is independent of distance, equation 1 can be rewritten for a fixed distance such that:

$$p_s(f,1,\theta) = p_{s,axis}(f,1)H(f,\theta)\,, \quad (3)$$

where r is 1 m and is the directional factor now normalized so that each frequency component has a corresponding value of θ, where $H(f,\theta_{max})=1$. We further define θ as the horizontal clockwise angle with respect to the bird's anterior–posterior axis, where $\theta=1$ directly in front of the displaying bird. Here, $p_s(f,1,\theta)$ is the free-field pressure field 1 m from the sound source (bird) measured as a function of frequency and angle. The pressure 1 m from the source on the acoustic axis is $p_{s,axis}(f,1)$, which reflects the frequency-dependence of the source level. It follows that for any one frequency:

$$p_{s,axis}(f,1) = MAX[p_s(f,1,\theta)]\,. \quad (4)$$

In a controlled setting, where interfering acoustic returns from the environment can be eliminated, the free-field values of $p_s(f,1,\theta)$ can be measured directly. From this, one can calculate the directional factor and a beam pattern for each frequency component. In contrast, our experimental design measures the acoustic field around a grouse calling just above the ground. Sound propagation near the ground is complicated by interference from multiple acoustic reflections. It is therefore necessary to correct for the transmission loss in order to determine the free-field values of $p_s(f,1,\theta)$.

The free-field source sound pressure field 1 m from the bird, $p_s(f,1,\theta)$, can be determined from measures of the acoustic field using:

$$p_s(f,1,\theta) = \frac{p_r(f,r,\theta)}{TL(f,r,\theta)}\,, \quad (5)$$

where $p_r(f,r,\theta)$ is the measured sound pressure, including all transmission effects, and $TL(f,r,\theta)$ is the transmission loss across the same propagation path. Previous field studies of source directionality have used a homogeneous geometric spreading model for transmission loss which is independent of frequency, $TL(r)=1/r$, and identical across all paths of equal distance (Archibald, 1974; Bennet-Clark, 1987; Forrest, 1991; Gerhardt, 1975; Narins and Hurley, 1982; Witkin, 1977). Our preliminary examination of sound propagation over the lek revealed that models such as this were insufficient for this environment. Therefore, we empirically measured the transmission loss curves for each propagation path (see Appendices A and B).

It is now possible, from equations 3, 4 and 5, to derive an equation for the directional factor $H(f,\theta)$ from the measures of the pressure field gathered by our receiver array and the independently measured transmission loss curves for each propagation path. This is:

$$H(f,\theta) = \frac{\dfrac{p_r(f,r,\theta)}{TL(f,r,\theta)}}{MAX\left[\dfrac{p_r(f,r,\theta)}{TL(f,r,\theta)}\right]}\,. \quad (6)$$

The two-dimensional directional factor $H(f,\theta)$ is cumbersome to visualize. It is helpful to extract the frequency-dependence by calculating a narrow-band average. As long as the band of frequencies is narrow, this simplification is appropriate. To do this, we calculate a band-averaged power Π_{band} using:

$$\Pi_{band}(\theta) = \frac{1}{\Delta f}\sum_{f_0}^{f_1}\frac{|p_r(f,r,\theta)|^2}{TL^2(f,r,\theta)}\,, \quad (7)$$

where $|p_r(f,r,\theta)|^2$ is the squared modulus of the pressure measurements, the power spectral density. This allows us to calculate a measure of the band-averaged squared directional factor, $H_{band}^2(\theta)$, using:

$$H_{band}^2(\theta) = \frac{\Pi_{band}(\theta)}{MAX[\Pi_{band}(\theta)]}\,. \quad (8)$$

From this, we can define the band-averaged beam pattern as:

$$b_{\text{band}}(\theta) = 10\log H_{\text{band}}^2(\theta)\,. \quad (9)$$

The samples of the acoustic field, $p_r(f,r,\theta)$, were gathered synchronously using an eight-microphone array encircling a displaying individual's territory (Fig. 3). The bird was unrestricted in its choice of display sites and moved constantly around its territory. For each call location, there were eight different propagation paths, each with a unique $TL(f,r,\theta)$. There was a practical limit to the number of transmission loss curves that could be measured. In this first application of our method, we restricted our measures of the directional factor to calls that had been generated near the four sites where we had measured the transmission loss along all eight paths. We used acoustic localization to identify these vocalizations. This method enabled us to measure the beam pattern of individual call elements from individual calls without averaging across calls and without unrealistic assumptions about sound propagation.

Study site

We constructed acoustic radiation maps from recordings of three males displaying at a lek (lek 8) in Long Valley, Mono County, California, USA (37°40′N, 118°50′W) from 4 to 21 April 1997. This spanned the main period of display activity in this year. Lek 8, like most of the leks in this region, is located on a mostly flat alkali meadow surrounded by rolling hills of sagebrush. The vegetation on the meadow (*Carex* sp. and saltgrass) was sparse and low (as seen in Fig. 1).

Array recordings

We deployed recording arrays (Fig. 3) at two focal sites chosen to overlap 1–2 male display territories where female visits were common. In both these areas, we arranged the circular eight-point arrays using a Sokkia measuring system (DIO343) to measure angle and a tape measure for distance. We positioned the microphones at each point on this array at approximately female head height (approximately 20 cm) so that their diaphragms faced the center of the array. On one side of the array, 20 m from the center, we positioned a hide that served as an observation and recording station (see Appendix A for details of the acoustic recording system). We stretched alkali-resistant microphone cables from the microphones to the hide. Sage grouse avoid exposed cables so we buried the cables in shallow (4 cm) ditches. This array design minimized disturbance to the birds' movements and activities.

Using the Sokkia measuring system, we also assessed the relief of the encircled area (Fig. 3). This was accomplished by marking the distance from a fixed plane above the lek, determined by the height of the leveled survey scope, to the ground below. We measured this distance at 1 m intervals along the eight radial paths from the array center to each microphone location. From these data, we constructed topographic maps using MATLAB's 'contour' function, with the heights converted so that they were relative to the array's lowest point.

We made synchronous video recordings for all focal studies

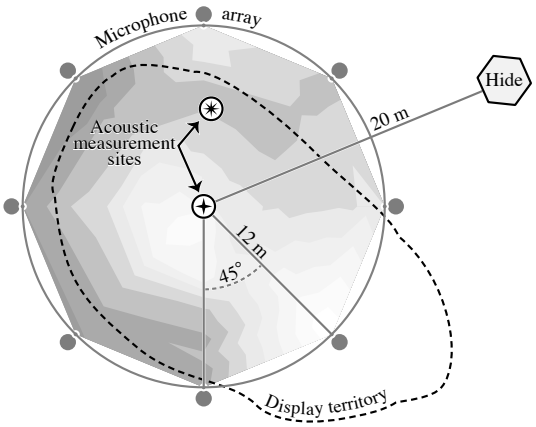

Fig. 3. Schematic drawing of the acoustic array deployment in relation to a male's display territory. An acoustic source was deployed for sound propagation measurement at two acoustic measurement sites, one of which was at the center of the array. The topography of the encircled area was measured when the array was deployed. A map of the relief is shown here with a contour interval of 10 cm.

using a Canon Hi-8mm ES2000 camera positioned in the hide approximately 0.75 m from the ground on a tripod. We synchronized the audio and video recordings by video-taping the running tape counter on the face of the audio recorder for a few seconds at the beginning of each recording session. Each day, we started recording as soon as there was sufficient light and continued until the males ceased their activity on the lek.

We designated two sites within each array as measurement positions: the center of the array and a position off center where the birds were seen calling. We measured transmission loss along each radial propagation path from these points as described in Appendices A and B. To minimize disturbance to the birds, we made these measurements in the birds' absence. Preliminary study showed that propagation properties are stable through the night and the display period (05:00–07:30 h), but change rapidly later in the morning (see Results and Fig. 4). These measurements were therefore made between 23:00 h and 03:30 h when the propagation effects are highly concurrent with those of the display period but the birds are absent.

Data acquisition

We digitally transferred all recordings to a Power Macintosh for analysis using an eight-track synchronous acquisition system (Digidesign ProTools v.4.1 with 888 I/O coupled to a TASCAM IF-88AE digital audio-interface unit). Using this software, we identified short sections of audio for detailed analysis, then created synchronized monaural files (22.05 kHz, wave format) for each track, which we transferred to MATLAB (MathWorks, 1998) for subsequent analyses.

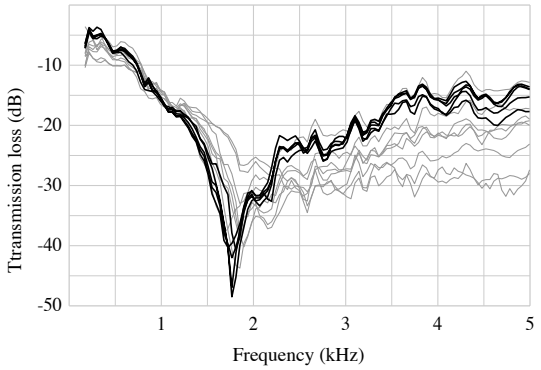

Fig. 4. Transmission loss functions for 12 measurements over the same 12 m stretch of the lek. Black lines show propagation during the period of display (05:00–07:30 h) and the period of calibration (23:30–03:30 h), while gray lines show the propagation at other times of day (08:00–23:00 h).

Acoustic localization

Our method for the mapping of acoustic radiation patterns required that vocalizations be produced near the designated measurement sites. We used acoustic localization to identify vocalizations produced in very close proximity to these calibrated sites ($\leqslant$1.5 m). Before localization, we preprocessed all signals with a highpass filter (second-order Butterworth with 200 Hz cut-off; MathWorks, 1998).

We employed a localization algorithm based on a least-squares best fit (Spiesberger and Fristrup, 1990) to equations that relate the sources' positions to the known locations of the microphones and the measured time delays in signal arrival between the microphones (Watkins and Schevill, 1971, 1972). We modified these equations in a number of ways. First, neglecting the small height variations of the lek surface, we reduced these equations to a two-dimensional case. Second, we employed the MATLAB function 'backslash' for the least-squares calculation of the over-determined set of linear equations (MathWorks, 1998). Third, the time delay estimates were taken from the peak location of the time-domain cross-correlation functions generated with the MATLAB function 'XCORR' (MathWorks, 1998; Shure and McClellan, 1997). Fourth, and most significantly, we calculated the final location estimate as the average location of eight semi-independent calculations made using each of the eight microphones as the designated reference. The algorithm requires the designation of a reference microphone, and previous users have designated a single receiver as this reference (Freitag and Tyack, 1993; Spiesberger and Fristrup, 1990; Watkins and Schevill, 1971, 1972). Our multi-reference algorithm increases the number of time delay estimates used in the calculation by a factor of four. In addition, only calls that showed a high correspondence between all eight location estimates were used in these analyses. We found that imperfections in the data (e.g. overlapping vocalizations, low signal/noise ratio) led to disparate estimates of location. This additional step allowed us to identify and purge these vocalizations from the data set.

Our system was well suited for acoustic localization using this algorithm. The method assumes that the speed of sound is known, that there is little wind and that receiver positions are accurately known (Spiesberger and Fristrup, 1990). Sound speed was calculated from air temperature measurements. Concurrent wind measurement allowed us to exclude data recorded during periods of wind in excess of 3 km h^{-1}. Receiver positions were definitely fixed and precisely known. Localization accuracy is high when the sound source is located near the microphone array (McGregor et al., 1997) and is best when the animal is completely encircled by receivers (Watkins and Schevill, 1971, 1972). Both were true of our experimental design. Also, the number of receivers, eight, far outnumbered the minimum (four) necessary to estimate the location unambiguously in two dimensions using this algorithm. In addition, the abrupt frequency and amplitude modulations of the sage grouse vocalization (Fig. 2) yielded sharp unambiguous peaks in the time-domain cross-correlation functions.

For each vocalization, the bird's location was combined with the orientation of the male relative to the receiver array to determine each receivers' value of θ for that call. The orientation could not be determined acoustically and was therefore estimated from the synchronous video recordings.

Beam pattern reconstruction

Band-averaged beam patterns, $b_{\mathrm{band}}(\theta)$, were then calculated for those calls that were generated at the measurement locations. The propagation delays, identified as part of the localization algorithm, were removed from the time series data in order to synchronize the signals. We then Fourier-transformed the data using a 128-point fast Fourier transform (with a zero-overlap Hanning window) and calculated the power spectral density, $|p_{\mathrm{r}}(f,r,\theta)|^2$. This, along with the measures of transmission loss, $TL(f,r,\theta)$, calculated as in Appendix B, were then substituted into equations 7 and 8 to yield the band-averaged beam pattern over a 5.8 ms time slice. The transmission loss corrections were truncated at the measurement-system noise floor, corresponding to TL=−45 dB.

The 5.8 ms duration of these time slices is arbitrary with respect to the vocalization. When we are interested in examining fluctuations in the beam pattern over short time scales, this time slice duration is useful. However, when the beam pattern is found to be fairly constant across an individual call component, it is more meaningful to map the beam patterns for the entire note of the acoustic display. Rather than just averaging the beam patterns of the individual time slices, we weight the time-averaged beam pattern so that the time slices that contain more acoustic energy contribute proportionally more to the measure of directionality. The

squared directional factor which is both band-averaged and time-averaged is:

$$H_{\text{band,note}}^2(\theta) = \frac{\frac{1}{n}\sum_{j=1}^{n}\Pi_{\text{band,j}}(\theta)}{MAX\left\{\frac{1}{n}\sum_{j=1}^{n}\Pi_{\text{band,j}}(\theta)\right\}}, \quad (10)$$

where n is the number of time slices over which the call component stretches; j is the time slice index and Π_{band} is the power in the frequency band defined in equation 7. Subsequently, the band-averaged beam pattern for that note is:

$$b_{\text{band,note}}(\theta) = 10\log H_{\text{band,note}}^2(\theta)\,. \quad (11)$$

Beam pattern comparison

Maps of the beam patterns allow for qualitative comparisons of directionality. In addition, we can calculate numerical measures of these patterns which encapsulate the variation and allow quantitative comparisons. In this paper, we employ four such quantitative measures. These are: (1) angle of maximum lobe, θ_{max}, defined such that $b(\theta_{max})$=0 dB; (2) angle of the radiation pattern minimum, θ_{min}, defined such that $b(\theta_{min})$=*MIN*[$b(\theta)$]; (3) beam pattern range in dB, $|b(\theta_{max})-b(\theta_{min})|$; and (4) the directivity index, DI, also in dB. These values are presented as means ± standard deviations.

The directivity index (DI) measures the degree to which a radiation pattern is concentrated. This index compares the intensity of the maximum lobe of a beam pattern with the intensity of a uniform source radiating the same total power output. In this way, the DI incorporates aspects of the radiation field off the maximum lobe whereas beam width measures do not. Derivations of DI are available elsewhere for three-dimensional radiation patterns (e.g. Kinsler et al., 1982). In Appendix C, we derive an analogous measure for radiation patterns resolved only in a single plane.

Results

Environmental acoustics

Transmission loss fluctuated with time of day but was stable from 22:30 to 07:30 h (Fig. 4). Therefore, late-night measurements made within a bird's territory while the animal was away were highly concurrent with propagation during the period of display. Below 1.2 kHz, these transmission loss measurements were extremely consistent, differing in value by a mean of 1.1±0.5 dB (N=5). The higher frequencies, 1.2–5.0 kHz, show more variation, 3.7±1.8 dB (N=5), across the time window of calibration and bird display. Because of this variation in the transmission loss curves over time, we estimate our error of measurement for beam pattern mapping to be ±2 dB below 1200 Hz and ±4 dB above 1200 Hz.

The transmission loss curves for sound propagation over the different paths of the lek (Fig. 5) show many similarities but also important differences. Measurements made from the center of each array are easiest to compare since the path lengths are equal (Fig. 5C,D). In both arrays, transmission loss curves for each path are highly concordant below 500 Hz. At these low frequencies, sound propagation was reliable across paths and less acoustic pressure was lost in transmission than in free-field spherical spreading. The low-frequency components of the sage grouse display (coos and pop 2) have most of their energy in this well-propagated frequency range (Fig. 2). Therefore, these components of the strut display must propagate reliably across fairly long distances.

In contrast, the higher-frequency whistle spans a less reliable frequency band from 0.6 to 3.2 kHz (Fig. 2). Sound in this range propagated far less effectively than free-field spherical spreading. Also in this frequency range we find a deep propagation minimum (notch) in the transmission loss curves of all paths. The exact position of this notch is variable between paths but is always between 1 and 2 kHz. Even outside the path-specific propagation notch, there are 10–15 dB differences in transmission loss between the paths. Long-distance communication in this frequency range is very unreliable, suggesting that the whistle component of the call might be an exclusively close-range component of sage grouse communication. Shorter paths show shallower notches and a concomitant decrease in the frequency-dependence of propagation (Fig. 5D,E).

The major features of our transmission loss curves (Figs 4, 5) are consistent with the measured curves and models of previous acoustic studies of sound propagation close to the ground (Embleton, 1996; Embleton et al., 1976, 1983). These major features include (1) low levels of loss for the low frequencies, (2) a stop-band notch in the intermediate frequencies due to interference between the direct and reflected paths and (3) lower levels of loss again for the higher frequencies where the reflected paths are less coherent. These features are expected for propagation near most surfaces.

There is, however, much heterogeneity between the transmission loss curves, even those with identical path lengths (Fig. 5C,D). Differences between these curves reveal propagation effects that arose from differences in topography (Fig. 5A,B) and soil composition. No extant acoustic model sufficiently explains the heterogeneity in the propagation curves that we have presented here. However, using our method, we were still able to reconstruct beam patterns for calls produced at sites where we had made empirical measures of the transmission loss. All these sites and their associated transmission loss curves are shown in Fig. 5.

Acoustic localization

We identified 39 vocalizations produced within 1.5 m of our calibration sites: 30 vocalizations from male A, seven from male B and two from male C. Although this sample is skewed towards a single individual, the range of directionality exhibited by male A subsumes the range of values exhibited by the other two males. Therefore, we consider each vocalization to be independent for statistical analysis. Where

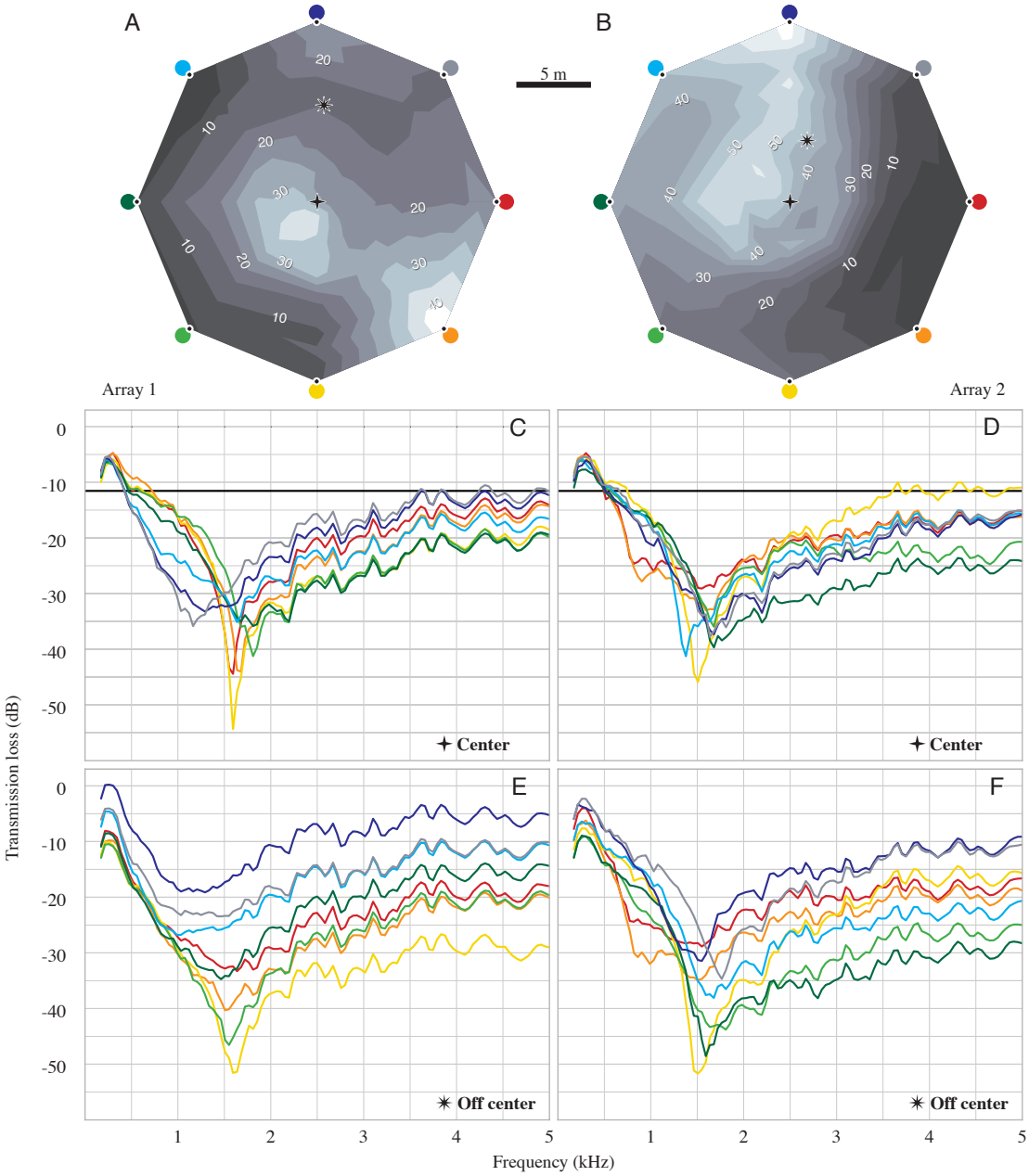

Fig. 5. Transmission loss curves for all propagation paths used for the reconstruction of acoustic radiation patterns and topographic maps of each recording array. (A,B) The maps of each array show topographic features (with elevation in cm) in relation to the location of the acoustic measurement sites and the microphones. The microphones are color-coded, corresponding to the line color of the transmission loss curve from the measurement site to that microphone. (C,D) Transmission loss for propagation paths from the center of the array to each of the microphones. The solid black horizontal line shows the level of transmission loss expected from spherical spreading alone. (E,F) Transmission loss for propagation paths from the off-center measurement site to each of the microphones. Since the propagation path lengths are unequal, the transmission loss expected due to spherical spreading alone is different for each path. For simplicity, these values are not shown.

appropriate, we also present directionality measures for each individual. In our subsequent studies, we will use an omnidirectional speaker that allows us to calibrate more sites within each array and thereby achieve sample sizes sufficient for comparisons between males.

Beam patterns

We found that the acoustic component of the sage grouse strut display is directional. This directionality showed high between-note variability in all measured vocalizations. However, we found that the coos and pops showed high within-note stability in their beam patterns. These notes, therefore, were best examined by calculating time-averaged beam patterns, $b_{band,note}(\theta)$. In contrast, the beam patterns of the frequency-modulated whistles varied significantly in time and consequently were examined as a series of discrete time slices, $b_{band}(\theta)$.

The coo notes had directional beam patterns (Table 1) which were consistent between the two coos of a single call but variable between vocalizations (Fig. 6). The beam patterns of the coos tended to be loudest to the front and quietest at the sides, with a variable amount of energy radiated behind the displaying bird. The orientations of the major lobes of the coo beam patterns were variable with respect to the anterior–posterior axis of the birds. In many vocalizations, the maximum lobe was rotated by up to 45° to either side of the bird, and in some examples the posterior lobe was actually slightly louder than the anterior lobe. Fig. 7 illustrates these trends as histograms of the maximum and minimum points on each beam pattern, θ_{max} and θ_{min}. These maxima and minima had significantly non-random angular distributions (Table 2).

The two pops showed markedly different beam patterns from the coos and from each other. Pop 1 was strongly directional (Table 1) but the angular distribution of the beam pattern maxima and minima was not distinguishable from random (Rayleigh test: combined data set, N=39, P>0.1). Pop 2 was much less directional (Table 1). The beam pattern range for many vocalizations fell below the noise floor of our technique, 4 dB in this frequency band. However, when we restricted our examination of the directionality to those pop 2 notes with a beam pattern range greater than the potential measurement error, we found that, when the beam pattern was significantly directional, this pop tended to be louder in front of the bird and quieter behind (Table 2).

During the duration of the whistle, both the dominant frequency and the air-sac geometry change extensively. This variation should be accompanied by fluctuations in the directionality of acoustic radiation. Such variability was seen in all whistles (Fig. 8). Despite this variability, all whistles showed a deep anterior null in the beam pattern. This null was not present for the entire whistle but was always present for at least part of it. In contrast to the beam patterns of the coo and pop notes described above, the modal positions of the whistles' beam pattern minima, mode[θ_{min}], were typically in front of the strutting bird (Fig. 9; Table 2). In addition, the modal maxima, mode[θ_{max}], of the whistles were never in front of the bird but were oriented to either side or behind. Thus, the angular distribution of the whistles' modal maxima and minima are the inverse of the coos' distributions. On average,

Table 1. *Directionality of the coo and pop notes of the sage grouse strut display*

Male	N	$b_{band, note}(\theta)$	Coo 1	Coo 2	Pop 1	Pop 2
A	30	Range (dB)	8.5±2.3	9.7±2.3	9.6±3.8	5.0±1.4
		DI (dB)	3.3±1.0	3.7±0.9	3.8±1.4	2.5±0.7
B	7	Range (dB)	8.6±2.6	7.6±1.6	11.4±3.3	6.2±1.5
		DI (dB)	3.4±1.5	3.2±1.3	4.3±1.0	2.5±0.8
C	2	Range (dB)	9.7±2.7	9.8±1.4	5.3±0.0	4.2±0.1
		DI (dB)	2.8±0.2	2.8±0.2	3.1±0.0	1.8±0.1
All	39	Range (dB)	8.6±2.4	9.4±2.3	9.7±3.8	5.2±1.4
		DI (dB)	3.3±1.1	3.6±1.0	3.8±1.3	2.5±0.7

The mean and standard deviation of two measures of directionality are shown for each individual and for the entire sample of vocalizations.

The top value is the range of the measured values of the beam patterns. The bottom value is the directivity index (DI) of those patterns. A uniform sound field has a DI of 0 dB and a dipole has a DI of 3.01 dB (see Appendix C).

$b_{band, note}(\theta)$, time- and band-averaged beam pattern.

Table 2. *Results of Rayleigh tests on the angular distribution of the beam patterns' maxima and minima, θ_{max} and θ_{min}*

Call note	Beam pattern measure	All males	Male A	Male B
Coo 1	θ_{max}, forward	z=7.81	z=5.34	z=2.86
		N=39	N=30	N=7
		P<0.001	P<0.005	P<0.1 (NS)
	θ_{min}, sideways	z=7.38	z=6.01	z=2.03
		N=39	N=30	N=7
		P<0.001	P<0.002	P<0.2 (NS)
Coo 2	θ_{max}, forward	z=19.02	z=13.75	z=3.56
		N=39	N=30	N=7
		P<0.001	P<0.001	P<0.05
	θ_{min}, sideways	z=12.17	z=9.44	z=4.56
		N=39	N=30	N=7
		P<0.001	P<0.001	P<0.01
Pop 2	θ_{max}, forward	z=9.19	z=5.38	z=2.94
		N=29	N=21	N=6
		P<0.001	P<0.005	P<0.1 (NS)
	θ_{min}, behind	z=9.25	z=8.82	z=3.84
		N=29	N=21	N=6
		P<0.001	P<0.001	P<0.02
Whistle	mode[θ_{max}], sideways	z=4.70	z=4.33	z=4.43
		N=39	N=30	N=7
		P<0.01	P<0.02	P<0.01
	mode[θ_{min}], forward	z=11.06	z=6.73	z=3.36
		N=39	N=30	N=7
		P<0.001	P<0.001	P<0.05

No tests were conducted for male C because the sample size was insufficient.

NS, not significant.

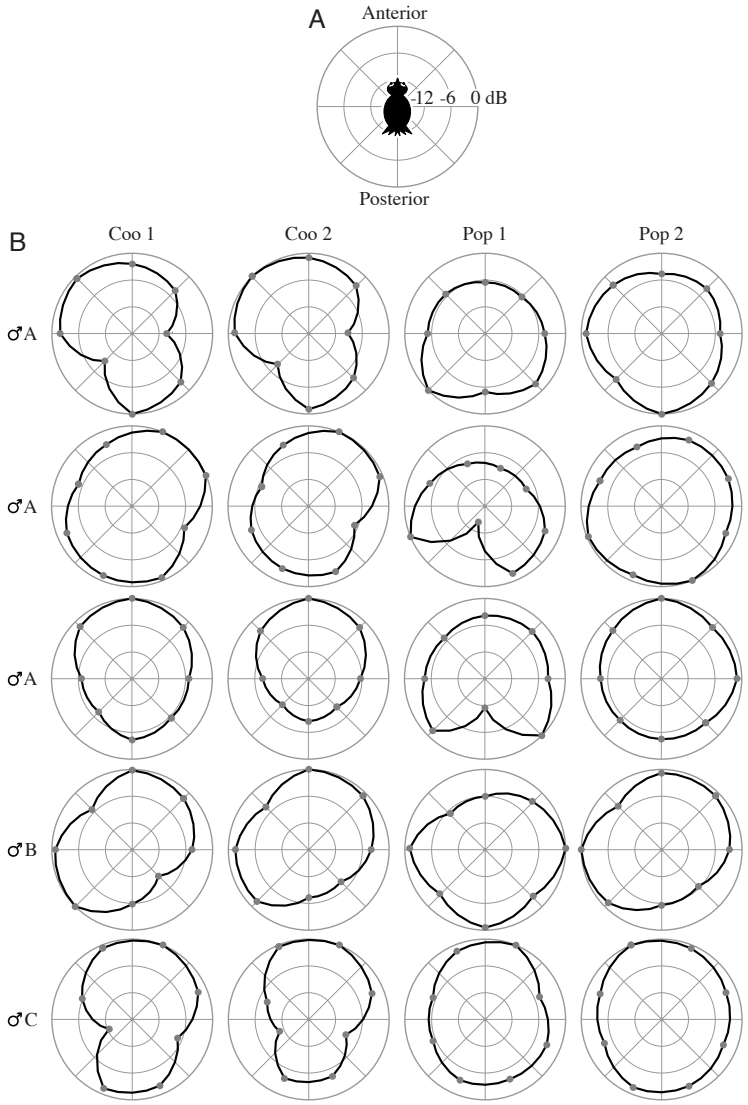

Fig. 6. Acoustic beam patterns, $b_{band,note}(\theta)$, for the coos and pops. (A) Polar diagram showing the format of all acoustic radiation plots used here. Viewed from above, the birds are standing at the center facing upwards. Divisions are 6 dB. Here, the dynamic range represented is 18 dB. (B) Beam patterns of five representative strut displays. The first three rows show the range of patterns observed from male A. The last two rows show one strut from each of the other two focal males (males B and C). The frequency bands used in the average were 300–600 Hz for coo 1, coo 2 and pop 2 and 600–1200 Hz for pop 1.

the whistle was highly directional and extremely variable (Table 3). At its most directional time slice, the average whistle was 22.9±3.4 dB less intense in front of the calling bird than it was at the sides (Table 3).

Discussion

The results described above show that sage grouse strut displays have strikingly directional patterns of acoustic radiation. Here, we compare these directional patterns with the patterns observed in other vertebrates and show that the sage grouse radiates sound in a fashion that is fundamentally different from that for any previously measured vertebrate (see Gerhardt, 1998, and below for review). To measure these patterns and map them accurately, we had to develop a new method for the measurement of acoustic directionality in the field. We start our discussion by explaining the major novelties and advantages of our method that allowed us to make these discoveries.

Methodological conclusions

There are two features of our method for measuring acoustic emission patterns that are advantageous relative to previous methods used in both laboratory and field studies:

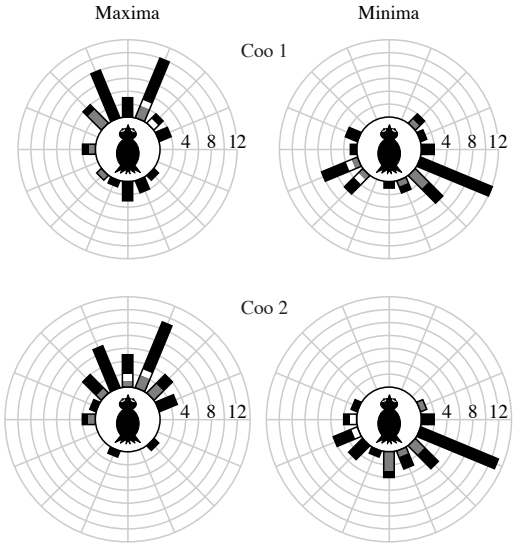

Fig. 7. Polar histograms showing the orientation of the beam patterns' major features relative to the anterior–posterior axis of the birds for coo 1 (top) and coo 2 (bottom). These frequency distributions show beam pattern maxima (left), θ_{max}, and minima (right), θ_{min}, for all 39 measured vocalizations. The contribution of each focal male is indicated by the density of the cell in each histogram bar; black is male A, gray is male B and white is male C.

Table 3. *Directionality of the frequency-modulated whistle of the sage grouse strut display*

Male	*N*	$b_{band}(\theta)$	Mean	Maximum	Minimum
A	30	Range (dB)	13.6±2.1	22.8±3.6	6.3±1.7
		DI (dB)	4.4±0.6	6.7±0.8	2.2±0.5
B	7	Range (dB)	16.1±2.1	23.6±3.2	8.5±1.2
		DI (dB)	4.6±0.3	6.8±0.5	2.7±0.4
C	2	Range (dB)	12.0±0.2	22.7±0.9	3.6±0.2
		DI (dB)	3.8±0.1	6.7±0.3	1.6±0.2
All	39	Range (dB)	14.0±2.3	22.9±3.4	6.5±1.9
		DI (dB)	4.4±0.5	6.7±0.7	2.3±0.6

The mean and standard deviation of two measures of directionality are shown for each individual and for the entire sample of vocalizations.

The top value is the range of the measured values of the beam patterns. The bottom value is the directivity index (DI) of those patterns.

$b_{band}(\theta)$, band-averaged beam pattern.

(1) synchronous recordings from multiple angles around the focal individual, (2) explicit measurement of environmental effects on propagation. Here, we examine the specific advantages associated with each of these features.

Advantages of synchronous recordings

Previous studies have made detailed beam pattern maps using two microphones by repeatedly repositioning a single receiver at various angles while another remains in a fixed position to correct for fluctuations in overall amplitude. This asynchronous, two-microphone method allows for fine spatial resolution in the mapping of acoustic fields and has been used to reconstruct some very complicated radiation patterns (Au et al., 1995; Bennet-Clark, 1987; Forrest, 1991; Hartley and Suthers, 1987, 1989, 1990; Hunter et al., 1986; Larsen and Dabelsteen, 1990). The only limit to the spatial resolution is the number of measurement sites chosen by the researcher. However, this method can only be used when the focal animal's position is fixed by behavior or design and the same vocalization can be coaxed or induced for repeated measures. In addition, using asynchronous measures to reconstruct radiation patterns assumes that beam patterns remain constant between vocalizations of the same type. Our synchronous recording technique allowed us to test this assumption in sage grouse. Our results show that the beam patterns for each call note vary between vocalizations. Therefore, this assumption may be inappropriate for some organisms, and synchronous recording is therefore preferred (Gerhardt, 1998). The trade-off associated with synchronous recording is that the spatial resolution of radiation maps is limited by the number of receivers deployed. This number has practical limitations, especially in the field. However, our eight-microphone design was sufficient to describe the major features of the radiation patterns produced by sage grouse.

Advantages of explicit environmental measures

Laboratory study of acoustic emission fields has one principal advantage over our method: a controlled environment. Anechoic recording chambers obviate detailed environmental calibration since the measures of the acoustic field are direct measures of the emission field. For many organisms, laboratory study is impossible or impractical and measures must be made in the field. Field study also allows for the measurement of acoustic directionality in the context of natural display behavior. Field studies must account for the complexities of propagation in natural environments. Previous field studies of acoustic directionality have dealt with the environment by either assuming or demonstrating (a) that sound propagation is not frequency-dependent over the measurement distance and (b) that environmental effects are homogeneous across the measurement paths. These simplifications allow the treatment of field measurements as if they were conducted in an anechoic chamber and thus require no explicit corrections for propagation effects. These simplifications may be appropriate (a) when the measurement propagation paths are very short, (b) when there are no nearby surface boundaries, and (c) when all paths are free from heterogeneous features. To make measurements on unrestrained and mobile sage grouse in the wild, our method used longer measurement distances over a heterogeneous surface boundary. Therefore, neither simplification was appropriate. Instead, we measured the precise transmission loss curve for each measurement path

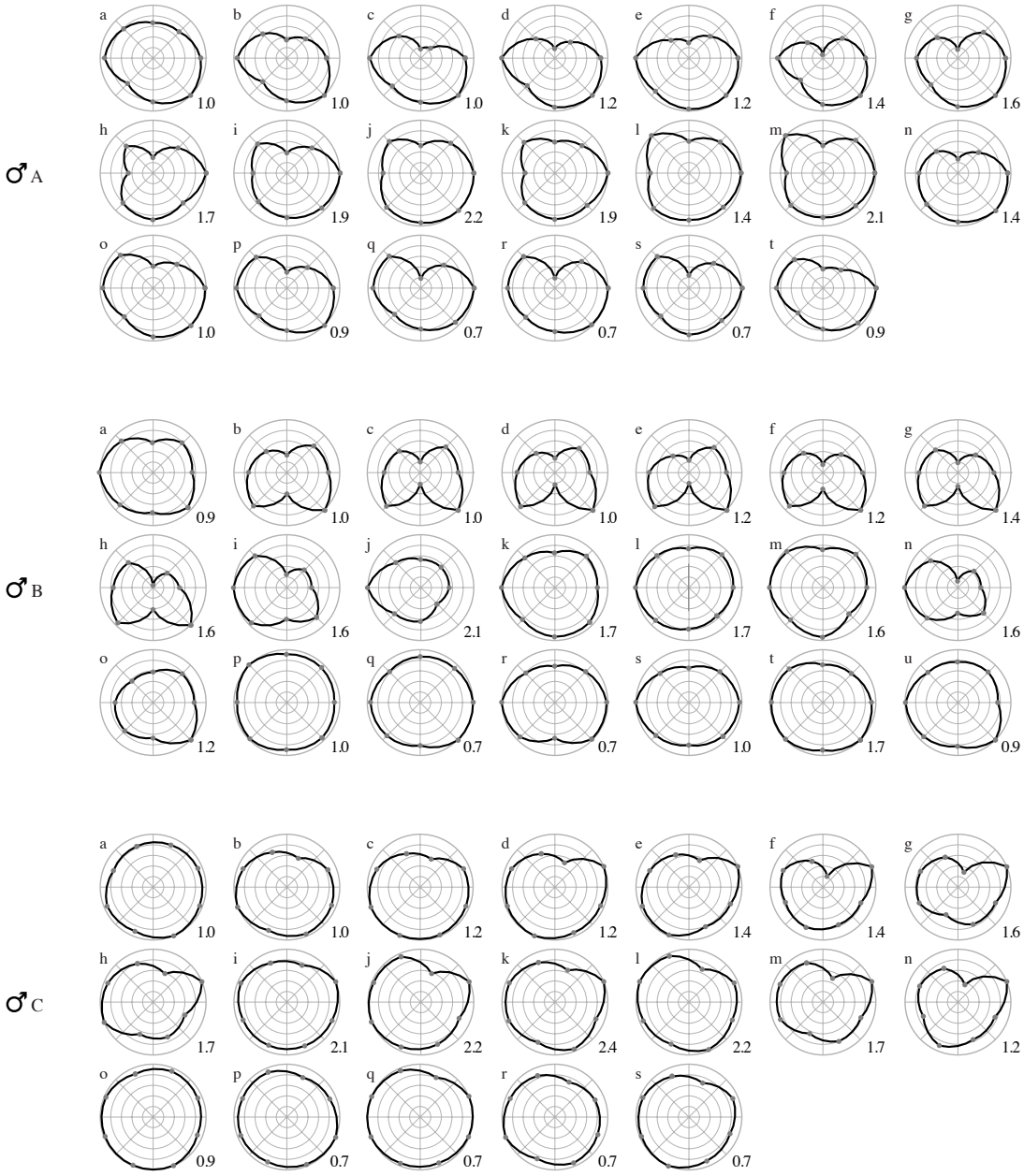

Fig. 8. Time-varying beam patterns, $b_{band}(\theta)$, for the whistle component of the strut display. The format is the same as in Fig. 6 except that the dynamic range of these plots is 30 dB. Each plot represents a time slice of 5.8 ms with no overlap. Time reads from left to right and from top to bottom, signified by the letters a–u. The value at the bottom right of each polar plot is the dominant frequency (kHz) for that time slice. One whistle from each focal bird is shown.

and explicitly corrected for propagation heterogeneity in frequency and space. In this way, our method makes acoustic-directionality research possible in a wider variety of organisms and environments.

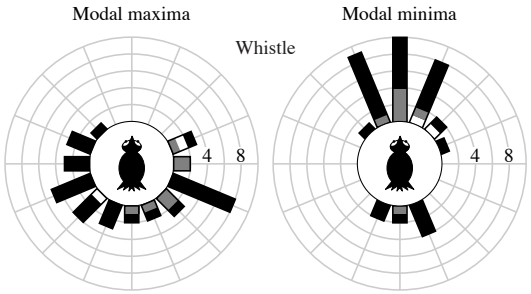

Fig. 9. Polar histograms showing the orientation of the beam patterns' major features relative to the anterior–posterior axis of the birds for the whistle. These frequency distributions show beam pattern modal maxima (left), mode[θ_{max}], and modal minima (right), mode[θ_{min}], for all 39 measured vocalizations. The contribution to the data set of each focal male is indicated by the density of the cell in each histogram bar; black is male A, gray is male B and white is male C.

Bioacoustic conclusions

Our measurements showed that sage grouse strut displays have markedly directional acoustic beam patterns. Although the directionality of these patterns varied both within a vocalization and between calls, clear patterns emerged. First, the coos were always intense in front of the animal and sometimes intense behind as well. The coos were least intense to either side. This maximal lobe rotated up to 45° to either side between vocalizations. The whistles showed a distinctly different beam pattern. While variable across the length of the note, the principal beam pattern that dominated the radiation of the whistle was laterally bilobate with a strong anterior null in the beam pattern. Pop 1 was strongly directional but highly variable in its orientation, whereas pop 2 had a much lower magnitude of directionality but was fairly stable in its directional pattern.

Comparisons with the directionality of other vertebrate vocalizations

The acoustic radiation patterns of a number of other vertebrate vocalizations have been measured and they conform to a general theme. Directional vertebrate vocalizations are bilaterally symmetrical with their maximal radiation point anterior to their site of acoustic radiation (mouth, nares or vocal sac). This is consistent with models of single-site acoustic radiation. The degree to which these fields are directional varies from a narrow beam to nearly or completely omnidirectional. The most directional vocalizations, with approximately 20–36 dB in beam pattern range, are the echolocation pulses of bats and of toothed whales (Au et al., 1995; Fuzessery et al., 1992; Hartley and Suthers, 1987, 1989, 1990; Pilleri et al., 1976; Purves and Pilleri, 1983; Schnitzler and Henson, 1980; Wotton et al., 1997). Few of the above studies resolved these patterns beyond the forward-facing 180°, so these range values are estimates and it would be inappropriate to estimate DIs. Intermediate directionality, with beam pattern ranges of 6–15 dB and DI between 2.0 and 3.5 depending on frequency, has been found in human speech and blackbird vocalizations (Flanagan, 1972; Larsen and Dabelsteen, 1990). Anuran calls are at the low end; the most directional of the measured frog calls has a beam pattern which ranges 6 dB from front to back (DI≈1.5) (Gerhardt, 1975). Most frogs vocalizations are much less directional and some have been found to exhibit a nearly omnidirectional pattern, DI≈0 (Gerhardt, 1975; Passmore, 1981; Prestwich et al., 1989).

To our knowledge, there are only two previously reported minor exceptions to the vertebrate theme that vocalizations are loudest in front and quieter behind. One species of toad, *Bufo americanus*, radiates sound in two equally intense lobes 180° apart, one in front and one behind, separated by a notch of approximately 3–4 dB (Gerhardt, 1975). The fairly shallow lateral null in this pattern is an interesting deviation from the standard vertebrate pattern and remains unexplained. Also, the call of the African frog *Cacosternum boettgeri* was reported to be 1–1.5 dB louder directly posterior (Passmore, 1981). This effect was extremely small, within the range of likely measurement error for working in the field. In addition, since this study did not account for propagation effects, it is possible that the skew was environmentally induced.

Portions of the sage grouse whistle show the greatest directionality of any strictly communicative vertebrate signal so far measured. Only vocalizations used for echolocation are known to be more directional. The sage grouse coos and pop 1 show the level of directionality commonly found in the communication signals of larger vertebrates, while pop 2 is more similar to the omnidirectional sounds of frogs. We expected that lower-frequency sounds, those with large wavelength-to-body size ratios, would be less directional than higher-frequency sounds (Bradbury and Vehrencamp, 1998; Prestwich, 1994). This held generally true in sage grouse since the whistle contains energy principally in wavelengths shorter than those of the less-directional coo and pop notes. However, despite having a similar spectral make-up, pop 2 is markedly less directional than the two coos. Also, the lower frequencies of the whistle, 500–1400 Hz, often exhibited the deepest anterior nulls and the strongest directionality. Therefore, we propose that the rapid movement of the esophageal air sac or associated structures is responsible for much of this between-note variation in magnitude of directionality.

While the magnitude of the directionality is not completely unprecedented, the shape of the beam patterns of the sage grouse strut is unlike any previously seen in vertebrates. The two most surprising results are the deep anterior null in the radiation pattern of the whistle and the bilateral asymmetry and variable direction of the peak in the radiation pattern of the coos and pop 1. Previous attempts to understand the patterns generated by vertebrate vocalization have used simple acoustic models of single-source radiation to arrive at a realistic estimate of radiation mechanisms. A model of the vocal apparatus as a vibrating piston suspended in a baffle has adequately explained the basic patterns observed in birds, bats,

cetaceans and humans (Flanagan, 1972; Hartley and Suthers, 1989, 1990; Hunter et al., 1986; Larsen and Dabelsteen, 1990; Mogensen and Møhl, 1979; Pilleri, 1990; Stevens, 1997; Strother and Mogus, 1970). Alternative models of single-site radiation have come closer to explaining the smaller side lobes in the acoustic field of bats (Hartley and Suthers, 1989, 1990). One dual-site radiation model argued that emission through a paired structure could lead to an increase in directionality for bats that call through their noses (Möhres, 1967; Sokolov and Makarov, 1971).

The beam patterns seen in the sage grouse do not fit those predicted by any of these models. The shape of the beam patterns for the coos and pops superficially resemble some of these patterns. However, since all the potential radiation sites (mouth and air sacs) face forwards for the duration of the vocalization, none of these models can explain the variability in the location of the peak or the intensity of the rearward-facing lobe. Furthermore, none of the models can explain the anterior null and lateral projection of the whistle component. Because of this lack of congruence with existing models, we suggest that the sound emission mechanism of the sage grouse is unlike that of any other vertebrate so far examined.

Directionality, display posture and the study of mate choice

Even directionality as low as 3–6 dB is likely to be behaviorally relevant because, given spherical spreading, this translates to a 40–100 % greater distance of propagation in the direction of the maximum lobe before the signal is lost. Directionality is a defining component of an acoustic signal's active space, although it is often overlooked (e.g. Brenowitz, 1982). When a sender knows (or can estimate) the location of its intended receiver, the signaler can reduce the cost of eavesdropping by predators and competitors by turning so that the peak of its beam pattern corresponds to the position of the receiver. The signaler can then produce just enough acoustic power to signal effectively to that individual (Klump and Shalter, 1984; Larsen and Dabelsteen, 1990). In addition, when competitors have overlapping signals, the sender can combine display orientation with a more powerful vocalization to decrease acoustic interference from its competitors and maximize the probability of response by the receiver. If the receiver can perceive the vocalization's directionality, then appropriate posture might also help to specify the intended recipient of the signal (McGregor and Krebs, 1984; Richards, 1981). In these ways, directional patterns of acoustic radiation can strongly influence the choice of display posture, allowing for more effective or efficient communication to receivers of known location. When the intended receiver's position is unknown, however, directional display can be a liability necessitating continual modification of display posture to maximize the probability of reception (Forrest, 1991). In situations like this, an omnidirectional vocalization may be favored. The directionality of vertebrate vocalizations is likely to be tuned to the social and environmental context of the display, and display posture is likely to reflect the degree and nature of that directionality.

Sage grouse males do not face females head on. Early observers of the mating display of the male sage grouse noticed that, although the display was dramatic, the efforts seemed to be unrelated to the locations of potential female mates. Simon (1940, p. 470) wrote that the males, 'seemed disinterested in the hens...[and] in strutting paid very little attention to [them]'. Indeed, while males rotate to different directions for successive calls, they rarely face a female head on (J. W. Bradbury and M. S. Dantzker, personal observation). Females turn with the male to help maintain an oblique angle between them (Wiley, 1973a). It is this indirect approach that fooled Simon (1940) into his incorrect inference that the sage cock was not in 'actual pursuit' of hens. We now know that lekking sage grouse are under intense sexual selection driven by female choice (Gibson and Bradbury, 1985; Hartzler, 1972; Hjorth, 1970; Lumsden, 1968; Patterson, 1952; Scott, 1942; Wiley, 1973b). The results of this study suggest that, despite maintaining an oblique orientation, male sage grouse might still reach females with the loudest portion of his acoustic signal. Beyond this, however, these data do not reveal the adaptive significance of the unusual radiation patterns we have described. While it is possible that these beam patterns evolved under direct selection, it is also possible that the patterns are an epiphenomenon of selection for loud or impulsive sounds. Alternatively, the patterns of acoustic radiation might have evolved to improve the efficacy of an already lateralized display that evolved first for other reasons.

Investigations of female sage grouse mate-choice have identified a number of spectral and temporal aspects of the strut display that are correlated with mating success (Gibson, 1996; Gibson and Bradbury, 1985; Gibson et al., 1991). While amplitude is likely to be an important determinant of mate attraction (Forrest and Raspet, 1994), these studies could not examine signal intensity since field measurements were not repeatable (J. W. Bradbury, personal observation). The results of the present study suggest that the unusual and variable beam patterns of the sage grouse display combined with the leks' heterogeneous transmission loss blocked these previous efforts from accurately measuring signal amplitude. These same factors, directionality and heterogeneous transmission loss, also stymie efforts to measure the amplitude of other species' acoustic displays (Gerhardt, 1998). Techniques such as the one we have described here facilitate the study of acoustic amplitude in the field and thereby allow more thorough investigation into the importance of amplitude and directionality in signal evolution.

Appendices

Appendix A: calibration of the acoustic system

The acoustic system, described below, had its own characteristic acoustic properties. These properties had to be identified and quantified before the system could be used to measure the transmission properties of the lek and the radiation pattern of the sage grouse. This Appendix outlines how this was accomplished. In what follows, we will assume that all

time variables have been Fourier-transformed so that we are dealing with the steady-state response of the system.

The acoustic system consisted of source and receiver components. The sound source was a Kudelski powered speaker driven by a Stanford Research DS340 signal generator. A single receiver channel consisted of an Audiotechnica MB1000L microphone coupled to a custom-built amplifier through an impedance-matching transformer. The output from the amplifier was recorded on a TASCAM DA88 digital recorder, which provides 96 dB of dynamic range from 10 Hz to 22.5 kHz.

The source sound pressure field measured 1 m from the front of the source can be related to the signal generator voltage by:

$$p_s(f) = \alpha_s(f) V_g(f) , \quad \text{(A1)}$$

where $V_g(f)$ is the voltage supplied by the generator and $\alpha_s(f)$ is a frequency-dependent constant, which depends on the source and has units of Pa V^{-1}. Similarly, the voltage at the output of the amplifier can be expressed as:

$$V_r(f) = \frac{p_r(f)}{\alpha_r} , \quad \text{(A2)}$$

where $p_r(f)$is the sound pressure at the microphone and α_r is a frequency-independent constant for the microphone/amplifier pair, which also has units of Pa V^{-1}. The frequency-independent response of the Audiotechnica microphone and custom-built amplifier was verified by comparison of the response with a calibrated APO microphone.

The third expression we require relates the acoustic field radiated by the source to the field that arrives at the microphone. For the acoustic system calibration, the source was positioned close to the microphone and away from the ground to prevent interference from multi-path arrivals. In this case, the relationship between p_s and p_r follows a spherical spreading law:

$$p_r = \frac{p_s}{r} , \quad \text{(A3)}$$

where r is the separation between the speaker and microphone. This relationship was tested and found to hold true by measuring the source spreading loss at three ranges, verifying that the calibration measurements were not made in the near field of the source and were free from multi-path effects.

To characterize the acoustic system, it was necessary to measure α_s and α_r. In our later calculations, these two constants will always appear as a dimensionless ratio, and so it is sufficient to measure α_r/α_s. Combining equations A1, A2 and A3, we have:

$$\frac{\alpha_r}{\alpha_s} = \frac{V_g}{V_r r} , \quad \text{(A4)}$$

where the explicit dependence on frequency has been dropped. The ratio defined in equation A4 was determined by measuring r and the variables V_r and V_g across a frequency band of 200 Hz to 5 kHz.

Appendix B: measurement of transmission loss across the lek

Acoustic transmissions close to the ground are characterized by frequency-dependent structure in the transmission loss caused by interference between airborne and ground-reflected arrivals. Absorption and refraction due to sound speed profiles in the air are not expected to be important over the short ranges and low frequencies of interest here (Piercy and Embelton, 1977). The ground-induced interference structure depends sensitively on the composition of the ground (Embleton et al., 1983) and ground relief. As the ground relief varied considerably along the transmission paths studied, the transmission loss along each path needed to be measured.

The subject of acoustic transmissions over ground is a subject area in its own right, and a full discussion of the phenomenon lies beyond the scope of the present paper. The interested reader is referred to the work of Embleton et al. (1976, 1983) and recent reviews by Embleton (1996) and Forrest (1994).

The transmission loss across a given stretch of the lek is defined by:

$$TL(f,r) = \frac{p_r(f,r)}{p_s(f)} , \quad \text{(B1)}$$

where $p_r(f,r)$ is the sound field pressure at the observation point as a function of range from the source, r, and frequency, f, and $p_s(f)$ is the free-space source sound pressure field measured 1 m in front of the source. Substituting equations A1 and A2 into equation B1, we obtain:

$$TL(f,r) = \frac{\alpha_r}{\alpha_s(f)} \frac{V_r(f,r)}{V_g(f)} , \quad \text{(B2)}$$

where the constants α_r and α_s depend on the acoustic measurement system (see Appendix A), V_r is the voltage measured at the microphone and V_g is the voltage used to drive the source. Since the ratio $\alpha_r/\alpha_s(f)$ is known, the transmission loss can be measured by measuring $V_r(r,f)$ and $V_g(f)$.

The actual measurement methodology for a given stretch of the lek was as follows. The measurement system was composed of the instruments described in Appendix A with the exception of the Stanford Research signal generator, which was replaced by a recording of the signal generator output. The Kudelski speaker was placed within the microphone array with its center 25 cm above the ground using a leveled stand and driven with a sinusoidal chirp linearly modulated with a triangle-wave from 200 Hz to 5 kHz. A complete chirp took 10 s to complete, providing sufficient time at any given frequency to allow for all multi-path arrivals. For each measurement path, we recorded four complete chirps of both the source excitation voltage and the microphone response voltage. At each acoustic measurement site, we repeated this measurement procedure eight times, rotating the speaker each time so that the speaker faced directly towards each microphone in the recording array. Like most loudspeakers, the Kudelski speaker is directional; however, the rotation of the speaker allowed us to calibrate our system with an effectively omni-directional source.

The most straightforward way to determine the ratio of voltages that appears in equation B2 would be to compute the ratio of the Fourier-transformed time series. However, in practice, it was found that this methodology was too sensitive to contamination from sources of ambient noise, which included wind and biological sources. Therefore, we employed a noise-reduction algorithm to improve the ratio estimates. The algorithm consisted of the following. For each transmission path, 30 s or three complete chirps of source excitation and microphone response voltages were digitally transferred from the tape to a computer. The digital data streams were pre-processed by cross-correlating the source and microphone voltages to determine the time delay in the transit of the airborne signal between the source and microphone. This time delay was then backed out of the microphone recording to synchronize the source and microphone time series so that the dominant frequency, f_j, within a given segment of source and microphone data was the same. The voltage ratio at f_j was then determined by taking the ratio of the spectral levels at f_j while ignoring all other spectral components. Thus, the ratio estimates were formed from data segments corresponding to the largest available signal-to-noise ratios.

Appendix C: the directivity index

The directivity index (DI) compares the intensity of the maximum lobe of a beam pattern with the intensity of a uniform source radiating the same total power output. The total power Π radiated by a directional sound source through a cylindrical surface of small height Δz enclosing the source is obtained by integrating the free-space sound pressure $p_s(r,\theta)$, so that:

$$\Pi = \frac{1}{2\rho_o c}\int_0^{2\pi} p_s^2(r,\theta)\Delta z r \mathrm{d}\theta\,, \qquad \text{(C1)}$$

where ρ_o is the density of sound in air and c is the speed of sound in air. (Note: angles in Appendix C are in radians.)

We can split the function for the free-space sound pressure field into the directional factor, $H(\theta)$, and the on-axis pressure, $p_{s,axis}(r)$, as in equation 1, then rewrite the above relationship for power as:

$$\Pi = \frac{1}{2\rho_o c}\, p_{s,axis}^2(r)\Delta z r \int_0^{2\pi} H^2(\theta)\mathrm{d}\theta\,. \qquad \text{(C2)}$$

A uniform source that generates the same acoustic power, Π_u, can be represented relative to the pressure amplitude $P_u(r)$ at r meters from the uniform source by:

$$\Pi = \Pi_u = \frac{1}{2\rho_o c}\int_0^{2\pi} p_u^2(r)\Delta z r \mathrm{d}\theta = \frac{2\pi}{2\rho_o c}\, p_u^2(r)\Delta z r\,. \qquad \text{(C3)}$$

It follows that the directional source will have a greater intensity along its acoustic axis than will the uniform source. The ratio of these intensities therefore gives us a measure of the directional concentration of the acoustic power. This ratio, called the directivity, D, can be represented as:

$$D = \frac{p_{s,axis}^2(r)}{p_u^2(r)}\,. \qquad \text{(C4)}$$

Setting equation C2 equal to equation C3, we can now solve for this above ratio and rewrite this equation as:

$$D = \frac{2\pi}{\int_0^{2\pi} H^2(\theta)\mathrm{d}\theta}\,. \qquad \text{(C5)}$$

The directivity index, DI, is the decibel equivalent of this quantity:

$$\mathrm{DI} = 10\log D\,. \qquad \text{(C6)}$$

Solving this equation for some simple radiation patterns shows us both the utility and limitations of this index. For a pulsating sphere where $H(\theta)=0$, we find that DI=0 dB. A hemispherical source mounted on a rigid baffle where $H(\theta)=0$ for $0<\theta\leqslant\pi$ and $H(\theta)=0$ for $\pi<\theta\leqslant 2\pi$ then has DI=3.01 dB. For a simple dipole radiation pattern where $H(\theta)=\cos^2\theta$, we find an equivalent DI=3.01 dB. This illustrates that the directivity index does not inform us as to the shape of the radiation pattern, only the degree to which the acoustic power is concentrated.

To calculate the directivity index of the measured radiation patterns from our eight-point array, we solved for a measure of the squared directional factor, $H^2(\theta)$, and approximated the integration in equation C5 using Simpson's rule. Substituting into equation C6, we arrived at the final solution:

$$\mathrm{DI} = 10\log \frac{2\pi}{\frac{\pi}{12}\left\{4\sum_{j=1,3,5,7} H_j^2 + 2\sum_{k=0,2,4,6} H_k^2\right\}}\,, \qquad \text{(C7)}$$

where $H(2\pi)=H(0)$ and H_0 was defined as the point where $H(\theta)=1$. In practice, our measure of the squared directional factor was $H_{band}^2(\theta)$ from equation 8 or $H_{band,note}^2(\theta)$ from equation 10.

For simple beam patterns, this approximation should not overestimate the value of DI. The degree to which the calculation approximates the true value of DI is dependent on where the eight samples of the beam pattern are taken. To illustrate this, we used this equation to calculate the DI of the dipole radiation pattern, $H^2(\theta)=\cos^2\theta$, 10 000 times choosing the position of the first of eight equally spaced samples randomly from $0\leqslant\theta<\pi/4$. This yielded a range of values (median 2.84 dB; range 2.32 dB<DI<3.01 dB). No values exceed the value calculated analytically above. We therefore suggest that our approximation of the directivity index is a conservative measure of the directionality of the true beam pattern.

List of symbols

$b(\theta)$	the beam pattern, the decibel equivalent of the directional factor H (dB)
$b_{band}(\theta)$	band-averaged beam pattern (dB)
$b_{band,note}(\theta)$	time- and band-averaged beam pattern (dB)

c	speed of sound ($m\,s^{-1}$)
D	directivity, a measure of the directionality of the sound field (dimensionless)
DI	directivity index, the decibel equivalent of D (dB)
f	frequency of vibration (Hz)
$H(\theta)$	the directional factor, a normalized function (dimensionless)
$H_{band}^2(\theta)$	frequency-band average of the squared directional factor (dimensionless)
$H_{band,note}^2(\theta)$	time- and frequency-band average of the squared directional factor (dimensionless)
H_0	point where $H(\theta)=1$
mode[θ_{max}]	beam pattern modal maximum (degrees)
mode[θ_{min}]	beam pattern modal minimum (degrees)
n	number of time slices
p_r	spectral density of the acoustic pressure measured at the receivers ($Pa\,H^{-1/2}$)
p_s	spectral density of the acoustic pressure generated by a source ($Pa\,H^{-1/2}$)
$p_{s,axis}$	spectral density of the acoustic pressure on the acoustic axis ($Pa\,H^{-1/2}$)
p_u	spectral density of the acoustic field generated by a uniform source ($Pa\,H^{-1/2}$)
r	distance from source (m)
TL	transmission loss (dB)
V_g	signal generator voltage (V)
V_r	output voltage from the microphone amplifiers (V)
z	vertical distance (m)
α_s	source frequency response, a frequency-dependent constant ($Pa\,V^{-1}$)
α_r	receiver response, a frequency-independent constant ($Pa\,V^{-1}$)
Π	acoustic power (W)
Π_{band}	frequency-band average of the acoustic power (W)
Π_u	acoustic power generated by a uniform source (W)
θ	horizontal angle relative to the front of the source (degrees; radians in Appendix C)
θ_{max}	value of θ at which $b(\theta)$ is a maximum (degrees)
θ_{min}	value of θ at which $b(\theta)$ is a minimum (degrees)
ρ_o	density ($kg\,m^{-3}$)

This work was supported by the National Science Foundation through a Graduate Research Fellowship (M.S.D.), a Doctoral Dissertation Research Grant IBN-9701201 (M.S.D. and J.W.B.) and grant IBN-9406217 (J.W.B.). We received additional field study support from a Mildred E. Mathias Graduate Student Research Grant through the University of California's Natural Reserve System (M.S.D.). Additional support was provided by NIH training grant T32GM-07240 (M.S.D.) and the US Office of Naval Research (G.B.D.). We thank the Sierra Nevada Aquatic Research Laboratory and Dan Dawson for providing field facilities and the Bureau of Land Management (Bishop, CA, USA) and Terry Russi for access to the field site. We thank Dahlia Chazan for her excellent assistance in the field. We thank Catherine DeRivera, Darren Irwin, Dr Jules Jaffe and two anonymous reviewers for critical comments on the manuscript and also Kathryn Cortopassi, Jami Dantzker and Alejandro Purgue for helpful discussions.

References

Archibald, H. L. (1974). Directional differences in the sound intensity of ruffed grouse drumming. *Auk* **91**, 517–521.

Au, W. W., Pawloski, J. L., Nachtigall, P. E., Blonz, M. and Gisner, R. C. (1995). Echolocation signals and transmission beam pattern of a false killer whale (*Pseudorca crassidens*). *J. Acoust. Soc. Am.* **98**, 51–9.

Bennet-Clark, H. C. (1987). The tuned singing burrow of mole crickets. *J. Exp. Biol.* **128**, 383–409.

Bradbury, J. W. and Vehrencamp, S. L. (1998). *Principles of Animal Communication*. Sunderland, MA: Sinauer Associates.

Brenowitz, E. A. (1982). The active space of red-winged blackbird song. *J. Comp. Physiol.* A **147**, 511–522.

Embleton, T. F. W. (1996). Tutorial on sound propagation outdoors. *J. Acoust. Soc. Am.* **100**, 31–48.

Embleton, T. F. W., Piercy, J. E. and Daigle, G. A. (1983). Effective flow resistivity of ground surfaces determined by acoustical measurements. *J. Acoust. Soc. Am.* **74**, 1239–1244.

Embleton, T. F. W., Piercy, J. E. and Olson, N. (1976). Outdoor sound propagation over ground of finite impedance. *J. Acoust. Soc. Am.* **59**, 267–277.

Flanagan, J. L. (1972). *Speech Analysis; Synthesis and Perception*. New York: Springer-Verlag.

Forrest, T. G. (1991). Power output and efficiency of sound production by crickets. *Behav. Ecol.* **2**, 327–338.

Forrest, T. G. (1994). From sender to receiver: Propagation and environmental effects on acoustic signals. *Am. Zool.* **34**, 644–654.

Forrest, T. G. and Raspet, R. (1994). Models of female choice in acoustic communication. *Behav. Ecol.* **5**, 293–303.

Freitag, L. E. and Tyack, P. L. (1993). Passive acoustic localization of the Atlantic bottlenose dolphin using whistles and echolocation clicks. *J. Acoust. Soc. Am.* **93**, 2197–2205.

Fuzessery, Z. M., Hartley, D. J. and Wenstrup, J. J. (1992). Spatial processing within the mustache bat echolocation system – possible mechanisms for optimization. *J. Comp. Physiol.* A **170**, 57–71.

Gerhardt, H. C. (1975). Sound pressure levels and radiation patterns of the vocalizations of some North American frogs and toads. *J. Comp. Physiol.* **102**, 1–12.

Gerhardt, H. C. (1998). Acoustic signals of animals: recording, field measurements, analysis and description. In *Animal Acoustic Communication: Sound Analysis and Research Methods* (ed. S. L. Hopp, M. J. Owren and C. S. Evans), pp. 1–25. Berlin, New York: Springer.

Gibson, R. M. (1996). Female choice in sage grouse: the roles of attraction and active comparison. *Behav. Ecol. Sociobiol.* **39**, 55–59.

Gibson, R. M. and Bradbury, J. W. (1985). Sexual selection in lekking grouse: phenotypic correlates of male strutting success. *Behav. Ecol. Sociobiol.* **18**, 117–123.

Gibson, R. M., Bradbury, J. W. and Vehrencamp, S. L. (1991). Mate choice in lekking sage grouse revisited: the roles of

vocal display, female site fidelity and copying. *Behav. Ecol.* **2**, 165–180.

Hartley, D. J. and Suthers, R. A. (1987). The sound emission pattern and the acoustical role of the noseleaf in the echolocating bat, *Carolia perspicillata*. *J. Acoust. Soc. Am.* **82**, 1892–1900.

Hartley, D. J. and Suthers, R. A. (1989). The sound emission pattern of the echolocating bat, *Eptesicus fuscus*. *J. Acoust. Soc. Am.* **85**, 1348–1351.

Hartley, D. J. and Suthers, R. A. (1990). Sonar pulse radiation and filtering in the mustached bat, *Pteronotus parnellii rubiginosus*. *J. Acoust. Soc. Am.* **87**, 2756–2772.

Hartzler, J. E. (1972). An analysis of sage grouse lek behavior. PhD thesis, University of Montana, Missoula, USA.

Hjorth, I. (1970). Reproductive behavior in Tetranidae, with special reference to males. *Viltrevy* **7**, 183–596.

Höglund, J. and Alatalo, R. V. (1995). Leks. In *Monographs in Behavior and Ecology* (ed. J. R. Krebs and T. Clutton-Brock), xiii, 248p. Princeton, NJ: Princeton University Press.

Honess, R. F. and Allred, W. J. (1942). Structure and function of the neck muscles in inflation and deflation of the esophagus in the sage cock. *Wyoming Game Fish Dept Bull.*, no. 2, 5–12.

Hunter, M. L. J., Kacelnik, A., Roberts, J. and Vuillermoz, M. (1986). Directionality of avian vocalizations: a laboratory study. *Condor* **88**, 371–375.

Kinsler, L. E., Frey, A. R., Coppens, A. B. and Sanders, J. V. (1982). *Fundamentals of Acoustics*. New York: Wiley.

Klump, G. M. and Shalter, M. D. (1984). Acoustic behaviour of birds and mammals in the predator context. I. Factors affecting the structure of alarm signals. II. The functional significance and evolution of alarm signals. *Z. Tierpsychol.* **66**, 189–226.

Larsen, O. N. and Dabelsteen, T. (1990). Directionality of blackbird vocalization. Implications for vocal communication and its further study. *Ornis Scand.* **21**, 37–45.

Lumsden, H. G. (1968). The displays of the sage grouse. *Ontario Department of Lands and Forests Reseach Report (Wildlife)* **83**, 1–94.

MathWorks (1998). *MATLAB*. Natick, MA: Math Works Inc.

McGregor, P. K., Dabelsteen, T., Clark, C. W., Bower, J. L., Tavares, J. P. and Holland, J. (1997). Accuracy of a passive acoustic location system: empirical studies in terrestrial habitats. *Ethol. Ecol. Evol.* **9**, 269–286.

McGregor, P. K. and Krebs, J. R. (1984). Sound degradation as a distance cue in great tit (*Parus major*) song. *Behav. Ecol. Sociobiol.* **16**, 49–56.

Mogensen, F. and Møhl, B. (1979). Sound radiation patterns in the freqency domain of cries from a vespertilionid bat. *J. Comp. Physiol.* A **134**, 165–171.

Möhres, F. P. (1967). Ultrasonic orientation in megadermatic bats. In *Animal Sonar Systems: Biology and Bionics*, vol. 1 (ed. R. G. Busnel), pp. 115–127. France: Laboratoire de Physiologie Acoustique.

Narins, P. M. and Hurley, D. D. (1982). The relationship between call intensity and function in the Puerto Rican coqui (Anura: Leptodactylidae). *Herpetologica* **38**, 287–295.

Passmore, N. I. (1981). Sound levels of mating calls of some African frogs. *Herpetologica* **37**, 166–171.

Patterson, R. L. (1952). *The Sage Grouse in Wyoming*. Denver, CO: Sage Books.

Piercy, J. E. and Embelton, T. F. W. (1977). Review of noise propagation in the atmosphere. *J. Acoust. Soc. Am.* **61**, 1403–1418.

Pilleri, G. (1990). Adaptation to water and the evolution of echolocation in the Cetacea. *Ethol. Ecol. Evol.* **2**, 135–163.

Pilleri, G., Zbinden, K., Gihr, M. and Kraus, C. (1976). Sonar clicks, directionality of the emission field and echolocating behaviour of the Indus River Dolphin (*Platanista indi* Blyth, 1859). In *Investigations on Cetacea*, vol. X (ed. G. Pilleri), pp. 157–188. Berne: Brain Anatomy Institute.

Prestwich, K. N. (1994). The energetics of acoustic signaling in anurans and insects. *Am. Zool.* **34**, 625–643.

Prestwich, K. N., Brugger, K. E. and Topping, M. (1989). Energy and communication in three species of hylid frogs: power input, power output and efficiency. *J. Exp. Biol.* **144**, 53–80.

Purves, P. E. and Pilleri, G. E. (1983). *Echolocation in Whales and Dolphins*. New York: Academic Press.

Richards, D. G. (1981). Estimation of distance of singing conspecifics by the Carolina wren. *Auk* **98**, 127–133.

Schnitzler, H.-U. and Henson, O. W. (1980). Performance of airborne animals sonar systems. I. Microchiroptera. In *Animal Sonar Systems* (ed. R. G. Busnel and J. D. Fish), pp. 801–827. New York: Plenum.

Scott, J. W. (1942). Mating behavior of the sage grouse. *Auk* **59**, 477–498.

Shure, L. and McClellan, J. (1997). *XCORR Cross-Correlation Function Estimates*. Natick, MA: Math Works Inc.

Simon, J. R. (1940). Mating performance of the sage grouse. *Auk* **57**, 467–471.

Sokolov, B. V. and Makarov, A. K. (1971). Direction of the ultrasonic radiation and role of the nasal leaf in *Rhinolophus ferrumequinum*. *Biologicheskie Nauki* **7**, 37–44.

Spiesberger, J. L. and Fristrup, K. M. (1990). Passive localization of calling animals and sensing of their acoustic environment using acoustic tomography. *Am. Nat.* **135**, 107–153.

Spurrier, M. F., Boyce, M. S. and Manly, B. F. J. (1994). Lek behaviour in captive sage grouse *Centrocercus urophasianus*. *Anim. Behav.* **47**, 303–310.

Stevens, K. N. (1997). Models of speech production. In *Encyclopedia of Acoustics*, vol. 4 (ed. M. J. Crocker), pp. 1565–1578. New York: Wiley.

Strother, G. K. and Mogus, M. (1970). Acoustical beam patterns for bats: Some theoretical considerations. *J. Acoust. Soc. Am.* **48**, 1430–1432.

Watkins, A. W. and Schevill, W. E. (1971). Four hydrophone array for acoustic three-dimensional location. *Woods Hole Oceanographic Institute Technical Report* 71-60.

Watkins, W. A. and Schevill, W. E. (1972). Sound source location by arrival-times on a non-rigid three-dimensional hydrophone array. *Deep-Sea Res.* **19**, 691–706.

Wiley, R. H. (1973a). The strut diplay of male sage grouse: a 'fixed' action pattern. *Behaviour* **47**, 129–152.

Wiley, R. H. (1973b). Territoriality and non-random mating in sage grouse, *Centrocercus urophasianus*. *Anim. Behav. Monogr.* **6**, 85–169.

Witkin, S. R. (1977). The importance of directional sound radiation in avian vocalization. *Condor* **79**, 490–493.

Wotton, J. M., Jenison, R. L. and Hartley, D. J. (1997). The combination of echolocation emission and ear reception enhances directional spectral cues of the big brown bat, *Eptesicus fuscus*. *J. Acoust. Soc. Am.* **101**, 1723–1733.

Young, J. R. (1994). The influence of sexual selection on phenotypic and genetic divergence among sage grouse populations. PhD thesis, Purdue University, USA.

Young, J. R., Hupp, J. W., Bradbury, J. W. and Braun, C. E. (1994). Phenotypic divergence of secondary sexual traits among sage grouse, *Centrocercus urophasianus*, populations. *Anim. Behav.* **47**, 1353–1362.

Acknowledgements

Chapter 3, in full, is a reprint of the material as it appears in Directional acoustic radiation in the strut display of male sage grouse, *Centrocercus urophasianus* in Journal of Experimental Biology 1999. Dantzker, Marc; Deane, Grant; Bradbury, Jack W. 1999. The dissertation author was the primary investigator and author of this paper.